Rui Pedro Silvestre dos Santos

Bachelor in Sciences of Biomedical Engineering

TIME SERIES MORPHOLOGICAL ANALYSIS APPLIED TO BIOMEDICAL SIGNALS EVENTS DETECTION

Dissertation submitted in the fufillment of the requirements for the Degree of Master in Biomedical Engineering

Advisor: Doctor Hugo Gamboa, FCT - UNL

Committee:

President: Doctor Mário António Basto Forjaz Secca
Examiner: Doctor Pedro Miguel Martins Encarnação
Vowel: Doctor Hugo Filipe Silveira Gamboa

FACULDADE DE CIÊNCIAS E TECNOLOGIA
UNIVERSIDADE NOVA DE LISBOA

December 2011

Time Series Morphological Analysis Applied to Biomedical Signals Events Detection

Acknowledgments

This dissertation work would not have been possible without the support of many people, both in scientific as in emotional levels, for whom I owe my deepest gratitude.

I am sincerely and heartily grateful to my advisor, Professor Hugo Gamboa, for all the encouragement, guidance and support given throughout this research work. I also thank the opportunity to work and learn in such a dynamic and creative environment, which definitely contributed to the achievements of this dissertation.

Through the networking experience this dissertation gave me, I had the opportunity to work with researchers from different scientific backgrounds, in which I found most of the motivation to carry it out. From those, I want to specially thank Professor Borja Sañudo, from the University of Seville, Spain, and Carlos J. Marques from the Physical Therapy and Rehabilitation Department at the Schön Klinik Hamburg Eilbek, Germany.

I would like to thank *PLUX - Wireless Biosignals, S. A.* and its collaborators for always letting me make feel part of this amazing team. A special thanks to Joana Sousa, who supervised this work at the company, showing a constant interest and giving a great contribution to make it go forward. I am also very grateful to João Santinha, my partner during a significant part of this work, for all the support, motivation words and knowledge exchange. I would like to express my gratitude to Ana Fé, André Modesto, Dário Bento, Gonçalo Martins, Lídia Fortunato, Nuno Cardoso, Nuno Santos, Paulo Aires, Ricardo Gomes, Neuza Nunes and Tiago Araújo for all the help and contribution for such a healthy work environment.

I would like to show my deepest gratitude to all of my friends, from those I know almost since we were born to those I have met at the faculty. Be assured that the meaning and the space you fill in my life is quite bigger than this single paragraph.

To Milene who always stood by me in such another important step of my life with love, friendship and dedication. Thank you for your constant support and for pulling me up when I most needed.

Um último e profundo agradecimento à minha família e, em especial, à minha irmã Raquel e aos meus pais, Jorge e Purificação, por todo o apoio e pela crença incondicional nas minhas capacidades. O vosso exemplo de trabalho, sacrifício e dedicação é sem dúvida a fonte de inspiração que conduz o meu trabalho e toda a minha vida, pela qual estarei eternamente grato. A vós dedico esta dissertação.

Abstract

Automated techniques for biosignal data acquisition and analysis have become increasingly powerful, particularly at the Biomedical Engineering research field. Nevertheless, it is verified the need to improve tools for signal pattern recognition and classification systems, in which the detection of specific events and the automatic signal segmentation are preliminary processing steps.

The present dissertation introduces a signal-independent algorithm, which detects significant events in a biosignal. From a time series morphological analysis, the algorithm computes the instants when the most significant standard deviation discontinuities occur, segmenting the signal. An iterative optimization step is then applied. This assures that a minimal error is achieved when modeling these segments with polynomial regressions. The adjustment of a scale factor gives different detail levels of events detection.

An accurate and objective algorithm performance evaluation procedure was designed. When applied on a set of synthetic signals, with known and quantitatively predefined events, an overall mean error of 20 samples between the detected and the actual events showed the high accuracy of the proposed algorithm. Its ability to perform the detection of signal activation onsets and transient waveshapes was also assessed, resulting in higher reliability than signal-specific standard methods.

Some case studies, with signal processing requirements for which the developed algorithm can be suitably applied, were approached. The algorithm implementation in real-time, as part of an application developed during this research work, is also reported.

The proposed algorithm detects significant signal events with accuracy and significant noise immunity. Its versatile design allows the application in different signals without previous knowledge on their statistical properties or specific preprocessing steps. It also brings added objectivity when compared with the exhaustive and time-consuming examiner analysis. The tool introduced in this dissertation represents a relevant contribution in events detec-

tion, a particularly important issue within the wide digital biosignal processing research field.

Keywords: Biosignals, Algorithms, Signal-Processing, Events Detection, Onsets, Transients

Resumo

As técnicas para aquisição e análise de biosinais têm-se tornado mais poderosas, particularmente ao nível da investigação em Engenharia Biomédica. Contudo, verifica-se a necessidade de melhorar os sistemas de reconhecimento de padrões e classificação, nos quais a detecção de eventos específicos e a segmentação automática de sinais são etapas de processamento preliminares.

Esta dissertação apresenta um algoritmo que detecta eventos em biosinais, independentemente do sinal considerado. Partindo da análise morfológica de uma série temporal, são calculados os instantes onde ocorrem as maiores descontinuidades no seu desvio padrão, segmentando os sinais. Uma etapa de optimização iterativa assegura um erro mínimo ao modelar esses segmentos como regressões polinomiais. O ajuste de um factor de escala garante diferentes níveis de detalhe na detecção de eventos.

A performance do algoritmo foi avaliada precisa e objectivamente. Ao aplicá-lo num conjunto de sinais sintéticos, com eventos conhecidos e pré-definidos, obteve-se um erro médio global de 20 amostras entre os eventos reais e os detectados, o que mostra a precisão desta ferramenta. A mesma provou também ser capaz de detectar o início de activações em sinais ou formas de onda transientes, com menos falhas do que métodos padrão para os sinais analisados.

Foram abordados casos de estudo onde o algoritmo desenvolvido pode ser aplicado. A sua implementação em tempo-real, como parte de uma ferramenta de processamento desenvolvida neste trabalho de investigação, é também reportada.

O algoritmo apresentado detecta eventos em sinais, com elevada precisão e imunidade ao ruído. A sua versatilidade possibilita a aplicação em diferentes sinais sem conhecimento prévio sobre as suas propriedades estatísticas ou etapas de pre-processamento específicas. Garante ainda uma objectividade acrescida quando comparado com a análise por peritos, tipicamente morosa e exaustiva. A ferramenta apresentada nesta dissertação traduz-se num

avanço na detecção de eventos, um tópico particularmente importante no processamento digital de sinais.

Palavras-chave: Biosinais, Algoritmos, Processamento de Sinal, Detecção de eventos, *Onset*, Transientes

Contents

List of Figures

List of Tables

List of Abbreviations

ACL Anterior Cruciate Ligament

ADC Analog to Digital Converter

API Application Programming Interface

BCI Brain-Computer Interface

BPTT Brake Pedal Travelling Time

BRT Brake Response Time

ECG Electrocardiography

EMG Electromyography

EOG Electrooculography

FFT Fast Fourier Transform

FTT Foot Transfer Time

GUI Graphical User Interface

f_s Sampling Frequency

H Hamstrings

HRV Heart Rate Variability

MSE Mean Squared Error

MIS Minimally Invasive Surgery

MT Movement Time

PSD Power Spectral Density

RF *Rectus Femoris*

RMS Root Mean Square

RT Reaction Time

sEMG Surface EMG

SNR Signal-to-Noise Ratio

STD Standard Deviation

TKA Total Knee Arthroplasty

T_s Sampling Interval

VGRF Vertical Ground Reaction Force

WBV Whole Body Vibration

Chapter 1

Introduction

1.1 Motivation

Automated techniques for acquiring and analysing data from scientific measurements have become increasingly powerful and accurate over the last decades. However, the need to improve signal pattern recognition and data-mining systems, for which the detection of specific events and the automatic signal segmentation is usually one of the first processing steps, is still verified. Those are considered fundamental tasks throughout physics and particularly at the biosignals analysis research field. The development of athletic performance evaluation tools, the initial motivation of this thesis, clearly exemplifies the importance of events detection and signal segmentation algorithms.

Sport practice has always been connected to competition, and therefore related to the comparison between the athletic performance of different subjects. As such, the continuous monitoring and evaluation of athletic performance is a valuable task. It allows the coaches to establish an optimal and customized training program for each athlete, according to their skills and their progress between training sessions. Likewise, it can also assume an important role when considering non-professional athletes, helping each individual to establish and achieve his own personal goals.

The evaluation of athletic performance is associated with the analysis of specific variables that provide information about the physical condition of the athlete. Generally, strength and power related variables are considered the gold standard for this evaluation [1]. Strength and power refer to the forces or torques generated during sport activity. Their assessment can help the sport researchers to quantify their significance and contribution to specific athletic events. This analysis can also help coaches to identify talented individuals who may be suited to particular sporting activities, monitor the effect of repeated training sessions and also per-

form the identification of specific deficiencies and program rehabilitation interventions [2].

Since a large number of indirect variables can be needed for assessment of the interest parameters and considering the fact that some devices only allow the posterior processing of the acquired signals, this kind of evaluation can have a high time complexity [1]. Therefore, the recent evaluation devices development is focused on real-time objective performance assessment, reducing the time spent to complete an evaluation session [1] and providing feedback not only to coaches, but also to the athletes, so they can modify their training patterns and achieve an optimal performance [1, 3]. Furthermore, the signal acquisition should preferentially be done under several degrees of freedom, by portable and miniaturized devices (to provide unobtrusiveness, comfort and user acceptability [4]), in order to approach the testing with the dynamic nature of sporting activities in unstructured environments. The impact of this evaluation systems is nowadays so remarkable that many athletes and coaches consider information derived from technological advances to be invaluable [3].

Given the wide variety of signals that can be considered when assessing the athletic performance, the analysis software tools available with the evaluation devices usually include several predefined protocols that the athletes or their coaches choose based on the specific training programs. But the basis of all the algorithms supporting those tools is related to the detection of the exact time period in which a specific movement is performed. Then, specific algorithms compute the interest variables depending on the chosen analysis protocol. As so there is a practical interest that those events detection and signal segmentation algorithms are as general as possible and fast enough to ensure a real-time processing.

This dissertation was developed at *PLUX - Wireless Biosignals, S.A.*, in partnership with national and international entities, with which the company R&D department is participating in research projects. Two papers regarding this research work were accepted for presentation in BIOSTEC 2012 conference and another paper was published in the *Journal of Strength and Conditioning Research*.

1.2 Objectives

The main goal of this thesis was the development of a signal-independent algorithm for biosignals events detection, segmentation and the subsequent parameters extraction. From the initial motivation described in section 1.1, it has become clear during the execution of the present research work that the development of that algorithm would involve an abstraction level above of that required by a specific athletic performance evaluation application, assuring also a wider contribution to the biosignals processing research field. The developed tools were

applied to distinct case studies, including the parameters analysis of signals acquired through the execution of specific sporting activities and the evaluation of reaction times and the time lag between muscles activation.

A robust off-line algorithm was introduced and its performance was evaluated from the comparison with other signal-specific standard events detection processing techniques and by applying on a database of synthetic signals for which the events were predefined. Its implementation in a real-time signal processing tool developed during this research is also described.

1.3 Thesis Overview

The structure of this thesis is schematically represented in Figure 1.1.

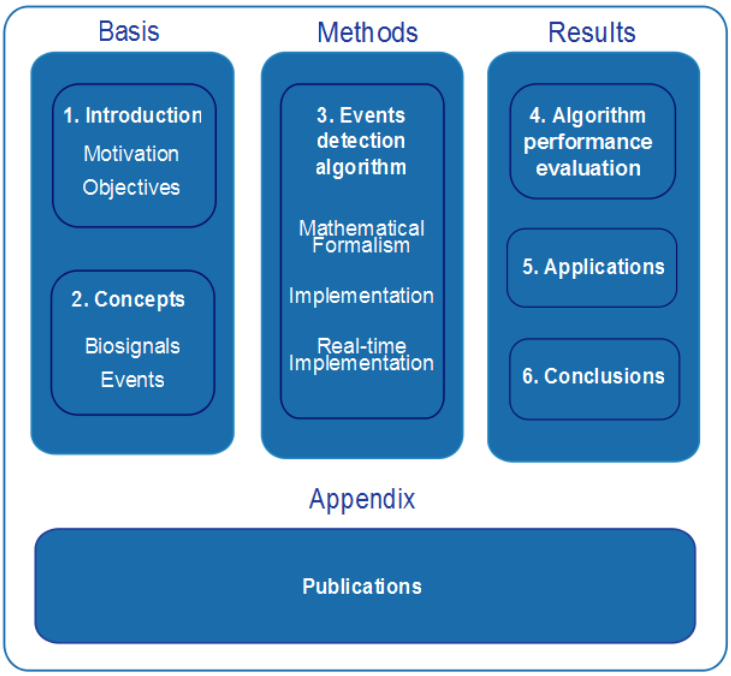

Figure 1.1: Thesis overview

In the first two chapters the basis that support this research work is exposed. The initial motivation, the present objectives and the concepts regarding the biosignals fundamentals and main characteristics, as well as the theory of events detection as part of a pattern recognition signal analysis procedure are presented. It is also made a brief definition of the main application areas of these class of algorithms and a review on some of the standard techniques in this research field is also reported.

Chapter 3 contains a detailed description of the methods applied in the context of this work. The algorithm regarding the events detection is presented in terms of its mathematical

formalism, adopted notation and the most efficient practical implementation solution. This chapter also explains the method by which the previously presented algorithm was implemented in real-time. As so, both the real-time processing tool developed towards this end and the implied constrains and the following adaptations the algorithm was subjected are exposed.

The following chapters address the results of this research work. The algorithm testing and performance evaluation is described in Chapter 4. Chapter 5 presents its application to specific case studies. Some final remarks and future work approach are presented in Chapter 6.

Appendix A contains the papers published in the context of this research work.

Chapter 2

Concepts

This chapter introduces the main concepts approached in the present dissertation. A review on the biosignals fundamentals and some theoretical concepts regarding the signals events detection algorithms are presented, as well as the main application areas and some of the standard methods in this research field.

2.1 Biosignals

A signal can be generically defined as a quantity associated with a physical, economical or social phenomenon that carries some kind of information about it [5]. Biosignals are used in biomedical fields for extracting and understanding the underlying physiological mechanisms of a specific biological event or system [6, 7].

2.1.1 Biosignals Classification

Biosignals can be classified according to their physiological origins, what may be useful when there is an interest in the basic physical characteristics of the process that resulted in that signal, in order to model it. The most important classifications are:

- **Bioelectric signals:** these are probably the most important biosignals and their source is the action potential generated by a nerve or muscle cell after being stimulated under certain conditions. Since the electric field propagates through the biologic medium the most of the times this potential may be acquired at specific anatomic regions on the surface, eliminating the need to perform invasive measurements.

- **Biomagnetic signals:** these records are originated by the magnetic signals associated with specific physiological activity at different organs such as heart, brain and lungs. Since these magnetic fields are typically very weak, biomagnetic signals have a low

signal-to-noise ratio (SNR) and their acquisition has to be done under very careful conditions.

- **Biomechanical signals:** are defined as the signals used in the biomedical field with origin in mechanical functions of the biological system, including motion, displacement, pressure and flow signals, among others. The measurement of these signals is very often forced to be invasive, since mechanical phenomena do not always propagate across the human tissues and organs, as the electric or magnetic biosignals.

- **Bioacoustic signals:** a special subset of biomechanical signals which involves vibration (motion) and is very useful because many biomedical phenomena create acoustic noise. Unlike other types of biomechanical signals, the acoustic energy propagates through the biologic medium. As so, bioacoustic signals may be conveniently acquired on the surface using acoustic transducers such as microphones or accelerometers.

Beyond the aforementioned, there are other types of commonly used biosignals, such as the Bioimpedance, Thermal, Biochemical or Biooptical signals [6].

From the point of view of signal analysis it may be more important to classify a biosignal according to the signal characteristics than correlating it with the respective physiological source. Figure 2.1 outlines some of those classification possibilities.

A broad classification makes distinction between continuous and discrete time signals. Continuous signals are defined over a continuum of time and are described by continuous variable functions [7]. Although the original biosignals are mostly defined in continuous time, the measured biosignals are normally defined in discrete-time, by a set of measurements taken sequentially (also called as time series). This is the result of a sampling of the original biosignals, a procedure very applied due to the powerful tools for discrete signal processing provided by current technology [8]. For a given continuous time signal x, which varies as a function of continuous time t [denotated by $x(t)$] the correspondent sampled signal [$x(n)$] is obtained from the sampling process defined by [6]:

$$x(n) = x(t)|_{t=nT_s} \qquad n \in \mathbb{Z} \tag{2.1}$$

where T_s is the sampling interval and $f_s = 2\pi/T_s$ is the sampling frequency.

Biosignals can also be classified as being either deterministic or stochastic. Deterministic signals can be exactly described by mathematical functions or graphically. A stochastic signal is a broadening of the concept of a random variable by the introduction of variations along time [8], being considered as a sample of a stochastic process. As so, stochastic signals cannot

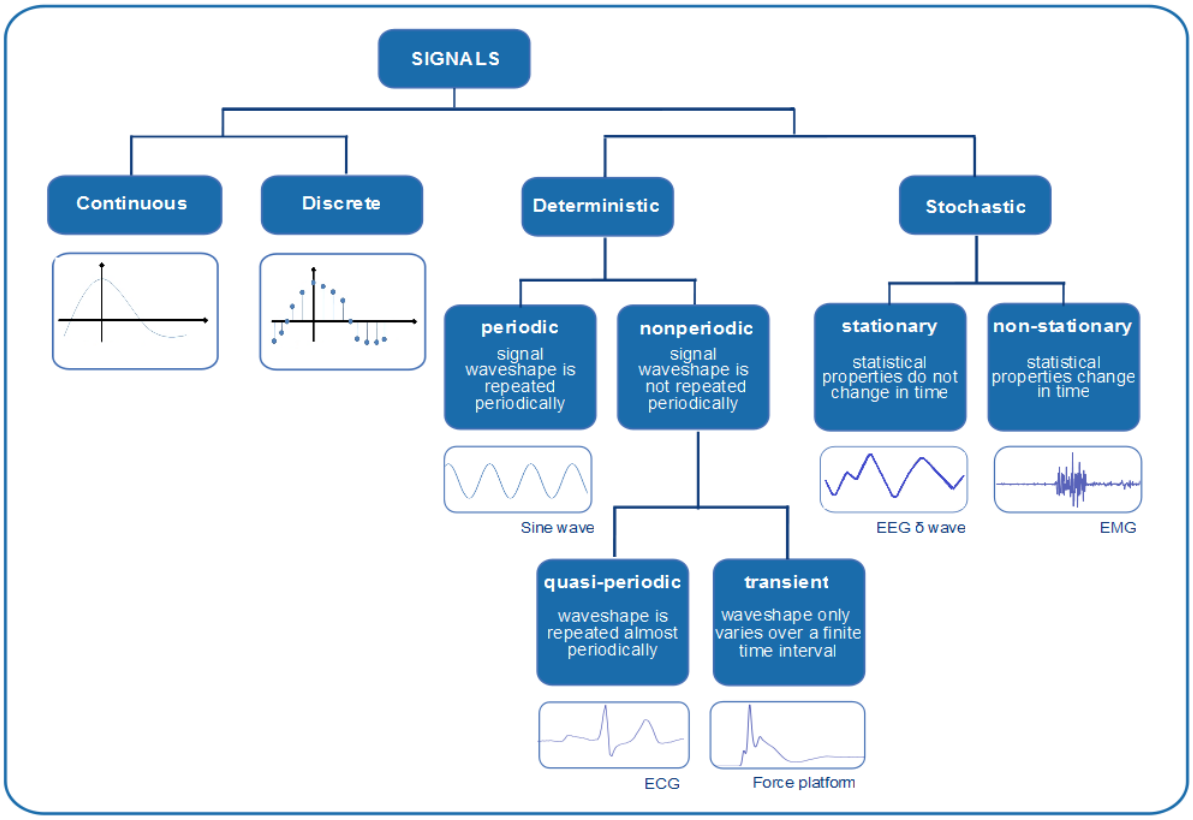

Figure 2.1: Biosignals classification according to the signal characteristics. Adapted from [6].

be expressed exactly and are described only in terms of statistical techniques as probabilities distributions or simple statistical measures such as the mean and the standard deviation [7]. Stationary stochastic signals are those for that the statistics or the frequency spectra remain constant over time. That is not usually verified and thus the most stochastic signals are non-stationary. Despite the fact that there is always some unknown and unpredictable noise added to the signals and that the underlying characteristics of a biosignal implies the possibility of some random parameters modification, rendering the signals nondeterministic, in practise there is often a signal modeling by means of a deterministic function [6].

Deterministic signals models allow their classification as periodic or nonperiodic. Periodic signals have a stereotyped waveform that repeats indefinitely. Considering that the waveform has a duration of T units (the period), the periodic signal verifies [7]:

$$x(t) = x(t + kT) \qquad k \in \mathbb{Z} \tag{2.2}$$

Nevertheless deterministic signals are mostly nonperiodic, being considered either as quasi-periodic (e.g. the ECG signal) or as transients, signals that vary only over a finite time interval and subsequently decay to a constant value as time progress. This research work focuses mostly on transient discrete biosignals that may be repeated either in a periodic

or non-periodic way.

2.1.2 Biosignals Acquisition

In order to extract meaningful information and understanding a particular physiologic system or event, sophisticated data acquisition techniques and equipments are commonly used. The fact that biomedical electronics must interface with a living body implies a unique set of safety requirements for those devices [8]. A blocks diagram representing the basic components in a bioinstrumentation system is shown in Figure 2.2.

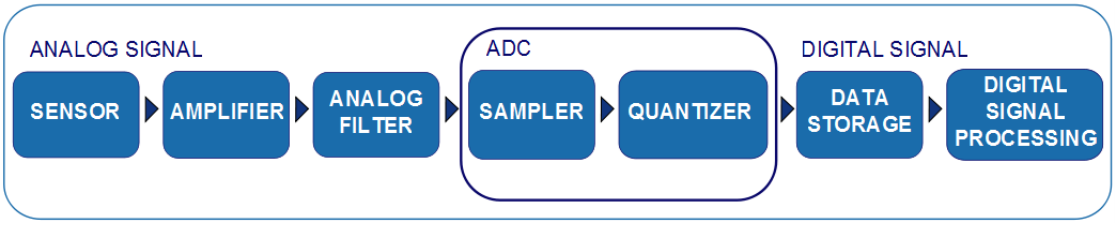

Figure 2.2: General acquisition procedure of a digital signal. Adapted from [6].

Biosignals are detected by using specific sensors which convert a physical measurand into an electrical output that can easily be treated, transmitted and stored. An analog preprocessing block is usually required to amplify and filter the signal, in order to make it satisfy some possible hardware requirements or to reduce the portion of undesired noise, while preserving the main information contained into the original waveform [6].

Analog-to-digital converters (ADC) are used to transform biosignals from continuous analog waveforms to digital sequences, i.e., series of numbers, discretized both in time and amplitude, that can be easily managed by digital processors. This conversion can be divided in two steps:

- **Sampling:** converts the continuous signal into a discrete time series, as described in sub-section 2.1.1. The sampling process must ensure that the continuous waveform can be perfectly reconstructed just from the series of sampled values [6]. This is accomplished by applying the sampling theorem, mathematically expressed by Nyquist. It states that a continuous time signal can be completely recovered from its samples if, and only if, the sample rate is greater than twice the original signal bandwidth B, i.e., its highest frequency component [5]:

$$f_s > 2B \tag{2.3}$$

- **Quantization:** assigns the amplitude value of each sample within a set of discrete values. The ADC resolution is related to the number of bits that are available for data storage. A quantizer with N bits is capable of representing a total of 2^N possible amplitude values. Typically, most ADC converters approximate the discrete samples with 8, 12 or 16 bits [7].

Biomedical acquisition systems are commonly connected to data storage devices, using one of the several available data transmission protocols [8].

2.1.3 Biosignals Processing

In general, biosignals information is not available directly from the raw recorded signals. Some additional processing is usually required to enhance the relevant information, which may be masked by other biosignals contemporaneously detected (endogenous effects) or buried in some additive noise (exogenous effects) [6].

Digital signal processing is concerned with the use of digital systems to analyse, modify, store or extract relevant information from digital signals [9], aiming at improving the understanding of the physiological meaning of the original parameters [7].

Techniques based on the extraction of waveforms features and estimation of spectral content are usually applied into noise reduction, artifact removal and extraction of information that may not be evident in raw signals. These features can be used for statistical analysis, trend detection or interpretation and classification purposes (further addressed in section 2.2) [8].

2.1.4 Biosignals Types

In this section the biosignals considered in this research work (electrocardiography, force, accelerometry and electromyography) are briefly described.

Electrocardiography

The electrocardiogram (ECG) is the recording, on the body surface, of the electrical activity generated by the heart. The heart muscle has four chambers; the two upper chambers are called the atria, and the two lower chambers are called the ventricles (Figure 2.3 a)). Located in the top right atrium there are a group of cells that act as the primary pacemaker of the heart [6]. Via a complex transformation of ion concentration in the membranes of those cells (source of continuous current), an extracellular potential field is created. The former excites the neighboring cells and propagates from one cell to the other, generating an electrical

event [8]. Because the body acts as a pure resistive medium, these potential fields extends to the body surface.

The ECG wave results from the electrical measure of the sum of the ionic changes within the heart. The observed waveform in the surface depends on the stimulated tissue mass and the current velocity [8]. A standard ECG pattern consists of a P wave, a QRS complex and a T wave (Figure 2.3 b)). P wave represents the atria depolarization and QRS complex is assigned to depolarization of the ventricles. Ventricular repolarization shows up as the T wave, while atrial repolarization is masked by ventricular depolarization [7].

A great research field within biomedical engineering is concerned about developing methods for acquiring and analysing ECG signals. Changes in the amplitude and duration of the ECG pattern provide useful diagnostic information. The length of time between QRS complexes also changes over time as a result of heart rate variability (HRV), also used as a diagnostic tool.

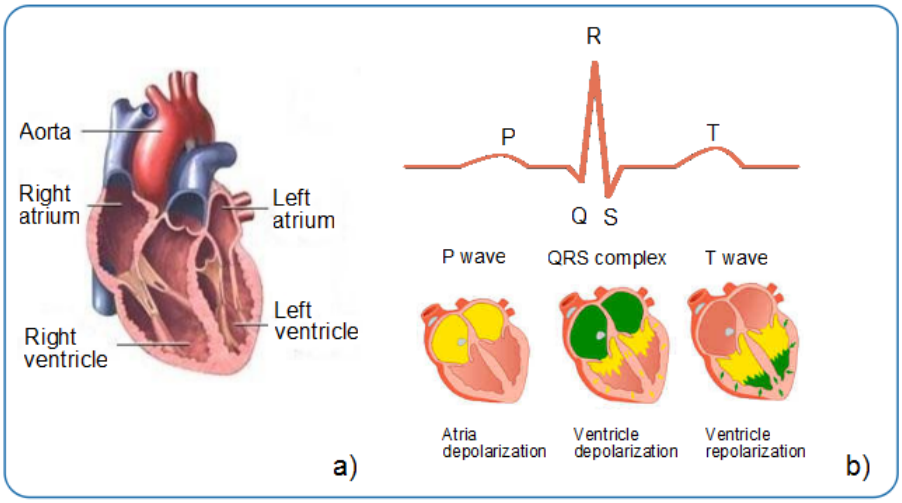

Figure 2.3: ECG signal principles: a) heart chambers b) ECG waveshape physiologic origin. Adapted from [10]

Force

Force is measured in a wide range of biomedical engineering activities, including gait analysis, implant development and testing, material property measurement, clinical diagnosis, and the study of structure and functional relationships in living tissue [8].

A common form of force sensor is the load cell. Apply a force to the load cell stresses its material, resulting in a strain that can be measured with a strain gauge. The strain is then proportional to the applied force (according to Hook's law) [6]. On the other hand, the three components of the ground reaction force vector, its point of application (i.e. the center of

pressure) and the vertical ground reaction torque are usually measured with force platforms embedded in the walkway [6]. A force platform is a rectangular metal plate with piezoelectric or strain gauges transducers attached at each corner to give an electrical output that is proportional to the force on the plate [11]. It can be useful when training stability of olympic shooters before pulling the trigger or training gymnasts during floor exercises by allowing the continuous monitoring of the center of pressure displacement below the feet [3]. In the context of strength and power assessment it is mainly applied to evaluate the performance of vertical jumps by athletes while standing on it (Figure 2.4), since jumping is generally used as a method of evaluation of reactive and explosive force in lower members [1].

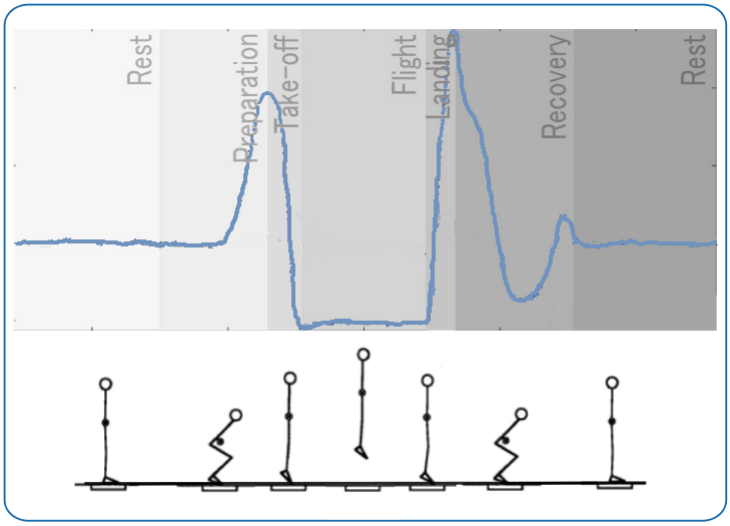

Figure 2.4: Illustration of the signal acquired from a force platform during the several phases of a counter-movement jump. Adapted from [12] and [11].

Accelerometry

Acceleration is the rate of change of either the magnitude or the direction of the velocity of an object, and it is measured in units of length per time squared (i.e., m/s^2) or units of gravity (g) (1 g = 9.81 m/s^2) [8]. Multiaxis accelerometers can be employed to measure both linear and angular accelerations (if multiple transducers are properly configured). Accelerometers are currently available with up to three orthogonal measurement axis (Figure 2.5). Velocity and position data may then be derived through numerical integration, although care must be taken with respect to the selection of initial conditions and the handling of gravitational effects. A three-dimensional (3D) accelerometer can also provide inclination information when not accelerated and, therefore, only sense gravity [4]. In that case, its sensitive axis pointing toward the center of the Earth will have an output equal to 1 g. This property is commonly used to calibrate the gain and zero offset of an accelerometer by positioning the

sensitive axis at a known angle relative to vertical and measuring the output [8].

Accelerometers are used in a wide range of biomedical applications. In motion analysis, e.g., lightweight accelerometers and recording devices can be worn by patients to study activity patterns and determine the effects of disease or treatments on patient activity [6]. Accelerometers are also widely applied on wearable systems for biomechanical analysis and assessment of physical activity. Being directly applied on the body segment to be monitored, those systems are also able to match the requirements of portability and user comfort in athletic performance evaluation usually not covered by the standard motion analysis instruments, such as force platforms [4, 13].

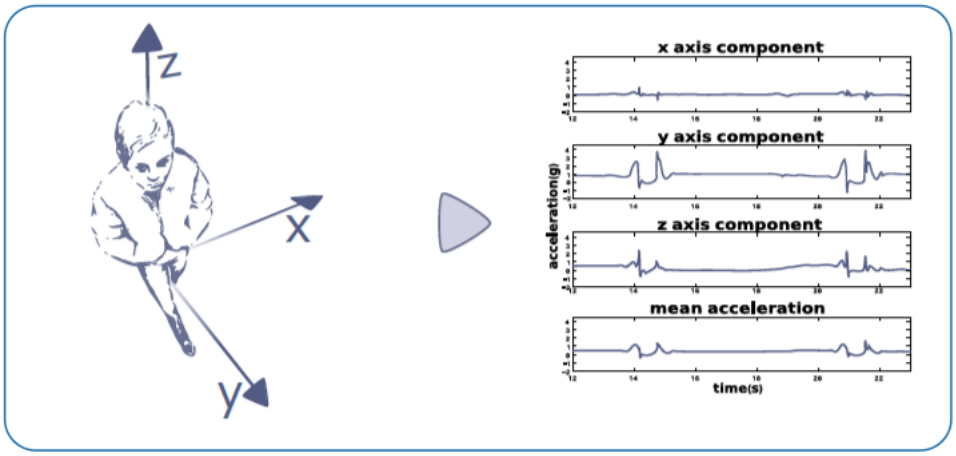

Figure 2.5: Acceleration signals acquired from the three axis components (x,y,z). The mean acceleration curve is computed by averaging the signal from each component. From [14].

Electromyography

Electromyography (EMG) signal arises from the flow of charged particles (ions) across the muscle membrane when its cells are electrically or neurologically activated. A set of muscle fibers innervated by the same motorneuron is defined as a motor unit. When a motor unit is recruited by the brain, the impulse (called action potential) goes through the motorneuron and to the muscle (Figure 2.6). EMG signal is typically obtained by measuring the action potentials from multiple motor units. The signal can be acquired either by fine wires inserted into muscle (intramuscular) or electrodes placed on the skin´s surface (surface EMG, sEMG) [6, 8]. In this dissertation the considered EMG signals were acquired by surface electrodes, even if not specifically referred as sEMG signals.

Data collection variables that affect the quality of EMG signal are the placement and the distance between recording electrodes, skin surface conditions, distance between electrodes and target muscle, signal amplification and filtering, and the rate of data acquisition [6].

Being an electrical recording of electrical activity in skeletal muscles, the EMG is generally used for the diagnosis of muscular disorders. Several authors have done a survey dealing with the relationship between the EMG signal and the related strength, coming to the conclusion that the root mean square (RMS) value of this signal has a close relationship with the exerted muscle strength [8]. Furthermore, it is possible to check the existence of exerted muscle strength and fatigue in frequency domain, e.g., with associated shifts for the median frequency in the EMG Power Spectral Density (PSD) [8, 15, 16].

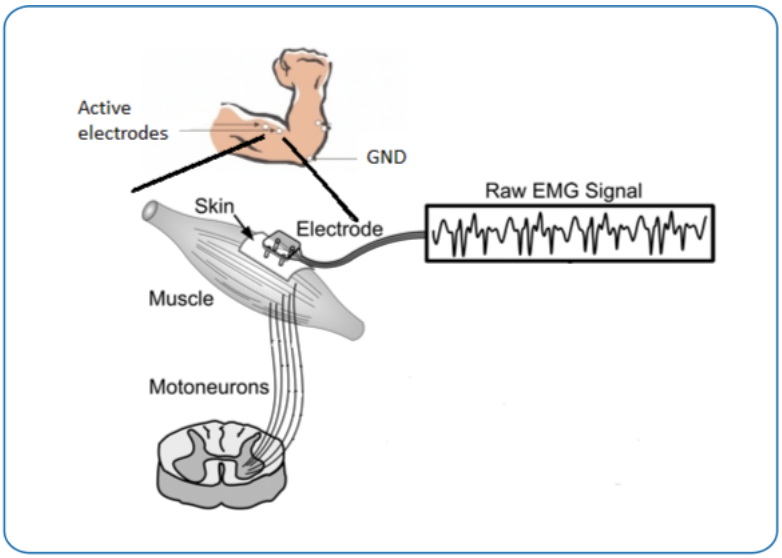

Figure 2.6: Surface EMG: after the action potential goes through the motorneuron and the muscle, it is collected by active electrodes at the skin's surface. A ground electrode is also necessary. Adapted from [17].

2.1.5 Statistical Concepts

Through this dissertation it is made reference to some statistical concepts that are standard when characterizing discrete-time signals. Following some brief definitions for those concepts are presented.

Considering a signal defined over a finite time window with length N and represented as time series $[x(n)]$, its **mean** (or expected value) corresponds to the average of all the values of that series [5]:

$$\mu = \frac{1}{N} \sum_{n=0}^{N-1} x(n) \tag{2.4}$$

The **variance** is used as a measure of how much the signal values are spread out from each other. It is computed as the average squared deviation of each value from the mean of the finite signal:

$$\sigma^2 = \frac{1}{N} \sum_{n=0}^{N-1} [x(n) - \mu]^2 \tag{2.5}$$

The **standard deviation** (STD) is the most commonly used measure of spread and it is defined as the square root of the variance.

A possible approach when trying to model a deterministic signal as a time dependent function is to use a **linear regression**, generally expressed by:

$$\hat{x}(n) = \alpha n + \beta \tag{2.6}$$

where α and β, the regression parameters, are computed in order to minimize the **mean squared error (MSE)**, a value that quantify the difference between the values implied by the linear regression and the true values of the original signal:

$$MSE = \frac{1}{N}\sum_{n=0}^{N-1}[x(n) - \hat{x}(n)]^2 \tag{2.7}$$

When modeling deterministic biosignals the use of a linear regression is restrictive. Therefore, a **polynomial regression**, by which the signal is modeled as a n^{th} order polynomial, may be a more accurate method of fitting a mathematical function to a time series data.

2.1.6 Synthetic Signals

Beyond being applied to the aforementioned biosignals, the tools developed in the context of this dissertation were also applied to synthetic signals, as part of the algorithm performance evaluation methodology. This sub-section presents the general mathematical formalism followed while defining those signals.

Synthetic signals are constructed by concatenating sections with predefined mean and STD values (referenced as zones, Z_i). In Figure 2.7 a block diagram outlining that construction process is presented. The mean values are given by float numbers, u_1, randomly sampled from a standard normal distribution and then multiplied by a factor m. The STD values are obtained by multiplying a random number u_2, sampled from a uniform distribution, within the interval $[0, 1]$ by a factor s.

Between those zones, transition events with known, randomly selected starting and ending points are also considered. Minimal values for mean and STD differences between successive zones are imposed and assigned to the m_d and sd_d variables, respectively. Thus, a new zone Z_i is rejected unless the following condition is verified:

$$|mean(Z_i) - mean(Z_{i-1})| \geq m\_d \bigwedge |STD(Z_i) - STD(Z_{i-1})| \geq sd\_d \tag{2.8}$$

Furthermore, before being added to the already constructed signal, the new zone is seg-

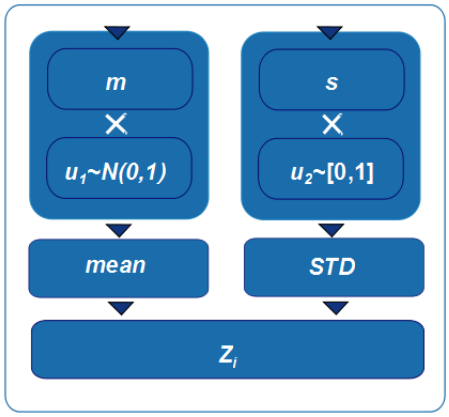

Figure 2.7: Blocks diagram describing the construction steps of a new zone to include in a synthetic signal.

mented into slices (Z_i^j) with 10% of the its length. Then, it is assured that mean and STD differences equal or bigger than m_d and sd_d, respectively, are not verified between successive slices within a zone:

$$|mean(Z_i^j) - mean(Z_i^{j-1})| \leq m\_d \bigwedge |STD(Z_i^j) - STD(Z_i^{j-1})| \leq sd\_d \tag{2.9}$$

Otherwise, the new zone is rejected. Depending oh the chosen m_d and sd_d parameters values, the aforementioned restrictions allow the successive zones of synthetic signals to be, or not, clearly distinct in terms of mean and STD values, without much variability of those parameters within each of the individual zones.

2.2 Events Detection and Signals Segmentation

Automated techniques for generating, collecting and storing data from scientific measurements have become increasingly precise and powerful. However, there is still a practical need to improve forms of data-mining, allowing the detection of specific events, the extraction of signals patterns, or even for distilling the scientific data into knowledge in the form of analytical natural laws [18].

The implementation of biosignal pattern recognition and interpretation systems must include the extraction of signal features (as structural characteristics or transforms) that are important to pattern classification [19]. Those can then be used either for comparison with stored data (allowing pattern detection, discrimination or classification) or for estimation of pattern parameters [19]. Since a large amount of data can be generated when considering these measurements, it should also be intelligently analyzed and archived to be most useful [20]. As so, the pattern parameters estimation can also play an important role towards

this end when applied to data compression algorithms [19].

An usual approach to recognition-oriented signal processing consists of using an automatic signal segmentation as the first processing step. This process can be described as the automatic segmentation of a given signal into stationary (or weakly nonstationary) segments, which length is adapted considering the local properties of the signal [21] and the analysis scale that is considered. The main goals are therefore the detection of the changes into the local characteristics, the estimation of the time points where the changes occur [21], and most of all have the ability to automatically distinguish between meaningful and insignificant changes.

2.2.1 Signal Events

An event is broadly defined as the change in state of the system under study [19]. After that the events are well marked on a signal representation of the system state, the respective patterns can be accessed by infering either the structure (a deterministic characterization of signal form, e.g. geometric and angular relationships) or the trend (the way in which a specific type of structure, expressed as the magnitude of the respective reference variables, changes in space or time) [19,22]. In the biosignals context the events could be e.g. heartbeats, EMG activations or even particular directed thoughts, for brain-computer interfaces (BCI) [23].

Despite the fact that pattern analysis problems in general, and the events detection in particular, become trivial under carefully controlled conditions, in practise that is not usually verified [19]. Biosignals are often nonstationary, being characterized by oscillations at specific frequencies, and contaminated by *in-band* noise, which is both periodical and stochastic [24]. These issues are particularly important when considering the application of these algorithms in signals acquired from portable devices: the artifacts caused by increased movement and the requirements for unobtrusive measurements causes the signal quality to be reduced compared to that achieved when performing measures in a laboratory environment [25]. Furthermore, there are many types of events (and we may be only interested in some of them) and the relationship between the actual event and the signal resulting from it may be quite complex, and often partially characterized.

Finding events in noisy signals is considered as a fundamental task throughout physics and particularly the biosignals analysis research field [23]. The main desired properties of an events detection and signal segmentation algorithm are few false positives and missed detections, and the low detection delay in the case of a real-time implementation [21]. Following, two of the main biosignal structural characteristics for that an event detection algorithm

should be able to mark clealry the change points (the determination of signal activation onset and the general transients detection) are presented. Some of the respective standard detection algorithms are also reported.

Onset

The accurate biosignals onset determination is useful in several studies of motor control and performance. It is widely applied on neurosciences studies with kinematic data analysis, allowing the extraction of several parameters such as the reaction time or the peak velocity time. Single-threshold velocity or acceleration methods are usually applied [26, 27]. These are, however, very sensitive to weak and abnormal response profiles, typical of some central motor disorders, introducing variability and systematic errors into the results. As such, more accurate onset detection methods have been proposed.

Gerhard Staude [26] introduced a model-based algorithm that comprises an adaptive whitening filtering step followed by a Log-Likelihood-Ratio test to decide whether a significant change occurred and estimate the change time. Despite the accuracy of this method and the possibility of improving its results by including *a priori* knowledge on the physiological background of the measured signals, it requires extensive modeling and computation. Less complex approaches have been developed, e.g. the onset detection method proposed by Botzen et al. [27]. This method employs a deterministic motor control model and a linear regression to estimate the change-point between a static and a movement phase, both of which are assumed to be corrupted by normal zero mean Gaussian noise.

When considering applications such as neurological diagnosis, neuromuscular and psychomotor research, sports medicine, prosthetics or rehabilitation it may also be important to measure the time difference between the muscle activation and the movement onset [27]. Furthermore, in order to allow comparisons between different muscles, experimental conditions and subjects, the accuracy of burst onset, duration and offset determination for EMG activity is crucial [28].

A comparative study regarding several methods for EMG signals onset detection is reported by Staude et. al [29]. The basic processing stages of all the analysed standard detection methods, for which a blocks diagram is represented in Figure 2.8, are:

- Signal conditioning: applied to reduce the high frequency noise;
- Detection unit: comprises a test function ($g[k]$) computed from the pre-conditioned signal and a decision rule. For each signal sample, X_k, the test function uses an intermediate signal within a window of N past samples. This function is then analysed by

the decision rule (which compares it with a specific threshold h) to determine when a change in the muscle activation pattern occurred;

- Post-processor: estimates the exact change time ($\hat{t_0}$) after that an event alarm (t_a) has been given by the detection unit processing stage.

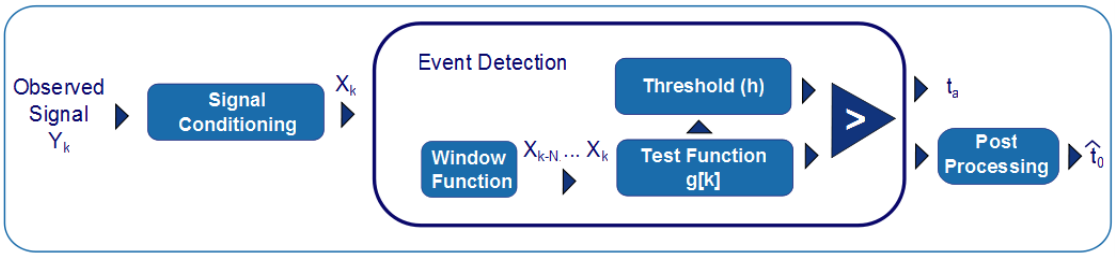

Figure 2.8: Typical onset detection scheme. Adapted from [30].

Apart from the intuitive but error-prone visual inspection, the simpler computational method approached by that study is the threshold-based Hodges detector [28]. After applying a lowpass filter to the rectified EMG wave, this algorithm computes the point where the mean of N signal samples exceeds the baseline activity level (the signal average value considering a samples segment prior to stimulus) by a specific number of standard deviations. As well as for other simple threshold-based methods, their results are highly dependent on the selected parameters (particularly the threshold level and the lowpass filter cutoff frequency). As such, Hodges detector is particularly suited to apply in high SNR conditions [29].

In conditions of low SNR the use of an adaptive pre-whitening filter, as proposed by Bonato [31], proved to be superior than a less specific lowpass filter [29]. Other model-based approaches based on statistically optimal decision rules are also compared. Despite their bigger accuracy, those methods depend on the *a priori* knowledge (or estimation) about the variance profiles before and after the change to be detected, being more complex and time-consuming than the previously referred algorithms [29].

Transients

Signal transients can be considered as a wider events class which are characterized by a sudden change into signal properties, such as the amplitude or the frequency, and with a short duration if compared to the observation interval [32].

Very important measurement information is often associated with the transients [33]. Abrupt changes or discontinuities encountered in biosignals may be symptomatic of functional disorders [34]. Thus, the ability to detect them is very important in medical prediction process [35]. On the other hand, disturbing sources sometimes produce undesired transients,

which corrupt the waveform to be analysed. In order to carry out an accurate measurement of the waveform and to identify probable sources and causes for those transients, they should be detected and also measured in terms of significant parameters such as duration and amplitude, possibly in very low SNR conditions [33].

Given their relatively short duration (considering all the signal observation interval), transients influence into the signal spectrum is limited [34]. Therefore, the standard methods for transients detection are mainly based on time-frequency analysis with the use of the *Wavelet transform* [32, 36]. The *Continuous wavelet transform* assures a good time resoultion that allows the evaluation of transients arrival times and their duration; the disembodying of the transient from the global waveform, for posterior parameters extraction, is achieved by performing a proper decomposition and a subsequent reconstruction of the original signal in frequency subbands by means of the *Discrete time wavelet transform* [32].

The present research work followed an alternative approach, by identifying time domain specific morphological parameters that can clearly distinguish those events from the complete observed signals. This chapter presented the base concepts that will be used in the following sections in order to describe the implementation and evaluation of the developed events detection algorithm.

Chapter 3

Events Detection Algorithm

In this chapter the events detection algorithm developed in the context of this dissertation is presented. The first section approaches the adopted mathematical formalism and the processing steps concerning its implementation are presented in section 3.2. Section 3.3 introduces the events detection algorithm real-time implementation approach.

3.1 Mathematical Formalism

3.1.1 Events and Signal Modeling

For a given signal defined as a time series, $x(t)$, with $t = 1, 2, ..., L$, a set of regions is created by slicing the signal. Considering E as the total number of events, a general event slicing signal regions is denoted by $e_i,\ i = 1, 2, ..., E$. According to the adopted notation e_1 and e_E are, respectively, the first and the last events of the considered time series. The complete modeled signal is expressed as defined in equation 3.1, for which further notation is described below:

$$\hat{x}(t) = \sum_{i=0}^{E-1} Q\Big(\frac{t}{e_{i+1} - e_i} - e_i\Big) M(t - e_i, A_i, \varepsilon) \tag{3.1}$$

$Q(t)$ is an unit pulse function expressed by:

$$Q(t) = \begin{cases} 1 & if \quad 0 \leq t \leq 1 \\ 0 & \text{otherwise} \end{cases} \tag{3.2}$$

Considering $\frac{t}{e_{i+1} - e_i}$ as the argument of this function, the time interval in which $Q(t) = 1$ corresponds to the signal segment length between those events. Subtracting e_i, that pulse is shifted to higher values in order to be aligned in time with the defined segment.

$M(t, A, \varepsilon)$ is a polynomial regression model defined by:

$$M(t, A, \varepsilon) = A(t) + \varepsilon \tag{3.3}$$

where A is the matrix with n polynomial parameters for a given signal region $(A(t) = a_0 + a_1 t + a_2 t^2 + ... + a_n t^n)$ and ε is an error term that is assumed to follow a normal distribution $(\varepsilon = N(\mu, \sigma^2))$ with $\mu = 0$.

After modeling the signal as described above, each one of the $E - 1$ signal segments can be described as:

$$\hat{x}^i(t) = \hat{x}(t)|_{t \in [e_i, e_{i+1}]} \tag{3.4}$$

3.1.2 Events Computation and Stopping Criteria

The set of events detected within a given signal are the result of an iterative process that considers different stopping criteria in order to return an optimal solution:

- **Maximal standard deviation gradient:** this parameter is evaluated by computing S, defined as the sum of the absolute standard deviation differences between successive segments $\hat{x}^i(t)$ within a signal:

$$S = \sum_{i=1}^{E} \left| std(\hat{x}^i(t)) - std(\hat{x}^{i+1}(t)) \right| \tag{3.5}$$

- **Minimal MSE**: the fitting quality of the applying model is also considered by computing D, defined as the sum of the mean squared error values through the successive regions (with length N_i):

$$D = \sum_{i=1}^{E+1} \left[\frac{\sum_{t=0}^{N_i} (x^i(t) - \hat{x}^i(t))^2}{N_i} \right] \tag{3.6}$$

- **Maximal number of events.**

The optimal solution is achieved by varying a set of implementation parameters P, further described in Section 3.2.2. P parameters include the length of the signal slices from which to compute a standard deviation difference sequence and a multiplying factor that affects the length of the moving average window considered in the smoothing filter to apply on the first derivative of that sequence. Another factor that will define the threshold to consider when computing the maximums and minimums within the resulting sequence is also included.

Those parameters are then iteratively changed in order to fulfill the following condition:

$$\underset{P}{\text{ArgMin}}[D - S - E] \tag{3.7}$$

3.2 Implementation

The following sub-sections introduce the main processing steps implemented in order to approach the mathematical formalism decribed in section 3.1. The algorithms were designed using Python programming language, with the Numpy [37] and the Scipy [38] packages.

3.2.1 Algorithm Design

The main goal of this algorithm is the signal segmentation into clearly distinct zones, by an accurate estimation of the time points in which significant changes into signal local features occur, as exemplified in Figure 3.1.

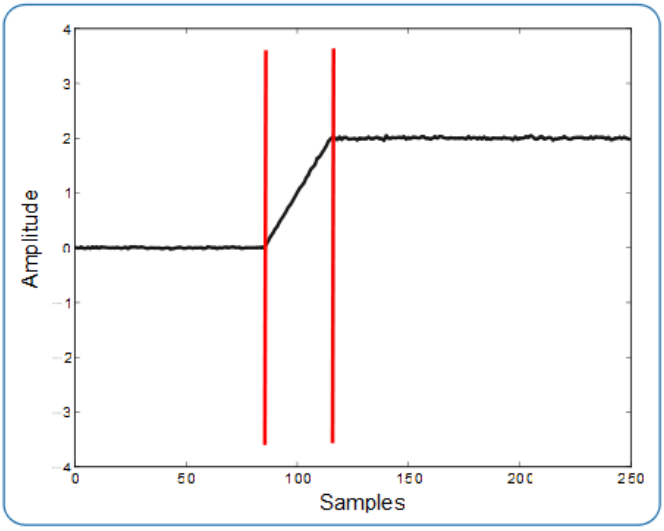

Figure 3.1: Example of a synthetic signal with marked events.

Those changes are evaluated by quantifying the differences between the standard deviation of successive regions within the signal. The sets of regions for which that differences are more pronounced are marked within the signal, being these marks called as notable points. The events definition is then achieved by applying a more accurate evaluation within those regions.

The `get_events` algorithm is the base function to identify the signal events. This algorithm was developed on a signal-independent basis, requiring no previous knowledge or

specific preprocessing steps. Nevertheless, beyond the signal, it can receive other parameters, by input, in order to run auxiliary functions (Table 3.1) responsible for each of the processing steps described below .

Table 3.1: `get_events` algorithm auxiliary functions

Function	**Input**	**Output**
`get_slices_std`	signal *slices_length*	STD sequence
`adjust_peaks`	signal *slices_length* peaks peaks_type	adjusted_peaks

The auxiliary functions input parameters are given during the optimization phase (described in section 3.2.2) and not directly by the user. Figure 3.2 shows a block diagram for `get_events` algorithm, which integrates either the input and output parameters, as well as the referred auxiliary functions. In Figure 3.3 the first processing steps of this algorithm applied to the signal on Figure 3.1 are graphically represented.

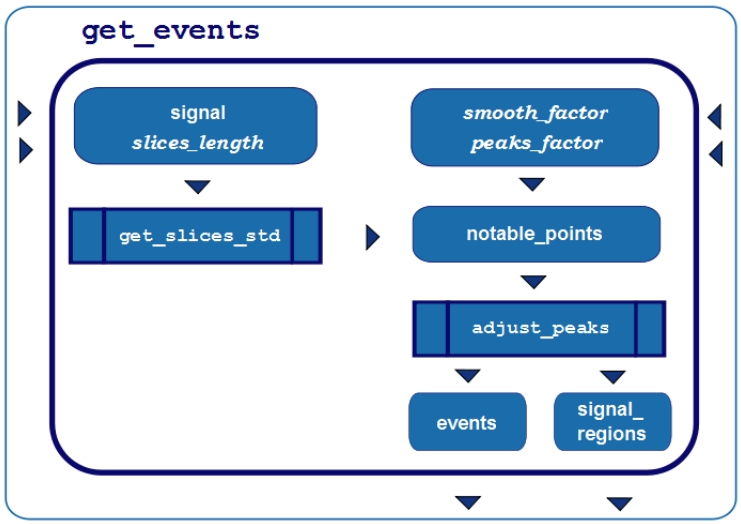

Figure 3.2: `get_events` algorithm flowchart diagram. This algorithm receives the signal and the *slices_length*, *smooth_factor* and the *peaks_factor* parameters as input. After slicing the signal, by applying the `get_slices_std` auxiliary function, its notable points are computed. The `adjust_peaks` auxiliary function is then applied to compute the events and the signal regions between those points, returned by this algorithm.

Signal Morphological Analysis

From a raw signal, the `get_slices_std` function divides the signal into slices with a defined length (*slices_length* in Figure 3.2), with exception for the last slice, that may be smaller (Figure 3.3 a)). This function returns an array containing the sequence of the successive

STD.

The signal morphological analysis follows by computing the first derivative of the standard deviation sequence previously defined. By analysing the resulting sequence (to select the signal notable points, as following described) the developed algorithm is able to perform a preliminary identification of the signal regions where the greatest pattern variability is verified.

The number of samples considered in each signal slice must always be bigger than 1. In practise, however, the number of samples in each slice should be bigger to allow the algorithm to distinguish natural random fluctuations from symptomatic tendencies. By default, that value is set to a minimum of 10 samples.

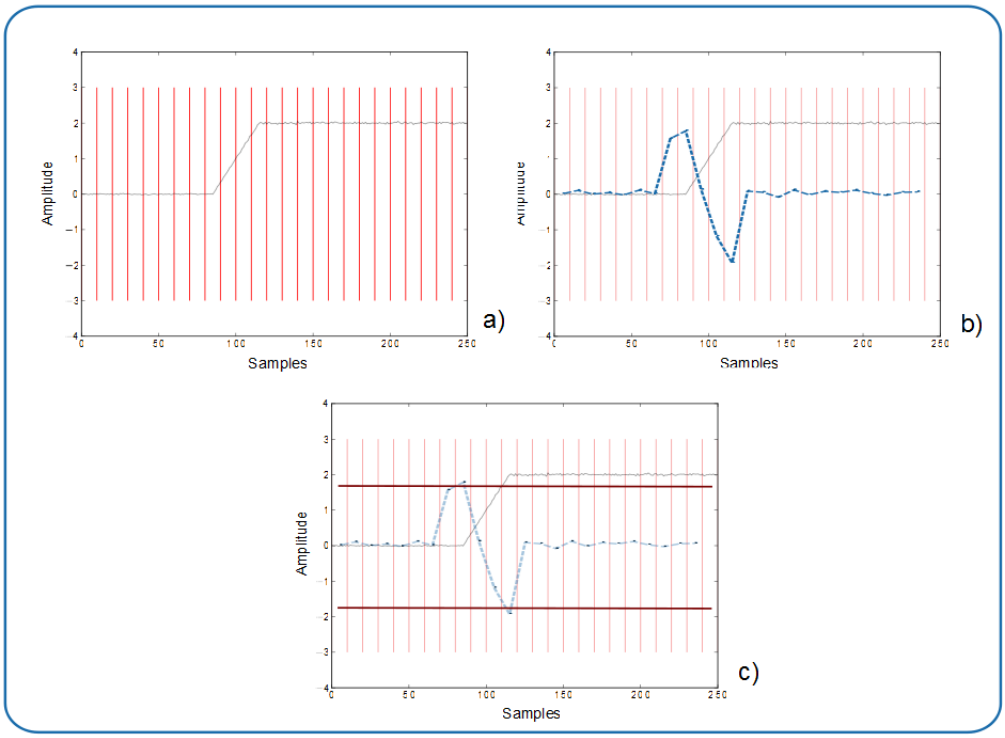

Figure 3.3: Illustration of the `get_events` algorithm first processing steps: a) Signal slicing; b) Smoothed STD sequence; c) Notable points selection.

Notable Points Selection

After the first derivative of the STD sequence is obtained, the resulting sequence is low-pass filtered. A smoothing filter, in which the number of points considered into the moving average window depends on the length of the sequence multiplied by a specific input ($smooth\_factor$) of this algorithm (Figure 3.3 b)), is applied.

The signal notable points (notable_points in Figure 3.2) are defined at the beginning of the slices where the correspondent filtered sequence points are computed as maximums/minimums

found above/below a specific threshold (Figure 3.3 c)). The former is defined multiplying the absolute sequence maximum/minimum by the $peaks\_factor$ input parameter (Figure 3.2).

Events Definition

After the preliminary signal notable points are computed, the `adjust_peaks` function is applied to these points aiming at an accurate events detection within the slices from which those were selected. This function receives the signal, the peaks, the considered peaks type (maximums or minimums) and the *slices_length* as input. For each peak this function considers the signal slice beginning in that point and then applies the `get_slices_std` algorithm on that signal segment (with a fixed *slices_length* of 5 samples). If a maximum peak is considered, it is then replaced by the point that maximizes the difference on the computed STD sequence. For minimums the procedure is analogous. This processing step ensures a more accurate events detection, with a minimum error of 5 samples.

At the end, the `get_events` algorithm returns the detected events and an array with the successive signal regions between those events.

3.2.2 Optimization Process

An optimization algorithm was defined, based on a iterative computation of the signal events by applying the `get_events` algorithm with a set of different input parameters. An optimal solution is returned with the set of parameters for that the stopping criteria defined in section 3.1 are better fulfilled. This is accomplished by applying the `get_opt_events` algorithm, for which a flowchart diagram is represented in Figure 3.4.

Parameters Range

The *slices_length* parameter range is defined by considering the signal length (L) and including increasing values (raising by one unit) between m and M, defined as follows:

$$\begin{cases} m = L/1000, & \forall\ L \geq 10^4 : m \geq 10 \\ M = m + L/100, & \forall\ L : M \leq 40 \end{cases} \tag{3.8}$$

As previously described the number of samples in each signal slice must be significant to allow the algorithm to evaluate if a change into the morphology should be marked as an event. Nevertheless, an excessive slices length can reduce the algorithm ability to distinguish two successive events if those are to close from each other. As such, for signals with less than

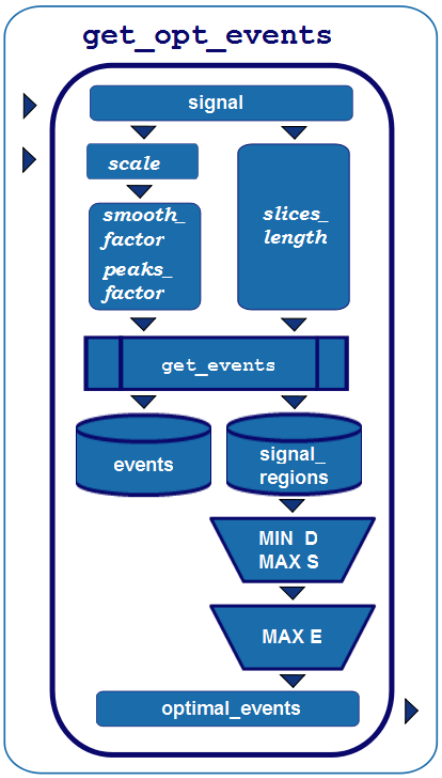

Figure 3.4: `get_opt_events` algorithm flowchart diagram. This algorithm performs the events detection optimization process. Its input parameters are the signal and the *scale* factor (optional). From those, $slices\_length$, $smooth\_factor$ and $peaks\_factor$ ranges are defined and the `get_events` algorithm is applied considering each combination of those input parameters. The solution that better fulfill the optimization criteria is then selected and returned by the `get_opt_events` algorithm.

10.000 samples m is set to 10. The upper limit is set to a maximum of 40 samples.

The following processing steps allow the algorithm to define the $smooth\_factor$ and the $peaks\_factor$ parameters range to be considered into the iterative optimization process:

- The signal is normalized dividing each sample by the mean value of the considered time series. From the resulting signal, for which the mean value is equal to 1, the standard deviation is computed and assigned to a specific variable (sm). By applying the normalization procedure it is ensured that the sm value does not depend upon the signal offset and only express its variability;

- A scale factor is also defined dividing L by successive higher powers of 10 until a value lower than 1 is reached. It can alternatively be given as an input, allowing the user to choose the level of detail, related to the minimum pattern discontinuity magnitude that will turn it into a detected event;

- A range specific factor, f, is also defined in order to compute its inner (i) and upper (u) limits as follows:

$$\begin{cases} i = \frac{f_i}{sm} \times scale \\ u = i + \frac{f_u}{sm} \times scale \end{cases} \tag{3.9}$$

Both $smooth\_factor$ and $peaks\_factor$ ranges limits follow the formalism described in equation 3.9. The considered f_i and f_u for each range are presented in Table 3.2, as well as the maximum values allowed for each limit.

- The step values are similarly defined for both the $smooth\_factor$ and $peaks\_factor$ ranges by analysing their inner limit values. In each case, if i is lower or equal to 0.1 the range step is 0.05. Otherwise, a step of 0.1 is considered.

Table 3.2: Specific parameters for $smooth\_factor$ and $peaks\_factor$ ranges.

	Inner limit		Upper limit	
	f_i	max	f_u	max
$smooth\_factor$	0.5	0.2	10	0.5
$peaks\_factor$	1	0.2	10	0.5

The followed implementation approach performs the $smooth\_factor$ and $peaks\_factor$ ranges shifting and expansion depending upon the scale factor and the global signal variability, represented by its normalized standard deviation value (sm).

In general, the range values vary inversely with the sm values. For a given signal, when a significant variability is verified in specific regions, rendering high sm values, the events detection is straightforward. As such, the moving average window to be considered when applying the smoothing filter to extract the signal notable points should be relatively small to ensure the detection accuracy is not compromised. Likewise, and since those notable points are clearly pronounced, the considered threshold levels when performing their selection are not to high, to avoid some possible missing detections.

In conditions of low sm values, the detection of significant pattern discontinuities may be more complex. Therefore, both the smoothing moving average window length and the threshold levels previously described should raise to avoid a false positive events detection.

Optimization

When considering global optimization problems, iterative methods are usually applied. In general, these techniques approach the solution through a series of guesses - where each successive guess is (usually, but not always) better than the previous one [39]. The basic and

perhaps most natural optimization approach passes by evaluating all the parameters domain, performing an exhaustive (or brute force) optimization. This method tests each potential solution, so the best combination of factors can be found [40, 41]. Following this exhaustive search model, all the experiments are conducted before any judgment is made regarding the optimal solution [42].

Alternatively, some searching techniques follow a different approach, by which the optimization is made sequentially (each new choice for the best solution is gathered from the preceding choices [39]). The Simulated Annealing [43, 44] and Step Size Algorithms [40] are examples of sequential optimization methods. Genetic algorithms, based on the mechanics of natural selection and genetic, are also widely applied [40, 45].

In general, exhaustive optimization is relatively inefficient compared to sequential search or genetic algorithms approaches, mostly because the time required to perform it is dramatically increased when the number of parameters increase [42, 45]. However, if the number and domain of those parameters is finite and relatively small, an exhaustive search is a simpler and reasonable approach [40]. Therefore, that was the methodology adopted at the optimization phase of the presented events detection algorithm.

For each set of parameters the `get_events` algorithm is applied. The results are then selected, applying the optimization criteria defined in sub-section 3.1.2. Either the solutions that have the minimum total MSE, considering all the signal segments modeled as 1^{st} order polynomials, or the maximum total standard deviation differences between those segments are selected in the same step. From those, the one for which the number of events is maximal is selected as the optimal solution.

3.3 Real-time Implementation

This section introduces a real-time signal processing application developed during this research work. The standard real-time processing constraints and the adopted events detection algorithm implementation approach are also discussed.

3.3.1 Real-time Signal Processing Tool

This appliaction for real-time signal processing was built on a general-purpose and object-oriented programming basis. It was developed using Python programming language (version 2.6.5.6) [46] with the Numpy [37], the Scipy [38], the wx [47] and the matplotlib [48] packages. The application uses the WXAgg backend [49] which comprises the WX Graphical User In-

terface (GUI), from matplotlib, together with the Antigrain drawing toolkit [50].

The signal acquisition is performed by bioPLUX research units [51]. The developed application uses a Python Application Programming Interface (API) available together with the bioPLUX unit, in order to control whether the device is acquiring the data and obtaining the digital raw signals from its several channels. By allowing the acquisition from up to two bioPLUX research units, this tool enables the data from sixteen independent sensor sources to be collected, visualized and processed in real-time. Both the raw and processed data can also be saved in text files for post-processing.

The objected-oriented programming approach allows a clear distinction between independent structural elements within the program, called as blocks. These are classes which may also use objects instantiated from other classes, in such a way that the blocks and the respective parameters are easily configured by the user. The organization and the data flow between the several blocks are described in Figure 3.5. Following this architecture and a brief description of the several structural blocks is reported.

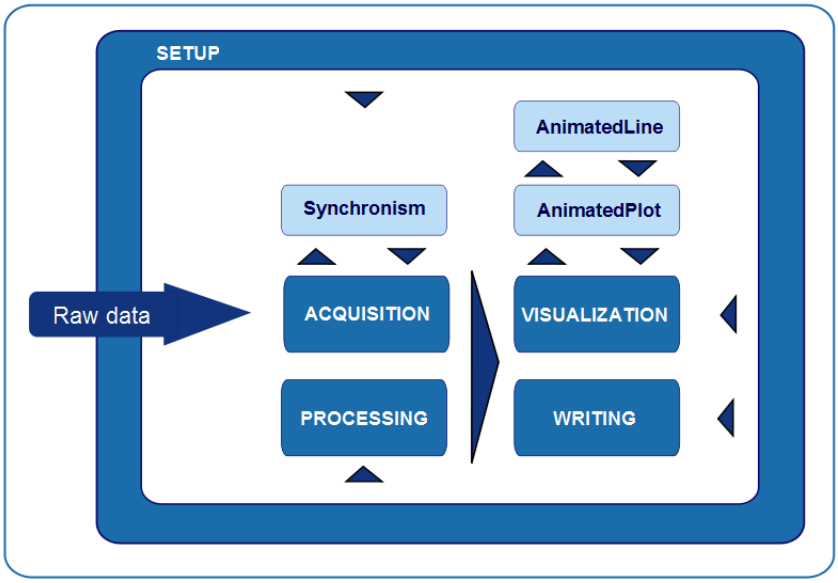

Figure 3.5: Real-time processing application: blocks description and data flow.

Structural Blocks Description

Acquisition class allows the connection to the bioPLUX units (by applying the Python API proper commands), the beginning of the acquisition and the repetition of this process at a user configurable rate. That rate defines the number of acquisition frames collected at a single time from the bioPLUX unit buffer, which are sequentially addressed to a specific variable, used as an input for the visualization, processing and writing blocks. This variable is a tuple in which each element is also a tuple with values corresponding to an acquisition

frame (or to the concatenation of the acquisition frames from two devices, if applicable). The acquisition end is also applied by a specific method of this class.

If the data from two bioPLUX devices is acquired, this block also calls an auxiliary Synchronism class. When the acquisition begins the main method of this class is able to find the time lag between the signals from both devices, by reading their digital port data (previously set with the same output value by successive commands execution). This lag is eliminated by acquiring and discarding the same number of frames only from the delayed device.

Visualization class is responsible for creating the GUI main window by instantiating an object from an auxiliary class (AnimatedPlot). The several subplots elements are then added in a predefined sorted way and the methods that perform the signal updated plot are also called in this block.

When using a matplotlib GUI to build animated plots, the basic approach passes by creating a figure and a correspondent callback function that updates it, which is passed to the specific GUI idle handler or timer [49]. In this application the AnimatedLine class allows the creation of the first lines to be plotted in each subplot element, defining the respective axis scales. This class includes also the necessary methods to update those lines with new data, as well as designing animated vertical markers above those lines. Those methods are then applied by a function of the AnimatedPlot class.

An higher performance on signal plotting is achieved, when applying the specific AnimatedPlot class method, by drawing a background and animating the necessary plot elements on top of it in each updating loop, as proposed in [49]. By default, the signals are only partially updated by the same predefined amount of samples (the same as the acquisition rate), but keeping a static background, in order to enable the visualization of its progress over time. It is also possible to obtain the visualization of the whole signal, updated at each loop, what is useful, e.g., when representing the signal spectrum (computed by applying the specific Processing block method).

Either the subplots labeling (according to the bioPLUX number, as ordered by the user when configuring the application, and the respective channel number, as exemplified in Figure 3.6) and sorting are assigned to the visualization class. The subplots sorting is done according to the following rules:

- The subplots are sorted primarily according to the bioPLUX device number and, between those, according to the channel source (Figure 3.6 a), c) and d)).

- If some processing is also required by the user the result is plotted, by default, after the correspondent raw signal position, whether the former is asked or not (Figure 3.6 b) and e)).
- The results of algebraic operations between signals is an exception, being always plotted after all the raw and processed single channel data (Figure 3.6 f)).

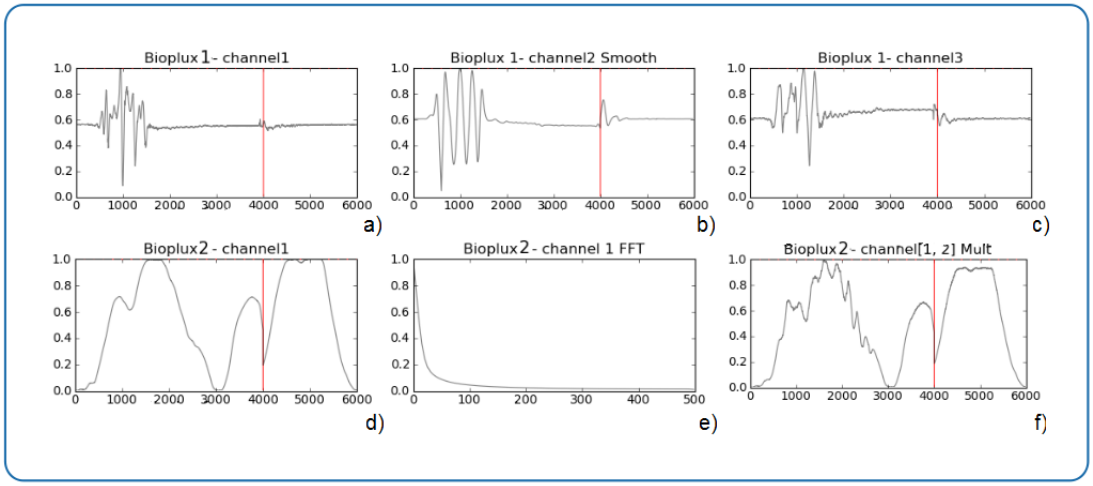

Figure 3.6: Real-time processing application GUI main window

Writing class allows the user to save the data acquired from the bioPLUX devices into a text file, so it can be post-processed. The data is presented in a column format. Each column contains the data from one of the selected channels. The order the data from the several channels is placed, as well as the information about from what bioPLUX device it belongs is explicit into the file header.

If some processing is required by the user the processed data is also written, by default, in successive columns after those that contain the raw data. The correspondence between each column and information about from what channel that processed data was originally acquired and what type of processing was performed is also provided in the header part of the file.

Processing the acquired data in real-time is the main feature of the developed application. Since the basic processing is done directly over the acquisition frames available at each updating loop, it is ensured no time lag between the raw and processed visualized data.

After the acquisition block returns the tuple containing the several acquisition frames, the processing block methods are responsible for selecting the signals to be processed, according to the parameters set by the user. Then, the specific processing is performed over each signal

and the result is also included on the original data tuple in order to be visualized and saved by the respective application blocks, as previously described.

The processed data management is common to all the basic processing functions, whereby this architecture is customizable and the application can be easily tailored to include other processing methods. Some of the basic signal processing already available includes a smoothing filter (with a default moving average window with length equal to half the number of acquisition frames), the FFT computation and basic algebraic operations between signals of different acquisition channels.

Setting up the developed application is an intuitive task, since its architecture allows an easy configuration of all the structural blocks and the respective parameters set.

In Figure 3.7 it is represented a possible implementation configuration which must be included into the Main part of the application. The `ACQ_FRAMES` parameter defines the number of acquisition frames collected at each update loop. `SOURCE_BIOPLUX` is a list containing between one and two bioPLUX research units MAC addresses, depending upon the number of devices from which the application is collecting data.

`BLOCKS_EXECUTION` is a list in which each element is also a list with a predefined structure that includes the following elements:

- `IN` and `OUT` (input and output variables): after the acquisition block execution, the output variable contains the data acquired from the bioPLUX devices. This variable is then given as input and returned as output, after the processed data is concatenated, through the several processing blocks methods execution. It is finally provided as input to the visualization and writing blocks. The writing block output variable is the name of the text file in which the data will be saved;
- `B`: blocks (or processing block methods) description;
- `BP`: a list containing the bioPLUX devices number (in accordance to the order of `SOURCE_BIOPLUX` list);
- `CH`: a list in which each element represents the analog channel from the corresponding bioPLUX device at the same `BP` list index.

The previously described setup steps can also be easily adapted in order to be configured and executed from specific commands to include into the already defined GUI. That update will certainly be accomplished in a following version of this application in order to improve its user-friendly features.

```
ACQ_FRAMES = 200

SOURCE_BIOPLUX = ['00:07:80:42:0F:92','00:07:80:40:DD:C8']

BLOCKS_EXECUTION = [[IN = None,   B = 'Acquisition',   BP = None,  CH = None,  OUT = 'data'],
                    [IN = 'data', B = 'Smooth' ,       BP = [1,1], CH = [1,2], OUT = 'data'],
                    [IN = 'data', B = 'FFT',           BP = [1,1], CH = [2,1], OUT = 'data'],
                    [IN = 'data', B = 'Mult',          BP = [1,1], CH = [2,2], OUT = 'data'],
                    [IN = 'data', B = 'Visualization', BP = [1,2], CH = [1,3], OUT =  None],
                    [IN = 'data', B = 'Writing',       BP = [1,1], CH = [1,2], OUT = 'Results.txt'],
                   ]
```

Figure 3.7: Application setup

3.3.2 Events Detection Algorithm Implementation

The simplicity of the algorithm developed during this research work makes it specially suited to perform the biosignals events detection in real-time. In this section some of the standard real-time processing features and constraints are discussed and the adaptations the algorithm suffered in order to be included into the application described in section 3.3.1 are also reported.

Real-time Processing: Features and Constraints

A real-time hardware or software system must operate according to strict constrains on its response time [52], which means that operational deadlines from events to response are imposed on that systems. The need of satisfying the requirements to meet processing deadlines usually brings an added complexity into these systems design [52].

Considering a real-time digital signal processing system, this must ensure that the time it takes to input and output a set of samples is independent of the processing delay [9]. A limitation of the digital signal processing for real-time applications is that the bandwidth of the system is limited by the sampling rate [9]. As such, the average processing time per sample should not be greater than the sampling period, whether the samples are processed individually or in groups. This criterium is also valid whether there are, or not, variable size data buffers, required in many types of signal processing functions. Likewise, the processing speed also determines the maximum rate at which the analog signal can be sampled [9], or, in the case of the developed application, the maximum rate at which the signal samples can be collected from the hardware buffer.

Even if the results of processing over a signal are significantly delayed from it, but that delay is bounded during a process that operates over an unlimited time, then that signal processing algorithm is still in real-time [9]. Although new and faster processors have continuously been introduced, there is still a limit to the processing that can be done in real-time. Furthermore, the usage of algorithms in consumer applications that implie a real-time pro-

cessing without any (expert) user interventions [25] implies some constraints to take into account, such as the inexistent knowledge of future events and the limited amount of data that can be buffered [53].

Implementation Approach

The events detection algorithm previously introduced in section 3.2 was quite simplified in order to perform an events detection with less processing, fitting the aforementioned real-time requirements.

All the optimization process was removed, as well as the `adjust_peaks` sub-function application. After smoothing the signal, considering, by default, a moving average window with half the points of the number of acquisition frames, the events are obtained by applying directly the `get_events` algorithm with fixed parameters.

In order to obtain a more accurate events detection, the number of data samples in which to apply the algorithm is usually bigger than the number of acquisition frames (N) available from a signal at each updating loop. As such, the raw data is sequentially saved into a circular buffer with fixed length W, as exemplified in Figure 3.8.

After that the acquisition begins the buffer is filled with samples of the signals from which to extract the events (Figure 3.8 a)). Once the buffer is full, the `get_events` algorithm starts to be applied. In each update loop, the algorithm considers all the signal samples the buffer contains (Figure 3.8 b)). However, only the events detected within the first N samples of the buffer are returned by the algorithm (being either visualized, by placing specific vertical markers under the signals, and saved into a text file). Those samples are then eliminated from the buffer and the new acquisition frames are included, following a *First IN, First OUT* data structure management concept. Nevertheless, the eliminated samples are still considered when computing the events of the new buffered data (Figure 3.8 c)). This procedure allows the inclusion of some past knowledge that may help the algorithm to distinguish if the events detected into the desired signal segment are actually significant or make part of a previously initiated waveform.

Given the present implementation approach, the delay between the input and output for this signal processing is constant and proportional to the buffer length. As such, this application ensures that the events are detected in real-time at the cost of bounded latency.

This implementation procedure is still ongoing and thus a further parameter optimization study, considering several types of signals, is still necessary. The studied parameters would include either the `get_events` inputs (`slices_length`, `smooth_factor` and `peaks_factor`),

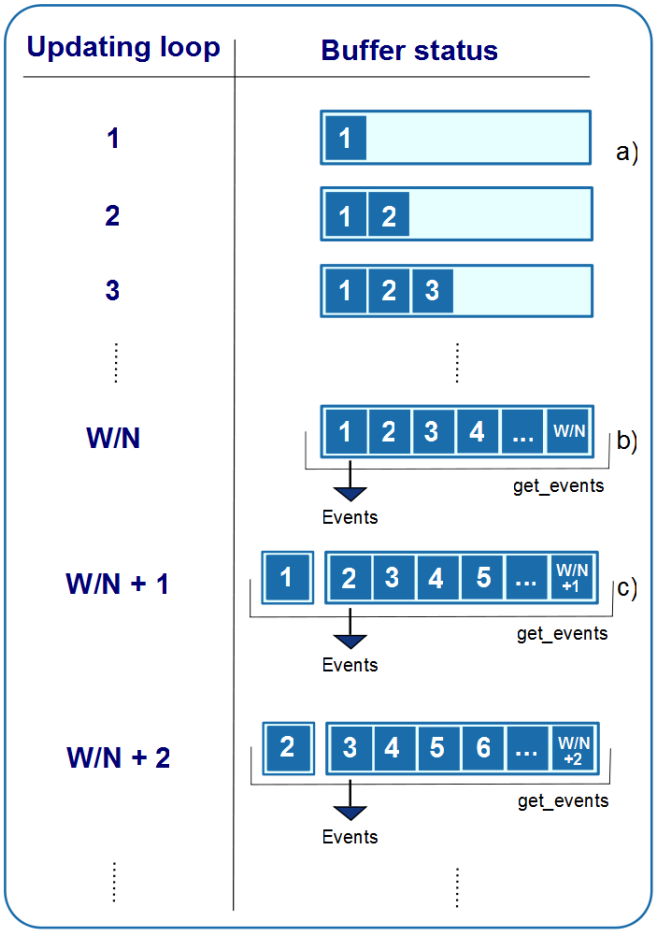

Figure 3.8: Real-time events detection implementation.

the smooth level to apply on signals before performing the events detection or the buffer length. The results would then be compared with those obtained applying the off-line algorithm, in order to compare the accuracy and efficiency of this real-time implementation.

Applying the `get_events` algorithm with the parameters set { `slices_length` = 10; `smooth_factor` = 0.2; `peaks_factor` = 0.4 } and considering a buffer of 1000 ms, some preliminary results were obtained. Despite the data and time constraints, those results point out the adapted algorithm's ability to perform the events detection in real-time, without a significant loss of accuracy.

Chapter 4

Algorithm Performance Evaluation

In this chapter the performance of the previously described events detection algorithm is evaluated. After some of the main issues regarding this kind of evaluation procedures are discussed, both the algorithm performance evaluated with synthetic data and by comparison with signal-specific standard techniques for EMG onset and ECG waveshape detection are presented.

4.1 Events Detection Performance Evaluation

When developing an algorithm to perform the detection of specific events within a signal, one major issue is evaluating the validity of the results. To achieve this, it is necessary to have some independent (and accurate) measure providing the characteristics of the events in which we are interested [23].

A profound performance test should be based upon relevant statistical analysis, which requires a large amount of data with properly preset signal parameters (ground truth data) [29]. That data should also be representative of the full range of data that the detection method in intended to be used for. This analysis is difficult or even impossible with real data, due to its poor parameter reproducibility. As such, commonly evaluation procedures apply the algorithm on synthetic signals, representative of real world data, for which the specific events were predefined based on some strict quantitative criteria [54].

It is likely that any model of a system used for data generation will only process some of the real data variables. As such, it has to be assured that the aspects considered when modeling the synthetic data are those that matter the most for interpretation techniques. An alternative approach would be to take some particularly good real data (for which the ground truth is clearly visible), and add noise to it, so that we have test signals for which we

know the ground truth, but in which this is not clearly visible [23].

Most of the studies regarding the performance evaluation of algorithms developed for events detection are related to the detection of onset in, e.g., EMG or kinematic data [27–29]. The most natural way to approach this problem is attempt to define onset times in line with human perception [54]. Visual inspection is a common method for resolving onset events, but it is limited to off-line analysis, can be time consuming and has poor reproducibility, being verified both inter- and intra rater variability [27, 29, 30]. This fact reinforce the importance of developing algorithms that accurately identify onset, as well as other signal events, apart from the experience or bias of the examiner and with an increased objectivity and reduced time to perform the analysis. Although it is acknowledge that visual determination of signal events is not optimal, it currently still provides a standard against which to compare computer methods [28].

4.2 Evaluation with Synthetic Data

Considering the issues approached in section 4.1, an accurate and objective performance evaluation procedure was designed in order to verify the efficiency of the proposed algorithm. Some strict quantitative criteria that a signal segment must have to be considered as an event were defined. The algorithm was then applied on a database of synthetic signals for which those events were known.

4.2.1 Synthetic Signals

Following the mathematical formalism previously introduced in sub-section 2.1.6, two different types of synthetic signals were defined by concatenating successive zones, according to the parameters in Table 4.1.

Table 4.1: Synthetic signals parameters. m and s are, respectively, the multiplying factors considered when computing the mean and standard deviation of signal's zones. m_d and sd_d represent, respectively, the minimum values allowed for mean and standard deviation differences between successive zones within a synthetic signal.

Synthetic signal	Type I	Type II
m	8	0.05
s	0.1	1
m_d	5	0.1
sd_d	0.05	0.5
Number of events	10	5

Type I signals were defined in order to get clearly distinct mean values between successive zones with low standard deviation values. These patterns are typically found, e.g., in signals acquired from Force platforms. However, in Type II signals the mean values difference between successive zones is not significant, but the standard deviations are clearly different, generating a typical pattern as those found in EMG signals.

4.2.2 Results

The developed algorithm was applied on a total of 25 Type I and 25 Type II synthetic signals, for which examples of graphic representations including marks on the detected events are given in Figure 4.1 . The default scale factor was used.

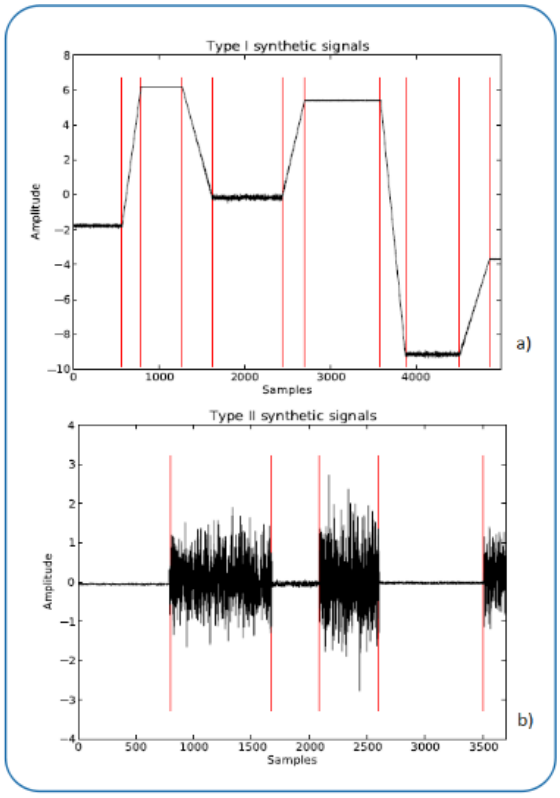

Figure 4.1: Example results for events detection on synthetic signals of a) Type I and b) Type II. The detected events are represented as vertical red marks.

Based on the comparison between the time instants where the events occur and the detected events, for each synthetic signal the detection mean error was computed by evaluating the mean of the differences between the detected events and the closer real event (in terms of the number of samples between those points). In Table 4.2 the mean and the standard deviation values for that parameter in both signal types are presented.

Table 4.2: Mean error values on events detection in Type I and Type II synthetic signals. The results follow the format *mean*(±*standard deviation*).

Synthetic signal	Type I	Type II
Mean error (samples)	11.84 (± 9.53)	28.81 (±16.81)

These results show that the mean error obtained when applying the algorithm in Type I signals is lower than the one verified for Type II signals. This suggests that the events detection is more accurate when there are significant changes into the mean value between successive regions, beyond the change into the standard deviation values.

An overall mean error of 20.32 (±16.01) samples between the detected and the real events was obtained. Considering those synthetic signals emulate biosignals acquired at a sampling frequency of 1000 Hz, one can conclude that the proposed algorithm performs the events detection with a mean error in the order of 20 ms, what shows its high accuracy. A paper regarding this performance evaluation study, as well as some applications in which this algorithm could be applied, was accepted to presentation in the BIOSTEC 2012 conference [55] [Appendix A.1].

4.3 Comparison with Standard Methods

4.3.1 Performance in Onset Detection

Overview

The ability to detect the activation onset of some types of signals, with high accuracy, is one of the most interesting applications of an events detection algorithm. This is particularly verified in what concerns with the onset of EMG activity, which detection is useful in several studies of motor control and performance [29]. As previoulsy mentioned in section 2.2, the onset detection algorithm proposed by Hodges et al. [28], which will be called as "*Hodges detector*" from now on, is one of the standard approaches to this problem.

In the present sub-section the performance of the events detection algorithm proposed in this research work, when detecting EMG signals onset, is compared with that achieved by *Hodges detector*. Following, the EMG signal acquisition method is described, as well as the implementation of both algorithms (including the specific *Hodges detector* preprocessing steps applied to those signals) and the results obtained from this comparison.

Acquisition Methods

The acquisition of EMG signals was made in the context of a study aiming at evaluating the effects on muscle activation thresholds before and after total knee arthroplasty, by testing the performance of an emergency brake in a car simulator [56], which will be further described in Chapter 5.

Surface EMG signals of the *Rectus Femoris*, *Vastus Medialis*, *Tibialis Anterior* and *Gastrocnemius* muscles were acquired using *emgPLUX* sensors [51], connected to a bioPLUX research unit [51] (Figure 4.2). This device performs the acquisition at a maximum sampling frequency of 1000 Hz, followed by analog to digital conversion (with a 12 bit ADC included). The data is then sent to a computer via Bluetooth. The system is portable (being miniaturized and lightweight) and allows the acquisition from 1 up to 8 analog channels plus one digital I/O port.

From the data set acquired while 3 subjects performed the emergency brake test, a total of 40 EMG signals, comprising 10 signals of each considered muscle, were considered for comparison between the events detection algorithm and *Hodges detector*. Typically, each signal includes an initial baseline region, followed by an activation pattern with origin from the emergency brake task [56].

Figure 4.2: bioPLUX research unit.

Processing

Since the basic features that guided the development of the events detection algorithm proposed in this thesis were the signal independence and the immunity to noise, no EMG specific preprocessing methods were applied to the signals before the algorithm performance evalu-

ation procedure described in this section. The developed algorithm was applied considering the default scale factor. The first event detected, after the signal first sample, was marked as the EMG onset instant.

The approach followed by *Hodges detector* implies the EMG signal to be preprocessed in order to reduce the high frequency noise and obtain the signal's envelope. After subtracting the mean value from the EMG signal and obtaining the rectified wave, a sixth-order digital butterworth lowpass filter with 50 Hz cutoff frequency was applied, following the implementation procedure described in [29], completing the envelope detection.

The muscle activity onset was identified as the instant from which the mean of the following N samples from the EMG envelope exceeds the baseline activity level by a specified multiple h of standard deviations. The baseline activity was adaptively determined, at each instant, by averaging M previous signal samples [29]. With a cutoff frequency of 50Hz, the set of criteria {N=25, h=3} and {N=50, h=1} are those reported as able to identify the EMG onset more accurately [28]. *Hodges detector* was implemented with both set of parameters, considering the baseline activity level computed from M=100 and M=200, respectively [29].

Results

The activation onset determined for each EMG signal was marked by vertical lines with different colors above the raw signals, as exemplified in Figure 4.3. The results were then compared with those obtained previously by visual inspection. In order to minimize the error from intra-rater variability, results from 3 examiners were considered and averaged, in each signal, to define the "true" onset value.

For each signal the difference between the onset, as defined from visual inspection, and those detected for each one of the implemented computational methods was computed. In case that a computational method detected no onset time, that was also registered. Table 4.3 exposes the mean error (considering only the signals for which the onset detection was achieved) and the percentage of missing detections verified for each of the compared methods.

Table 4.3: Results obtained from the proposed events detection algorithm and *Hodges detector* while performing the EMG signals onset detection. The "true" onset values were determined by visual inspection. The results follow the format *mean*(±*standard deviation*).

	Events detection algorithm	*Hodges detector* {N=25, h=3}	*Hodges detector* {N=50,h=1}
Mean error (samples)	-22.94 (± 115.09)	—	12.65 (± 81.85)
Percentage of missing detections	0%	100%	5%

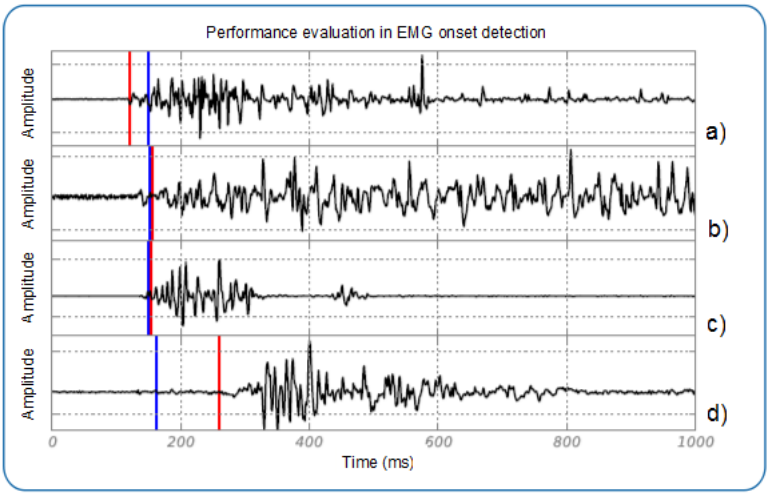

Figure 4.3: Graphic example of detected EMG onset (vertical lines) applying the events detection algorithm (in red) and *Hodges detector* with the parameter set {N=50, h=1} (in blue). EMG signals from a) *Rectus Femoris*; b) *Vastus Medialis*; c) *Tibialis Anterior* and d) *Gastrocnemius* muscles are represented.

These results show that the proposed events detection algorithm achieved a superior, though not significant, absolute mean error than that verified for *Hodges detector* implemented with the parameter set {N=50, h=1}. An high standard deviation value was verified for mean error values of both approaches. Therefore, there is no clear tendency of either the algorithms to perform an early or late onset detection.

Considering the events detection algorithm results, no missing onset detections were verified. *Hodges detector* implemented with the parameters set {N=50, h=1} missed 2 out of 40 onset detections. However, when applied with the criteria {N=25, h=3}, no onset was detected applying Hodges algorithm. This clearly exemplifies the sensibility of this single-threshold based algorithm to its input parameters, in agreement with that previously reported in other studies [28, 29].

Considering that the events detection algorithm showed a comparable accuracy and more reliability on EMG onset detection, when compared with *Hodges detector*, this represents a more suitable tool to apply in such usual signal processing requirement.

4.3.2 Performance in Transient Waveshape Detection

Overview

The detection of signal transients is considered as one of the main applications for an algorithm designed to detect significant signal events. As previously mentioned in section 2.2.1, transients are characterized by a sudden change into signal properties, such as the amplitude or frequency, over a short time interval when compared with the length of the signal being

analysed [32]. Under this definition, it is valid to consider the ECG standard waveshape as a transient segment within an electrical baseline signal.

ECG signal processing comprises a set of algorithms that condition the signal with respect to different types of noise and artifacts, detect heartbeats, extract basic measurements concerning the waveshape and comprises the data for efficient storage or transmission [8]. From those, the heartbeat detection and its occurrence time is one of the basic information required in several types of ECG signal processing tools. Since the QRS complex is the waveform that is most easily discerned from the ECG, beat detection is mostly achieved by detecting those complexes, and particularly the R-peaks, usually the higher peaks among those in ECG cycle [8, 57].

Standard QRS complex detectors are usually divided into two stages: a pre-processor (to emphasize the QRS complex) and a decision stage to threshold the QRS enhanced signal. More complex approaches have been proposed, such as the use of *Wavelet transforms* [58, 59], in order to consider the time-varying morphology of the QRS complex.

In this sub-section the performance of the introduced events detection algorithm on detecting heartbeats within an ECG signal is compared with that of a standard QRS complex detector proposed by Pan and Tompkins [60], adapted as described in [57]. After that the database from which the ECG signals considered in this performance evaluation study were collected is described, the main processing steps in order to implement *Pan and Tompkins* algorithm and the results of the comparison between both algorithms are also posteriorly exposed.

Database

A total of 26 ECG signals was considered on this performance evaluation study. Those signals, which were obtained from a public database (PhysioBank) at PhysioNet library [61], were acquired from healthy people, with normal sinus rhythm. Each acquisition was made during 4 seconds, at a sampling frequency of 125 Hz.

Processing

Such as in the previous performance evaluation tests described in this dissertation, the events detection algorithm was applied in ECG signals with no preprocessing steps. The default scale factor was also considered.

In order to implement the adaptation of *Pan and Tompkins* algorithm [60], ECG signals were first filtered by applying a 2^{nd} order Butterworth lowpass filter with a 30 Hz cutoff

frequency, to remove some possible high frequency noise due to electronic devices interference. A 2^{nd} order Butterworth high pass filter with 2 Hz cutoff frequency was also applied to remove some possible baseline fluctuations and other respiration artifacts [57].

The implemented R-peak detection algorithm consists of three main components [57]:

- **Signal transformation:** ECG signal is differentiated and squared to enhance QRS wave slopes, particularly that of R-peak, independently of the signal polarity. The resultant signal is then integrated into a moving window, producing a signal that includes information about both the slope and width of the QRS complex [60];
- **Adaptive thresholding:** a single threshold is determined dynamically, corresponding to a fraction of the differentiated signal in each moment;
- **Local search:** Considering each set of points where the integrated signal crosses the threshold, the R-peak occurrence is defined at the time instant where the amplitude value of those points is maximal. Given the electrical properties of cardiac tissue, once a valid R-peak is recognized a refractory period of 200ms is initiated, where the search for new peaks is disabled.

Results

For each ECG signal, after running both the algorithms, the detected events and R-peaks were marked by vertical lines with specific colors, as exemplified in Figure 4.4.

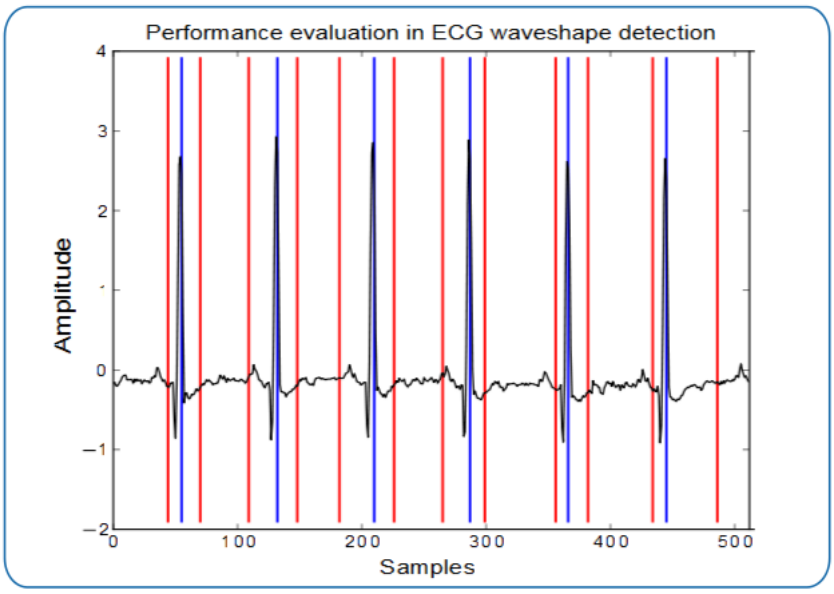

Figure 4.4: Graphic example of detected ECG waveshapes (vertical lines) applying the events detection algorithm (in red) and *Pan and Tompkins* algorithm (in blue).

Considering *Pan and Tompkins* adapted algorithm, a ECG waveshape is considered to be detected if the R-peak is marked. However, the waveshape discrimination by the events detection algorithm implies the detection of two events, i.e., an onset and an offset instant. An exception was made on signal's extremities, where only an offset (detected at the beginning) and an onset (detected at the end) was enough to consider the ECG transient waveshape had been detected.

The resulting graphics were then visually examined and, for both algorithms, the percentage of detected ECG waveshapes and the number of extra detected events were registered. Table 4.4 exposes the mean values of those parameters, in both algorithms, considering the total of 26 analysed signals.

Table 4.4: Results obtained from the proposed events detection algorithm and from *Pan and Tompkins* adapted algorithm while performing the ECG signals QRS complex detection. The results follow the format *mean*(±*standard deviation*).

	Events detection algorithm	*Pan and Tompkins* algorithm
Percentage of detected ECG cycles	93.84% (± 15.64 %)	92.63% (± 21.90%)
Number of extra detections	1.35 (± 1.52)	0.38 (± 1.06)

These results show that the mean percentage of detected events within a given signal is significant for both algorithms, being slightly bigger for the events detection algorithm proposed in this dissertation.

Considering the number of extra detections, however, this is more significant when considering the events detection algorithm than for *Pan and Tompkins* adapted algorithm. This extra events detection is mostly due to the detection of some pronounced T waves in some signals. A parameter optimization study regarding the algorithm *scale* factor could improve its efficiency at this level.

Pan and Tompkins algorithm reduces the extra detection rate by applying a signal-specific preprocessing step and defining the 200 ms latency period after a R-peak detection. However, the referred preprocessing steps are highly dependent on specific parameters such as the filters order and cutoff frequency, as well as the signal sampling rate.

In general, the algorithm proposed in this dissertation showed to have a comparable efficiency with that of a standard QRS complex detector, without the previous knowledge or specific preprocessing steps required in the last approach, what makes it suitable to apply in this important signal processing task.

Chapter 5

Applications

This chapter presents some applications for which the algorithm introduced in this dissertation allows the events detection with added accuracy and objectivity. Those applications are mostly based on projects developed in parallel with the research work here presented, which contributed in great part to its motivation. At the end of this chapter other possible applications are also exposed.

5.1 Case Study: Knee Stability Analysis

5.1.1 Overview

This project was developed in partnership with researchers from the Department of Physical Education and Sport of the University of Seville (Spain).

Whole body vibration (WBV) is currently considered as an effective method by which muscle strength or balance can be improved, in addition to other physiological benefits. However, there is still no clear consensus on the mechanisms by which WBV enhances muscle strength and power [62, 63].

There is evidence that preventive training programs can reduce the incidence of sport injuries of the lower extremity, particularly the knee anterior cruciate ligament (ACL) [64]. Those programs should also consider the subject gender they are designed for, since several authors have suggested that females demonstrate a substantially greater risk of suffering acute injury of the ACL, compared to males [65, 66].

A comprehensive understanding of WBV effects on neuromuscular control of the knee joint, depending on the subject gender, is particularly important for the most serious sports-related injuries and their prevention. That was the main motivation for the study here presented.

The protocol followed on this study included the performance of single-legged drop jumps from a 30 cm elevated platform to the ground level. After a set of three pretest landings, forty-five healthy volunteer participants (age: 22 ± 3 yr) completed one set of six bouts of WBV (with 4 mm of oscillation amplitude and a training frequency of 30 Hz) of 1 minute, each one followed by another single-leg drop jump (Figure 5.1).

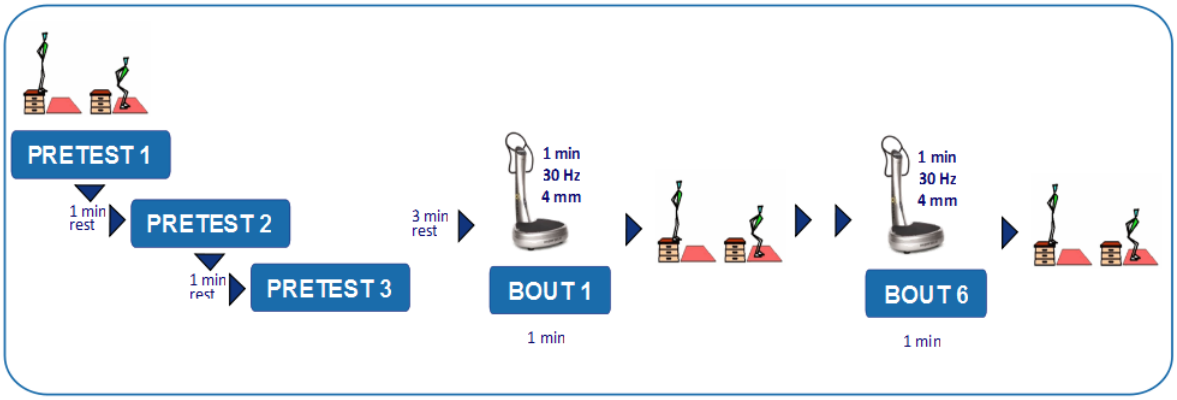

Figure 5.1: Schematic illustration of knee stability study testing protocol.

Among other variables, such as vertical ground reaction forces (VGRF) and knee angles, surface EMG signals in *Rectus Femoris* (RF) and *Hamstrings* (H) muscles of the dominant leg were acquired, in each jump trial, using two *emgPLUX* sensors [51]. Two tri-axial accelerometers *xyzPLUX* were placed at the tibial condyle and at the peroneal malleolus levels, in order to acquire knee and ankle acceleration signals, respectively. The referred sensors were connected to a bioPLUX research unit [51][1].

The data analysis performed in this study, which will be further described for EMG and acceleration signals in sub-section 5.1.2, was divided in two main parts with specific purposes, as following exposed.

Acute Effects of WBV Training on Knee Stability

This part of the study aimed at investigating whether WBV training influences the landing technique, the lower limbs muscle activity and knee medial-lateral acceleration, and hence its stability. The analysis outcomes showed that the time to stabilize the knee was significantly lower after WBV and that the EMG signal mean frequency, before and after activation, was also lower after that WBV training was introduced between the drop jumps trials. Those results suggest that WBV enhances knee stability, which may have clinical significance and help in the design of rehabilitation programs.

[1]The described signal acquisition procedure was fully done by Borja Sañudo, from the Department of Physical Education and Sport of the University of Seville (Spain).

Gender Differences in Knee Stability in Response to WBV

The purpose of this part of the study was to determine whether gender differences existed in muscle activity and knee kinematics of healthy people when performing a landing maneuver, after exposure to WBV. The data analysis showed that while females displayed a significantly greater VGRF and H activity (before the ground contact), an acute bout of WBV might reduce those values, increasing co-contraction. No gender differences in neuromuscular activity of the *quadriceps* were observed after WBV. However, WBV decreased females medial-lateral acceleration in both knee and ankle. The reported gender differences underline the necessity to perform specific neuromuscular training programs. A paper regarding the second part of the study was accepted for publication in the *Journal of Strength and Conditioning Research* [67], [Appendix A.2].

5.1.2 Data Analysis Methodology

In order to extract important features from the EMG and acceleration signals (e.g. the mean frequency or RMS values), the applied data analysis methodology began with a preprocessing phase.

EMG signals preprocessing included the offset removal and full-wave rectification, followed by lowpass filtering in order to obtain the signal's envelope. Acceleration signals were lowpass filtered and calibrated to g-units, as described in [68].

From the EMG envelope, the signal activation onsets and offsets were determined by applying a single threshold method. Likewise, the jump phase on the acceleration signals was identified from its maximum value, applying then specific time thresholds to define either the jump, as well as pre- and post-jump intervals. All the parameters to be considered in the applied preprocessing functions were selected on a signal-specific basis, implying an exhaustive and time-consuming optimization study.

The algorithm introduced in this dissertation would simplify the previously described analysis, allowing the posterior parameters extraction with enhanced accuracy. The EMG onset and offset detection, already approached in sub-section 4.3.1, would discard the envelope detection step and assure an higher accuracy compared with that achieved by a single-threshold method.

Applying the events detection algorithm, with the default scale factor, to the acceleration signals the obtained result is exemplified in Figure 5.2 a). The jump would be marked by two events surrounding the landing phase record, which is characterized for the greater instability within the signal. A more accurate description of the acceleration pattern during the jump

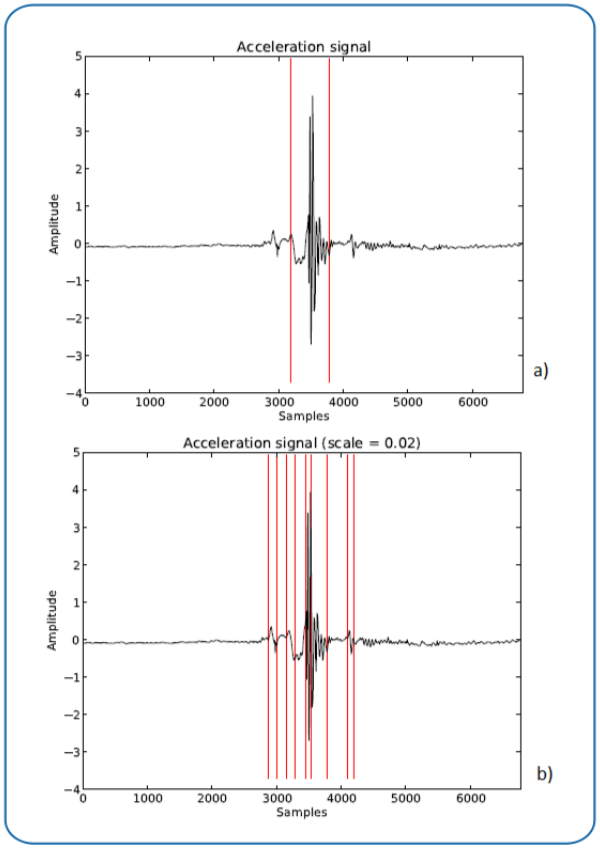

Figure 5.2: Medial-lateral knee acceleration signal with marked events. The events detection algorithm was applied considering: a) the default scale factor and b) a scale factor of 0.02.

task is achieved by using this algorithm with a proper pre-defined scale factor. The results presented in Figure 5.2 b), where a scale factor of 0.02 was used, allow to distinguish the knee acceleration while preparing the jump from the platform, the flying phase (with a slight and longer acceleration instability) and the landing phase, where the instability increases significantly for a short time period. The time the knee takes to recover the stability from the jump can also be estimated by accessing the posterior signal segments, what could be very useful given the main goals of the presented study.

5.2 Case study: Brake Response Time and Muscle Activation Thresholds

5.2.1 Overview

This ongoing project is being developed in partnership with researchers from the Faculty of Human Kinetics at the Technical University of Lisbon (Portugal) and the Physical Therapy and Rehabilitation Department at the Schön Klinik Hamburg Eilbek (Germany).

After total knee arthroplasty (TKA) it is documented that there is an increase in the brake

response time (BRT) [69–72], an important human factor used in traffic accident prevention and research. As such, there is evidence that TKA affects peripheral aspects related with the movement execution. Those performance impairments may be caused by soft tissue lesions, which were reduced with the introduction of Minimally Invasive Surgery (MIS) techniques for TKA.

The main goals of this study are the comparison of the effects of MIS and standard approach for TKA on BRT components and on muscle activation thresholds of four muscles involved in an emergency brake task.

A randomized controlled trial was designed [56]. Surface EMG signals of *Rectus Femoris*, *Vastus Medialis*, *Tibialis anterior* and *Gastrognemius* are recorded, using four *emgPLUX* sensors [51], while the patients perform 10 emergency brake trials in a car simulator (Figure 5.3). Those sensors are connected to a bioPLUX research unit [51], which also acquires the digital signal from one trigger, which commands a stimulus light (red LED) turn on/off, and from two load cells connected with the brake and accelerator pedals [2]. The digital signal is used to slice the signals in the 10 brake trials for each task, thus the analysis can be done considering the signals from a single emergency brake.

In the following sub-section the data analysis and features extraction procedure created to achieve the previously defined goals will be briefly described.

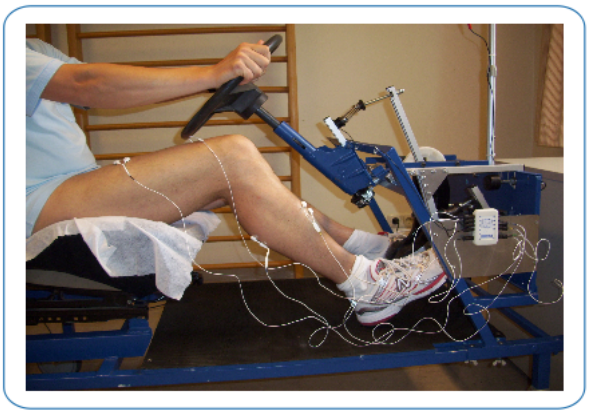

Figure 5.3: Car simulator with the bioPLUX research unit and four *emgPLUX* sensors placed above the muscles involved in the emergency brake task. From [56].

5.2.2 Data Analysis and Primary Outcome Results

In a first approach the study protocol used an adaptation of Hodges EMG onset detector [28], created to be used on force and EMG signals, either on positive or negative transitions [56]. As verified in the context of the performance evaluation test in sub-section 4.3.1, prelimi-

[2]The described signal acquisition procedure was fully done by Carlos J. Marques, researcher at the Physical Therapy and Rehabilitation Department at the Schön Klinik Hamburg Eilbek (Germany)

nary results using this approach showed the onset detection to be highly dependent upon the signal-specific preprocessing steps that were applied. The events detection algorithm developed in the context of this research work is a much suitable procedure in terms of reliability and signal independence.

Since the patient selection to this study is still taking place and the number of cases for which data is available is still small and an unbalanced distribution of male and female patients is verified, a paper presenting only the primary outcome results of two female patients was accepted to presentation in the BIOSTEC 2012 conference [73] [Appendix A.3].

In Figure 5.4 an example of a graphical representation of the results, enhancing the activation onset detected for each signal considering the default scale factor, is presented. Force signals were calibrated and the EMG signals were lowpass filtered by applying a smoothing filter with a moving average window of 10 points. Despite the fact that no other preprocessing steps were applied in the EMG signals before the onset detection, in Figure 5.4 those thresholds are marked above the EMG envelope, allowing a more intuitive visualization. From the EMG signal, the envelope was computed subtracting its mean value, obtaining the rectified wave and then applying a smoothing filter with a moving average window of 20 points.

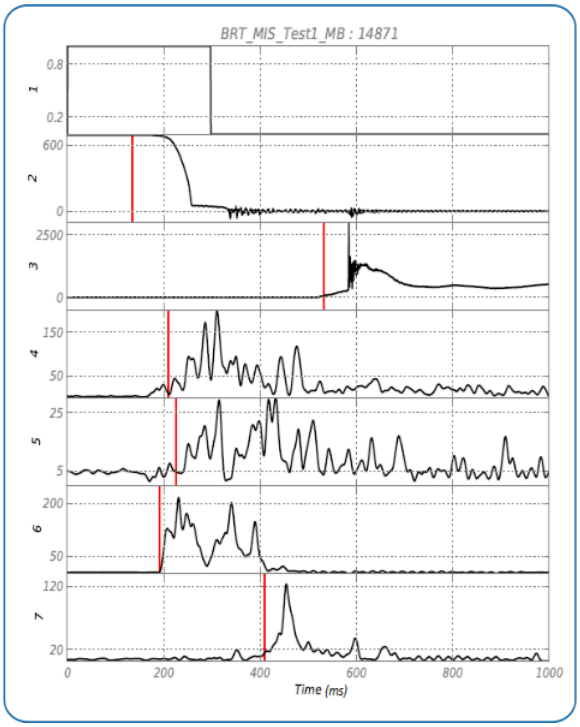

Figure 5.4: Graphic representation of onset detection results in an emergency brake trial, with the 7 signals (1 Trigger; 2 Accelerator; 3 Brake pedal; 4-7 EMG envelope signals of the 4 muscles) and the vertical red lines marking the detected thresholds for each signal.

After the activation onset times of force signals were determined the following outcomes could be computed [56]:

- BRT (Brake Response Time)- time frame between the onset of the red LED and the achieving of a brake force on the brake pedal of 150N (ms);
- RT (Reaction Time)- time frame between the onset of the red LED and the initiation of the movement of the foot on the accelerator pedal (ms);
- FTT (Foot Transfer Time)- time frame between the initiation of the movement of the foot on the accelerator pedal and the first contact with the brake pedal (ms);
- BPTT (Brake Pedal Travelling Time)- time frame between the first contact with the brake pedal and the achieving of a brake force of 150N on the brake pedal (ms);
- MT (Movement Time)- sum of the FTT with BPTT.

The mean RT, FTT, BPTT and BRT were calculated out of the 10 test trials for each task. The outcomes of the two considered cases suggest that surgery had different effects on the mean BRT of both patients. A more exhaustive analysis is ongoing, considering a bigger data sample, in order to find out whether the observed trends are related with the surgery technique the patients underwent, as well as verifying the technique influence on muscle activation thresholds of four muscles involved in the emergency brake task.

5.3 Other applications

Besides the aforementioned applications, there is a wide range of signals, acquired under different scenarios, for which the algorithm developed in this research work would be able to perform the detection of significant events. Some of those applications are exemplified in this section.

In Figure 5.5 a) a force signal obtained from a drop jump task and the corresponding detected events are represented. The events detection algorithm here introduced was applied without defining a specific scale factor. The landing process phases are clearly marked within the signal, but generally a higher level of accuracy is required by this specific signal analysis.

The vertical ground reaction forces during the landing phase have a constant pattern with well defined peaks [74]. Considering only the signal segment corresponding to the first landing phase, previously defined in Figura 5.5 a), and applying the algorithm with a proper scale factor (set to 0.025), as exemplified in Figure 5.5 b), an automated accurate access to these peaks, as well as the respective onset and offset points, is achieved. This processing can help sport researchers on studying the forces distribution at the landing path and on developing lower members specific training protocols and rehabilitation interventions, adapted

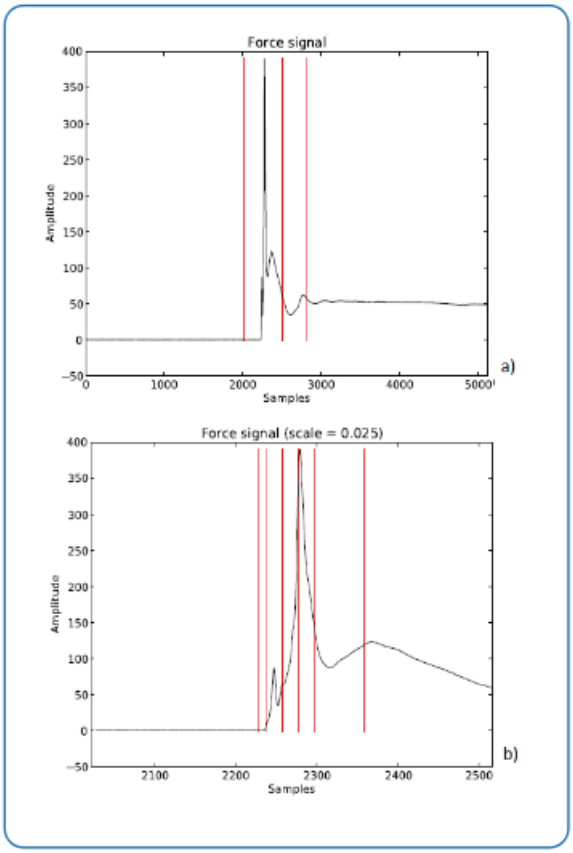

Figure 5.5: Signal acquired from a force platform, during a drop jump, with marked events. The events detection algorithm was applied considering: a) default scale factor; b) signal segment between the two first events detected in a) and a scale factor of 0.025.

to prevent injuries usually assigned to the landing phase of a jump [74].

The real-time implementation of the algorithm introduced in the context of this dissertation is already ongoing, as further described in Chapter 3. Performing an accurate and reliable events detection in real-time, this algorithm could be included in tools for diagnosis or athletic performance evaluation in a wide variety of scenarios.

Another possibility would be the inclusion of this tool in BCI applications, such as Electrooculography (EOG) and EMG based virtual keyboards [75]. Such a project, already under development in *PLUX* R&D department, aims at allowing the user select the letters, sequentially highlighted across a virtual keyboard, using a frown expression. The correspondent muscular activation is measured by EMG sensors placed in specific positions at the facial surface. A correct EMG onset and offset detection, together with a time threshold establishing a minimum duration between those points would allow the distinction between actual intended and involuntary frowns, minimizing the number of false detections. This BCI would be very useful, e.g., for people suffering from Locked-in syndrome, spinal-cord injury or amyotrophic lateral sclerosis, who only have control over specific parts of their facial expression [75].

Chapter 6

Conclusions

The work developed and presented in the context of this dissertation was strongly motivated by the necessity of performing an automated detection of significant events within a signal. From a specific and concrete processing requirement, regarding the design of an athletic performance evaluation system, the robust tools developed through this work achieved an higher abstraction level, with proved applicability in a wide range of biosignals acquisition scenarios.

A signal-independent off-line algorithm, which is able to detect significant events in a biosignal, was introduced. The algorithm performs the events detection based on a time series morphological analysis, followed by an iterative optimization process.

An accurate and objective performance evaluation procedure was designed to verify the efficiency of the proposed algorithm. When applied on a set of synthetic signals, with known and quantitatively predefined events, an overall mean error of 20.32 ($\pm$ 16.01) samples between the actual events and those which were detected showed the high accuracy of this approach.

The algorithm also proved its ability to perform the detection of signals activation onset and transient waveshapes with similar or, in some cases, higher accuracy and reliability when compared with signal-specific standard methods.

Based on signal processing requirements created in the context of some research projects, developed in parallel to this dissertation, some applications in which the introduced algorithm is suitable at performing the events detection were also presented. The initial steps of the algorithm´s implementation into a real-time processing tool were also reported.

In the context of this research work a couple of papers were published, regarding either the algorithm introduction and performance evaluation, as well as the aforementioned application case studies. Two papers were accepted for presentation in BIOSTEC 2012 conference and

another paper was published in the *Journal of Strength and Conditioning Research*. Those publications are presented in Appendix A.

In general, the algorithm proposed in this dissertation performs an efficient and accurate events detection when both synthetic or real biosignals are considered, with good noise immunity. Its versatile design allows the application in different signals without previous knowledge on their statistical properties or specific preprocessing steps. The adjustment of a scale factor also allows the achievement of different detail levels in specific applications.

The added objectivity of the tools here described when compared with the exhaustive and time-consuming standard examiner analysis, by visual inspection, also represents a relevant contribution in events detection, a particularly important issue within the wide digital signal processing research field.

6.1 Future Work

There are a few aspects in this research work for which there is the intention of performing additional development and optimization studies in the future:

- **Further validation:** A more exhaustive performance evaluation study concerning the developed algorithm is still needed, considering synthetic signals with different events patterns or a wider range of biosignals from more subjects and acquired at distinct experimental scenarios;
- **Noise immunity tests:** Since no preprocessing steps are required to apply the events detection, it is important to characterize its noise immunity. As such, testing the algorithm performance at different signal to noise ratio (SNR) conditions is a future path for additional research.
- **Scale factor characterization:** A further characterization of the relationship between the scale factor and the minimum pattern discontinuity magnitude to be considered as an event is also a future goal of this research work. A parameter optimization study would allow the definition of the best scale factor values to consider in specific applications;
- **Integration in pattern recognition/classification systems:** Given the ability of this tools to perform an accurate signal segmentation, extracting characteristic waveshapes, there is the intention to include it in data-mining systems with specific tools for pattern recognition and classification of these signal segments.

- **New applications:** Beyond the applications described in this dissertation, when approaching the performance evaluation tests and specific case studies, there is the intention of using the developed algorithm in new applications, adding accuracy and functionality to the already developed tools;

- **Real-time integration:** The events detection algorithm integration into a real-time processing tool is already under development. Given the satisfactory preliminary results, a further parameter optimization study is now necessary to assure that the events detection in real-time is performed with residual loss of accuracy, when compared of that achieved by the off-line version. This ability would allow the developed algorithm to integrate software tools in which a real-time objective feedback from signal processing outcomes is essential, such as those used in health monitoring, diagnosis or athletic performance evaluation.

Bibliography

[1] H. Silva, G. Martins, S. Palma, P. Mil-Homens, and M. Valamatos, "An Automated Athlete Performance Evaluation System," in *Proceedings of Biodevices 2009, Porto, Portugal*, 2009.

[2] P. Abernethy, G. Wilson, and P. Logan, "Strength and power assessment. Issues, controversies and challenges." *Sports medicine (Auckland, NZ)*, vol. 19, no. 6, p. 401, 1995.

[3] D. Liebermann, L. Katz, M. Hughes, R. Bartlett, J. McClements, and I. Franks, "Advances in the application of information technology to sport performance," *Journal of Sports Sciences*, vol. 20, no. 10, pp. 755–769, 2002.

[4] P. Veltink and D. De Rossi, "Wearable technology for biomechanics: e-textile or micromechanical sensors?[Conversations in BME]," *Engineering in Medicine and Biology Magazine, IEEE*, vol. 29, no. 3, pp. 37–43, 2010.

[5] R. S. H. Ramos, F. Coito and M. Ortigueira, *Análise de sinais em engenharia biomédica.* FCT-UNL, 2009.

[6] J. Bronzino, *The biomedical engineering handbook.* CRC Pr I Llc, 2000.

[7] J. Enderle, J. Bronzino, and S. Blanchard, *Introduction to biomedical engineering.* Academic Press, 2005.

[8] M. Akay, *Wiley encyclopedia of biomedical engineering.* Wiley-Interscience, 2006.

[9] S. Kuo, B. Lee, and W. Tian, *Real-Time Digital Signal Processing.* Wiley Online Library, 2006.

[10] Southwest Tennessee Community College (2010), "Principles of Anatomy and Physiology I & II" [online] Available at: http://faculty.southwest.tn.edu/rburkett/heart_lab.htm, [Accessed 17 September 2011].

[11] N. Linthorne, "Analysis of standing vertical jumps using a force platform," *American Journal of Physics*, vol. 69, p. 1198, 2001.

[12] S. Palma, H. Silva, H. Gamboa, and P. Mil-Homens, "Standing standing jump loft time measurement: an acceleration based method," in *Proceedings of Biodevices 2008, Madeira, Portugal*, 2008.

[13] P. Picerno, V. Camomilla, and L. Capranica, "Countermovement jump performance assessment using a wearable 3D inertial measurement unit." *Journal of sports sciences*, p. 1, 2010.

[14] N. Nunes, "Algorithms for time series clustering applied to biomedical signals," Master's thesis, Faculdade de Ciências e Tecnologia- Universidade Nova de Lisboa, 2011.

[15] M. Cifrek, V. Medved, S. Tonkovic, and S. Ostojic, "Surface emg based muscle fatigue evaluation in biomechanics," *Clinical Biomechanics*, vol. 24, no. 4, pp. 327–340, 2009.

[16] C. Camic, T. Housh, G. Johnson, C. Hendrix, J. Zuniga, M. Mielke, and R. Schmidt, "An emg frequency-based test for estimating the neuromuscular fatigue threshold during cycle ergometry," *European journal of applied physiology*, vol. 108, no. 2, pp. 337–345, 2010.

[17] C. De Luca, A. Adam, R. Wotiz, L. Gilmore, and S. Nawab, "Decomposition of surface emg signals," *Journal of neurophysiology*, vol. 96, no. 3, p. 1646, 2006.

[18] M. Schmidt and H. Lipson, "Distilling free-form natural laws from experimental data," *Science*, vol. 324, no. 5923, p. 81, 2009.

[19] E. Ciaccio, S. Dunn, and M. Akay, "Biosignal pattern recognition and interpretation systems," *Engineering in Medicine and Biology Magazine, IEEE*, vol. 12, no. 3, pp. 89–95, 1993.

[20] A. Bar-Or, J. Healey, L. Kontothanassis, and J. Van Thong, "Biostream: A system architecture for real-time processing of physiological signals," in *Engineering in Medicine and Biology Society, 2004. IEMBS'04. 26th Annual International Conference of the IEEE*, vol. 2. IEEE, 2004, pp. 3101–3104.

[21] M. Basseville and I. Nikiforov, *Detection of abrupt changes: theory and application*. Citeseer, 1993, vol. 15.

[22] W. Melek, Z. Lu, A. Kapps, and W. Fraser, "Comparison of trend detection algorithms in the analysis of physiological time-series data," *Biomedical Engineering, IEEE Transactions on*, vol. 52, no. 4, pp. 639–651, 2005.

[23] L. Smith, S. Shahid, A. Vernier, and N. Mtetwa, "Finding events in noisy signals," in *Proc. of Irish Signals and Systems Conference*. Citeseer, 2007, pp. 31–35.

[24] G. Clifford, "A novel framework for signal representation and source separation: Applications to filtering and segmentation of biosignals," *Journal of Biological Systems*, vol. 14, no. 2, pp. 169–184, 2006.

[25] S. de Waele, G. de Vries, and M. Jager, "Experiences with adaptive statistical models for biosignals in daily life," in *Affective Computing and Intelligent Interaction and Workshops, 2009. ACII 2009. 3rd International Conference on*. IEEE, 2009, pp. 1–6.

[26] G. Staude, "Precise onset detection of human motor responses using a whitening filter and the log-likelihood-ratio test," *Biomedical Engineering, IEEE Transactions on*, vol. 48, no. 11, pp. 1292–1305, 2001.

[27] L. Botzer and A. Karniel, "A simple and accurate onset detection method for a measured bell-shaped speed profile," *Frontiers in Neuroscience*, vol. 3, 2009.

[28] P. Hodges and B. Bui, "A comparison of computer-based methods for the determination of onset of muscle contraction using electromyography," *Electroencephalography and Clinical Neurophysiology/Electromyography and Motor Control*, vol. 101, no. 6, pp. 511–519, 1996.

[29] G. Staude, C. Flachenecker, M. Daumer, and W. Wolf, "Onset detection in surface electromyographic signals: a systematic comparison of methods," *EURASIP Journal on Applied Signal Processing*, vol. 2001, no. 1, pp. 67–81, 2001.

[30] N. Alves and T. Chau, "Automatic detection of muscle activity from mechanomyogram signals: a comparison of amplitude and wavelet-based methods," *Physiological measurement*, vol. 31, p. 461, 2010.

[31] P. Bonato, T. D'Alessio, and M. Knaflitz, "A statistical method for the measurement of muscle activation intervals from surface myoelectric signal during gait," *Biomedical Engineering, IEEE Transactions on*, vol. 45, no. 3, pp. 287–299, 1998.

[32] L. Angrisani, P. Daponte, and M. D'Apuzzo, "A method for the automatic detection and measurement of transients. part i: the measurement method," *Measurement*, vol. 25, no. 1, pp. 19–30, 1999.

[33] Q. He, Z. Feng, and F. Kong, "Detection of signal transients using independent component analysis and its application in gearbox condition monitoring," *Mechanical systems and signal processing*, vol. 21, no. 5, pp. 2056–2071, 2007.

[34] B. Sankur, E. C. Güler, and Y. Kahya, "Multiresolution biological transient extraction applied to respiratory crackles," *Computers in biology and medicine*, vol. 26, no. 1, pp. 25–39, 1996.

[35] A. Geva, K. Todros, B. Levi, D. Solomon, and D. Kerem, "Adaptive prediction of changes of physiological/pathological states using processing of biomedical signals," May 29 2007, uS Patent 7,225,013.

[36] P. Addison, J. Walker, and R. Guido, "Time–frequency analysis of biosignals," *Engineering in Medicine and Biology Magazine, IEEE*, vol. 28, no. 5, pp. 14–29, 2009.

[37] T. Oliphant, *A Guide to NumPy*. Trelgol Publishing, 2006, vol. 1.

[38] Jones, E., Oliphant, T., Peterson, P. (2001), SciPy: Open source scientific tools for Python. [online] Available at: http://www. scipy. org/ [Accessed 20 September 2011].

[39] R. Miller, *Optimization: foundations and applications*. Wiley-Interscience, 2000.

[40] Z. Zabinsky, *Stochastic adaptive search for global optimization*. Springer Netherlands, 2003, vol. 72.

[41] Multicharts(2008) 21st Century Technical Analysis and Trading Platform - Optimization Strategies [online] http://www.multicharts.net/optimize.php [Accessed 17 October 2011].

[42] S. Rao and S. Rao, *Engineering optimization: theory and practice*. Wiley, 2009.

[43] N. Metropolis, A. Rosenbluth, M. Rosenbluth, A. Teller, and E. Teller, "Simulated annealing," *Journal of Chemical Physics*, vol. 21, pp. 1087–1092, 1953.

[44] S. Kirkpatrick, C. Gelatt, and M. Vecchi, "Optimization by simulated annealing," *Science*, vol. 220, no. 4598, p. 671, 1983.

[45] Tradecision(2011) Advanced trading software: technical analysis and neural network - Strategy Optimization [online] http://www.tradecision.com/product/trading_systems/strategy_optimization.htm [Accessed 17 October 2011].

[46] G. Van Rossum and C. voor Wiskunde en Informatica, *Python reference manual*. Centrum voor Wiskunde en Informatica, 1995.

[47] N. Rappin and R. Dunn, *wxPython in Action*. Manning, 2006.

[48] J. Hunter and D. Dale, "The matplotlib user's guide," *Electronical edition*, 2006.

[49] Matplotlib animations (2009). [online] Available at: http://www.scipy.org/Cookbook/Matplotlib/Animations/ [Accessed 11 September 2011].

[50] Shemanarev, M. (2007) Anti-Grain Geometry. [online] Available at: http://www.antigrain.com/ [Accessed 11 September 2011].

[51] PLUX (2007) PLUX - Wireless Biosignals, S. A.. [online] Available at: http://plux.info/ [Accessed 23 September 2011].

[52] M. Ben-Ari, *Principles of concurrent and distributed programming.* Addison-Wesley Longman, 2006.

[53] D. Karantonis, M. Narayanan, M. Mathie, N. Lovell, and B. Celler, "Implementation of a real-time human movement classifier using a triaxial accelerometer for ambulatory monitoring," *Information Technology in Biomedicine, IEEE Transactions on*, vol. 10, no. 1, pp. 156–167, 2006.

[54] S. Dixon, "Onset detection revisited," in *Proc. of the Int. Conf. on Digital Audio Effects (DAFx-06)*, 2006, pp. 133–137.

[55] R. Santos, J. Sousa, B. Sañudo, C. J. Marques, and H. Gamboa, "Biosignals events detection - a morphological signal-independent approach," in *Proceedings of the International Conference on Bio-inspired Systems and Signal Processing (BIOSIGNALS 2012)*, Vilamoura, Portugal, 2012.

[56] C. J. Marques, H. Gamboa, F. Lampe, J. Barreiros, and J. Cabri, "Muscle activation thresholds before and after total knee arthoplasty - protocol of a randomized comparison of minimally invasive vs. standard approach," in *Proceedings of the International Conference on Bio-inspired Systems and Signal Processing, pages 544-547. DOI: 10.5220/0003318505440547*, 2011.

[57] J. Medeiros, "Development of a heart rate variability analysis tool," Master's thesis, Faculdade de Ciências e Tecnologia- Universidade de Coimbra, 2010.

[58] S. Kadambe, R. Murray, and G. Boudreaux-Bartels, "Wavelet transform-based qrs complex detector," *Biomedical Engineering, IEEE Transactions on*, vol. 46, no. 7, pp. 838–848, 1999.

[59] S. Mahmoodabadi, A. Ahmadian, M. Abolhasani, M. Eslami, and J. Bidgoli, "Ecg feature extraction based on multiresolution wavelet transform," in *Engineering in Medicine and Biology Society, 2005. IEEE-EMBS 2005. 27th Annual International Conference of the.* IEEE, 2006, pp. 3902–3905.

[60] J. Pan and W. Tompkins, "A real-time QRS detection algorithm," *Biomedical Engineering, IEEE Transactions on*, no. 3, 1985.

[61] PhysioBank - physiologic signal archives for biomedical research (2009) [online] Available at: http://physionet.ph.biu.ac.il/physiobank/ [Accessed 17 September 2011] .

[62] P. Marín and M. Rhea, "Effects of vibration training on muscle power: a meta-analysis," *The Journal of Strength & Conditioning Research*, vol. 24, no. 3, p. 871, 2010.

[63] P. Marín and M. Rhea, "Effects of vibration training on muscle strength: a meta-analysis," *The Journal of Strength & Conditioning Research*, vol. 24, no. 2, p. 548, 2010.

[64] A. Von Porat, M. Henriksson, E. Holmström, and E. Roos, "Knee kinematics and kinetics in former soccer players with a 16-year-old acl injury–the effects of twelve weeks of knee-specific training," *BMC Musculoskeletal Disorders*, vol. 8, no. 1, p. 35, 2007.

[65] T. Hewett, G. Myer, and K. Ford, "Anterior cruciate ligament injuries in female athletes," *The American journal of sports medicine*, vol. 34, no. 2, p. 299, 2006.

[66] K. Ford, G. Myer, and T. Hewett, "Valgus knee motion during landing in high school female and male basketball players," *Medicine & Science in Sports & Exercise*, vol. 35, no. 10, p. 1745, 2003.

[67] B. Sañudo, A. Feria, L. Carrasco, M. Hoyo, R. Santos, and H. Gamboa, "Gender differences in knee stability in response to whole body vibration," *The Journal of Strength & Conditioning Research*, 2011.

[68] H. Myklebust, N. Nunes, J. Hallén, and H. Gamboa, "Morphological analysis of acceleration signals in cross-country skiing," in *Proceedings of the International Conference on Bio-inspired Systems and Signal Processing*, 2011.

[69] C. Marques, J. Cabri, J. Barreiros, A. Carita, C. Friesecke, and J. Loehr, "The effects of task complexity on brake response time before and after primary right total knee arthroplasty," *Archives of physical medicine and rehabilitation*, vol. 89, no. 5, pp. 851–855, 2008.

[70] C. Marques, J. Barreiros, J. Cabri, A. Carita, C. Friesecke, and J. Loehr, "Does the brake response time of the right leg change after left total knee arthroplasty? a prospective study," *The Knee*, vol. 15, no. 4, pp. 295–298, 2008.

[71] D. Dalury, K. Tucker, and T. Kelley, "When can i drive?: brake response times after contemporary total knee arthroplasty," *Clinical Orthopaedics and Related Research®*, pp. 1–5, 2010.

[72] M. Liebensteiner, F. Birkfellner, M. Thaler, C. Haid, C. Bach, and M. Krismer, "Driving reaction time before and after primary fusion of the lumbar spine," *Spine*, vol. 35, no. 3, p. 330, 2010.

[73] C. J. Marques, R. Santos, H. Gamboa, F. Lampe, J. Barreiros, and J. Cabri, "Brake response time before and after total knee arthroplasty- tracking possible effects of the surgery technique on motor performance: report of two cases," in *Proceedings of the International Conference on Bio-inspired Systems and Signal Processing (BIOSIGNALS 2012)*, Vilamoura, Portugal, 2012.

[74] J. Abián, L. Alegre, A. Lara, J. Rubio, and X. Aguado, "Landing differences between men and women in a maximal vertical jump aptitude test," *Journal of sports medicine and physical fitness*, vol. 48, no. 3, pp. 305–310, 2008.

[75] H. Dhillon, R. Singla, N. Rekhi, and R. Jha, "Eog and emg based virtual keyboard: A brain-computer interface," in *Computer Science and Information Technology, 2009. ICCSIT 2009. 2nd IEEE International Conference on.* IEEE, 2009, pp. 259–262.

Appendix A

Publications

This appendix contains the three papers submitted in the context of this dissertation work. The first publication, regarding the introduced algorithm and its performance evaluation, is entitled *Biosignals Events Detection- A Morphological Signal-Independent Approach*. This paper was accepted for presentation in BIOSIGNALS 2012, which is a co-located conference of the 5^{th} International Joint Conference on Biomedical Engineering Systems and Technologies, to be hold in Vilamoura, Portugal, in February 2012. Two other papers are related to the application case studies presented in this thesis. The first, called *Gender Differences in Knee Stability in Response to Whole Body Vibration*, was accepted for publication in the *Journal of Strength and Conditioning Research*. In this appendix an ahead of print publication, already available online, is presented. The second, entitled *Brake Response Time Before and After Total Knee Arthroplasty- Tracking Possible Effects of The Surgery Techniques on Motor Performance: Report of Two Cases*, was also accepted for presentation in BIOSIGNALS 2012.

A.1 *BIOSIGNALS 2012*

Biosignals Events Detection - A Morphological Signal-Independent Approach

BIOSIGNALS EVENTS DETECTION
A Morphological Signal-Independent Approach

Rui Santos[1], Joana Sousa[2] , Borja Sañudo[3], Carlos J. Marques[4,5] and Hugo Gamboa[1,2]
[1]*Physics Department, FCT-UNL, Lisbon, Portugal*
[2]*PLUX- Wireless Biosignals, S.A., Lisbon, Portugal*
[3]*Department of Physical Education and Sport, University of Seville, Seville, Spain*
[4]*Faculty of Human Kinetics at the Technical University of Lisbon, Lisbon , Portugal*
[5]*Physical Therapy and Rehabilitation Department at the Schön Klinik Hamburg Eilbek, Hamburg, Germany*
rui_pss@hotmail.com, jsousa@plux.info, bsancor@us.es, carlos.marques@web.de, hgamboa@plux.info

Keywords: Biosignals, Signal-processing, Events, Detection and Identification, Signal-independent

Abstract: This study presents a signal-independent algorithm, which detects significant events in a biosignal, without previous knowledge or specific pre-processing steps. From a morphological analysis, the algorithm computes the instants when the most significant standard deviation discontinuities occur. An iterative optimization step is then applied. This assures that a minimal error is achieved when modeling the signal segments (between the detected instants) with a polynomial regression. The detection scale can be modified by an optional input scale factor. An objective algorithm performance evaluation procedure was designed, and applied on two types of synthetic signals, for which the events instants were previously known. An overall mean error of 20.32 ($\pm$16.01) samples between the detected and the real events show the high accuracy of the proposed algorithm. The algorithm was also applied on accelerometry and electromyography raw signals collected in different experimental scenarios. The fact that this approach does not require any previous knowledge and the good level of accuracy represents a relevant contribution in events detection and biosignal analysis.

1 INTRODUCTION

Automated techniques for generating, acquiring and storing data from scientific measurements have become increasingly precise and powerful. However, there is still a practical need to improve tools for signal pattern recognition and interpretation systems, in which the detection of specific events and the automatic signal segmentation must be one of the first processing procedures (Ciaccio et al., 1993). An event is broadly defined as the change in state of the system under study (Ciaccio et al., 1993). Biosignals are often characterized by oscillations at specific frequencies and contaminated by *in-band* noise, which is both periodic and random (Clifford, 2006). Identifying the underlying biosignal and its specific events among trivial changes can become extremely difficult.

The accurate onset determination of electromyographic (EMG) activity is an application of events detection algorithms. A comparative study regarding several methods for EMG signals onset detection, including those proposed by Hodges (Hodges and Bui, 1996) and Bonato (Bonato et al., 1998), is reported by Staude (Staude et al., 2001). Another possible application is related to the detection of general transient events. Abrupt changes or discontinuities encountered in biosignals may be symptomatic of functional disorders (Sankur et al., 1996). The ability to detect them has great importance to the medical prediction process, as well as in sport and rehabilitation research fields.

In the present work we've developed an algorithm for biosignals events detection. Based on a morphological analysis, it is able to identify time domain specific shape parameters that can clearly distinguish those events from the complete observed signals. The algorithm's design follows a signal-independent approach, requiring also no prior information or preprocessing steps, but allowing the user to control the detail on the event detection by optionally changing a specific scale factor.

The algorithm was applied on acceleration and EMG digital raw signals. An objective performance evaluation procedure was designed and applied on synthetic signals, for which the events were known.

2 MATERIALS AND ACQUISITION METHODS

2.1 Synthetic Signals

Synthetic signals were constructed by concatenating sections with predefined mean and standard deviation (STD) values (referenced as zones). The mean values where given by float numbers randomly sampled from a standard normal distribution and then multiplied by a factor m. The STD values were obtained by multiplying a random number sampled from a uniform distribution, within the interval $[0,1]$ by a factor s. Between those zones transition events with known randomly selected starting and ending points were also considered. Minimal values for mean and STD differences between successive zones were imposed and assigned to the m_d and sd_d variables, respectively. Two different types of synthetic signals were defined according to the parameters in Table 1.

Table 1: Synthetic signals parameters.

Synthetic signal	Type I	Type II
m	8	0.05
s	0.1	1
m_d	5	0.1
sd_d	0.05	0.5
Number of events	10	5

2.2 Data Acquisition

The EMG and acceleration signals were acquired, respectively, using surface bipolar EMG sensors (emgPLUX) and triaxial accelerometers (xyzPLUX), connected to a bioPLUX research unit (PLUX, 2007). Signals were sampled at frequency of 1000 Hz.

For acquiring acceleration signals drop jumps from a 40 cm elevated platform to the ground level were executed. The accelerometer was placed next to the knee (at the tibial condyle level) and orientated so its x axis was pointing upward. Only the signal acquired from the z axis (the acceleration in the Medial-Lateral axis) was considered. The testing protocol that was followed to obtain EMG signals aimed at accessing the performance of an emergency brake in a car simulator (Marques et al., 2011). From the set of signals acquired in the context of that study we consider the EMG records from the Tibialis anterior muscle during the foot transition from the accelerator to the brake pedal.

3 EVENTS DETECTION ALGORITHM

3.1 Mathematical Formalism

For a given signal defined as a time series, $x(t)$, with $t = 1,2,...,L$, a set of regions is created by slicing the signal. Considering E as the total number of events, a general event slicing signal regions is denoted by $e_i,\ i = 1,2,...,E$. The complete modeled signal is expressed as defined in equation 1, for which further notation is described below:

$$\hat{x}(t) = \sum_{i=0}^{E-1} Q\left(\frac{t}{e_{i+1}-e_i} - e_i\right) M(t-e_i, A_i, \varepsilon) \quad (1)$$

$Q(t)$ is an unit pulse function expressed by:

$$Q(t) = \begin{cases} 1 & if\ \ 0 \leq t \leq 1 \\ 0 & \text{otherwise} \end{cases} \quad (2)$$

$M(t,A,\varepsilon)$ is a polynomial regression model defined by:

$$M(t,A,\varepsilon) = A(t) + \varepsilon \quad (3)$$

where A is the matrix with n polynomial parameters for a given signal region $\left(A(t) = a_0 + a_1 t + ... + a_n t^n\right)$ and ε is an error term that is assumed to follow a normal distribution $\left(\varepsilon = N(\mu, \sigma^2)\right)$ with $\mu = 0$. Increasing the order of M makes the polynomial regression to better model the signal, decreasing the Mean Squared Error (MSE), but also renders this algorithm less sensitive to abrupt changes within that signal.

After modeling the signal as described above, each one of the $E-1$ signal segments can be described as:

$$\hat{x}^i(t) = \hat{x}(t)|_{t \in [e_i, e_{i+1}]} \quad (4)$$

3.2 Implementation

3.2.1 Events Detection

The `get_events` algorithm is the base function to identify the signal events (Figure 1). Beyond the signal, it can receive other parameters, by input, in order to run auxiliary functions responsible for each of the processing steps described below.

From a raw signal, the `get_slices_std` function divides the signal into slices with a defined length ($slices\_length$). This function returns an array containing the sequence of the successive slice's STD. The STD sequence first derivative is then calculated and low-pass filtered by applying a smoothing filter, in which the number of points considered into the moving average window depends on the length of the sequence multiplied by the $smooth\_factor$

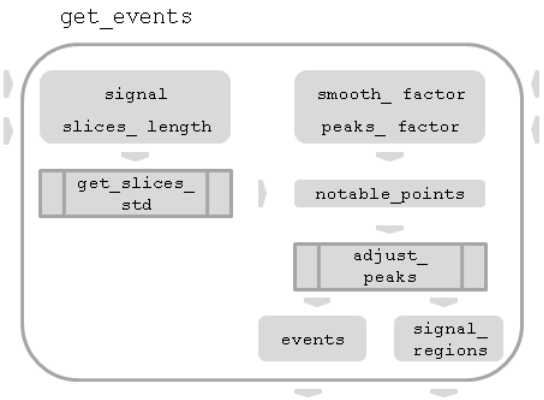

Figure 1: `get_events` algorithm flowchart diagram.

value (Figure 1). From the filtered sequence, the signal notable points are computed from the local maximums/minimums found above/below a specific threshold. The former is defined multiplying the absolute sequence maximum/minimum by the *peaks_factor* input parameter (Figure 1).

The `adjust_peaks` function is then applied. For each peak this function considers the signal slice beginning in each notable point and then applies the `get_slices_std` function on that signal segment (with a fixed *slices_length* of 5 samples). If a maximum peak is considered, it is then replaced by the point that maximizes the difference on the computed STD sequence. For minimums the procedure is analogous. This processing step ensures a more accurate events detection, with a minimum error of 5 samples. At the end, the `get_events` algorithm returns the detected events and an array with the successive signal regions between those events.

3.2.2 Optimization

The optimization processing step is based on an iterative change into the input parameters of the `get_events` algorithm (*slices_length*, *smooth_factor* and *peaks_factor*). The respective ranges depend on a *scale* factor, defined with base on the signal's length. It can alternatively be an input of the optimization algorithm, allowing to increase or decrease the level of detail (the number of detected events). For each set of parameters the `get_events` algorithm is applied. Either the solutions that have the minimum total MSE, considering all the signal segments ($\hat{x}^i(t)$ in equation 4) modeled as 1st order polynomials, or the maximum total standard deviation differences between those segments are selected in the same step. From those, the one for which the number of events is maximal is selected as the optimal solution.

4 RESULTS AND DISCUSSION

4.1 Algorithm Performance Evaluation

The developed algorithm was applied on a total of 25 Type I and 25 Type II synthetic signals, for which examples of graphic representations, including marks on the detected events, are given in Figure 2. The default *scale* factor was used. For each synthetic signal the detection mean error was computed by evaluating the mean of the differences between the detected events and the closer real event. An overall mean error of 20.32 ($\pm$16.01) samples show the high accuracy of the proposed algorithm.

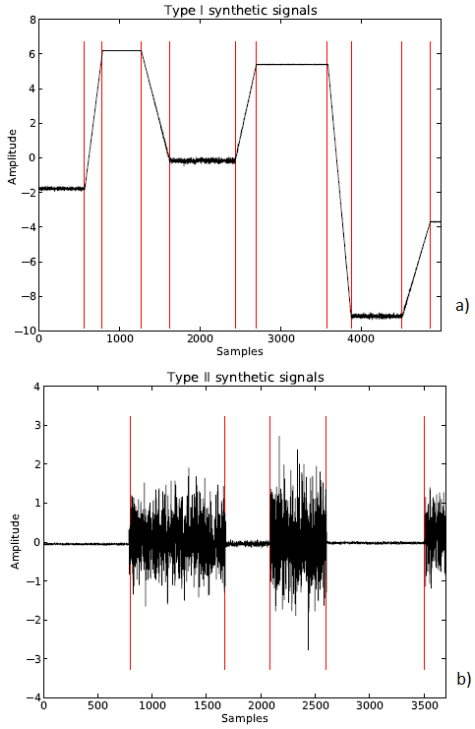

Figure 2: Synthetic signals results: a) Type I and b) Type II. The detected events are represented as vertical red marks.

4.2 Application to Biosignals

The default mode algorithm application to knee acceleration signals (Figure 3a)) marks the drop jump event by selecting mostly the landing phase record, which is characterized for the greater instability and amplitude within the signal. A more accurate description of the acceleration pattern is achieved with a proper *scale* factor. The results presented in Figure 3b), with a *scale* factor of 0.02, allow to distinguish the knee acceleration while preparing the jump from

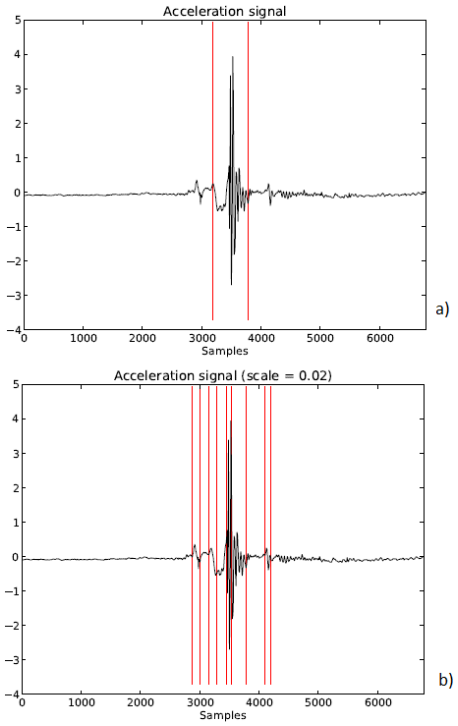

Figure 3: Acceleration signal results considering: a) default *scale* factor and b) a *scale* factor of 0.02.

the platform, the flying phase (with a slight and longer acceleration instability) and the landing phase, where the instability increases significantly for a short time period. The time spent recovering the knee stability can also be estimated by accessing the posterior signal segments. When applied to EMG signals, the default mode events detection allowed a clear distinction between activation and rest phases with an acute onset and offset detection. Being able to detect multiple events and requiring no EMG specific pre-processing steps, this algorithm presents advantages when compared with the standard onset detection techniques (Staude et al., 2001).

5 CONCLUSIONS AND FUTURE WORK

The proposed algorithm performs an efficient events detection within a signal. Its versatile design allows the application in different signals, without previous knowledge on their statistical characteristics and the adjustment of a *scale* factor to achieve different detail levels in specific applications. The added accuracy and objectivity of this algorithm when compared with the standard visual inspection also represents an advance in events detection from biosignals analysis.

In future work there is the intention of applying the algorithm to a wider range of biosignals and evaluate its performance when compared with signal specific processing techniques. Its integration into a real-time processing tool is already under development. Preliminary results point out the application's ability to detect the events in real-time, without a significant loss of accuracy.

ACKNOWLEDGEMENTS

This work was partially supported by National Strategic Reference Framework (NSRF-QREN) under projects "LUL" and "Affective Mouse", and Seventh Framework Programme (FP7) program under project ICT4Depression, whose support the authors gratefully acknowledge.

REFERENCES

Bonato, P., D'Alessio, T., and Knaflitz, M. (1998). A statistical method for the measurement of muscle activation intervals from surface myoelectric signal during gait. *Biomedical Engineering, IEEE Transactions on*, 45(3):287–299.

Ciaccio, E., Dunn, S., and Akay, M. (1993). Biosignal pattern recognition and interpretation systems. *Engineering in Medicine and Biology Magazine, IEEE*, 12(3):89–95.

Clifford, G. (2006). A novel framework for signal representation and source separation: Applications to filtering and segmentation of biosignals. *Journal of Biological Systems*, 14(2):169–184.

Hodges, P. and Bui, B. (1996). A comparison of computer-based methods for the determination of onset of muscle contraction using electromyography. *Electroencephalography and Clinical Neurophysiology/Electromyography and Motor Control*, 101(6):511–519.

Marques, C. J., Gamboa, H., Lampe, F., Barreiros, J., and Cabri, J. (2011). Muscle activation thresholds before and after total knee arthoplasty - protocol of a randomized comparison of minimally invasive vs. standard approach. In *Proceedings of the International Conference on Bio-inspired Systems and Signal Processing*.

PLUX (2007). PLUX - Wireless Biosignals, S.A. [online] Available at: http://plux.info/ [Accessed 5 September 2011].

Sankur, B., Güler, E. C., and Kahya, Y. (1996). Multiresolution biological transient extraction applied to respiratory crackles. *Computers in biology and medicine*, 26(1):25–39.

Staude, G., Flachenecker, C., Daumer, M., and Wolf, W. (2001). Onset detection in surface electromyographic signals: a systematic comparison of methods. *EURASIP Journal on Applied Signal Processing*, 2001(1):67–81.

A.2 *Journal of Strength and Conditioning Research*

Gender Differences in Knee Stability in Response to Whole Body Vibration

Journal of Strength and Conditioning Research Publish Ahead of Print
DOI: 10.1519/JSC.0b013e31823b0716

Gender differences in knee stability in response to whole body vibration.

Borja Sañudo[1], Adrian Feria[1], Luis Carrasco[1], Moisés de Hoyo[1], Rui Santos[2,3], Hugo Gamboa[2,3]

1 Department of Physical Education and Sport. University of Seville, Spain
2 Plux Wireless Biosignals. Lisbon. Portugal
3 Department of Physics. Universidade Nova de Lisboa, Portugal

Abstract

The purpose of this study was to determine whether there are kinematic and electromyographic (EMG) differences between males and females in how the knee is controlled during a single-legged drop landing in response to whole body vibration (WBV). Forty-five healthy volunteers, 30 males (22 +/- 3 yr; 76.8 +/- 8.8 kg; 179.0 +/- 6.8 cm) and 15 females (22 +/- 3 yr; 61.0 +/- 7.7 kg; 161.9 +/- 7.2 cm) were recruited for this study. Knee angles, vertical ground reaction forces and the time to stabilize the knee were assessed after single-legged drop landings from a 30-cm platform. Surface EMG in rectus femoris (RF) and hamstrings (H) and knee and ankle accelerometry signals were also acquired. Participants performed three pretest landings, followed by 3 min recovery and then completed 1 min of WBV (30 Hz - 4 mm). Before vibration the female subjects had a significant higher peak vertical force value, knee flexion angles and greater H pre-activity (EMGRMS 50 ms before activation) than the male subjects. In addition, although not significant, the medial-lateral (ML) acceleration in both knee and ankle was also higher in females. After WBV no significant differences were found for any of the other variables. However there was a decrease in the RF to H activation ratio during the pre-contact phase and a increase in the ratio during the pos-contact phase just in females which leads a decrement in ML acceleration. The gender differences reported in knee stability in response to WBV underline the necessity to perform specific neuromuscular training programs based on WBV together with instruction of the proper technique which can assist the clinician in the knee injury prevention.

Keywords: gender; injury prevention; knee; neuromuscular control; vibration training.

Borja Sañudo, PhD
Physical Education and Sport Department. University of Seville
Campus Pirotécnia. C/ Pirotécnia s/n
41013 Seville (Spain)
Tel.: +34 955420462
Fax: +34 954555985
Email: bsancor@us.es

INTRODUCTION

A large body of literature suggests that females demonstrate a substantially greater risk, approximately four to eightfold higher, to suffering acute injury of the anterior cruciate ligament (ACL) compared to males (20,13). Most of these injuries used to occur in non-contact situations such as landing activities due to the rapid changes in the forces applied to the knee joint (3,16). Therefore identification of risk factors that predispose female athletes for ACL injury has high clinical relevance.

The potential underlying mechanism to these differences between genders has been categorized in anatomical, hormonal, and biomechanical or neuromuscular imbalances (18) but there is clear consensus that sex differences in neuromuscular and biomechanical function may be the most compelling factors to explain the different rates of injury in men and women. It has been suggested that the absence of dynamic knee joint stability or neuromuscular control of the lower extremity in female athletes contributes to an increased knee injury rate (16). In addition, gender-specific muscle activation patterns as well as lower limb kinematics and kinetics have been documented (20). Differences in muscle activation have been reported in some studies supporting a tendency to higher activation of quadriceps and lower activation of hamstrings (H) in females compared to males, thus females show quadriceps/H deficits and have delayed H reactions in response to anterior stress on the ACL (7,11,17,20,43,46,49). Several electromyographical studies have evaluated gender differences and also indicate that female athletes display different neuromuscular responses, including timing (33) and magnitude (49) of muscle activation in situations where ACL injuries occur (2). This situation has also been related with the lower muscle stiffness produced by females in comparison to male athletes (49).

While there has been considerable interest in determining whether males and females differ in muscular activation, timing, recruitment patterns, musculotendinous stiffness or a combination of these factors, in order to provide a potential explanation for the disparity in ACL injury rates, more research in needed to contribute to the understanding of the potential prevention mechanism. It is widely accepted that efficient neuromuscular control is essential to dynamic joint stability and recent data support that neuromuscular training should be utilized in female athletes to decrease the incidence of ACL injuries (4). However, a better understanding of how exercises affect knee stability is of importance in order to enhance injury prevention.

To date injury-prevention programs have successfully incorporated unilateral landings (20) and strengthening in their protocols (15) due to muscle contraction can decrease the incidence of injury to the knee. Other studies have investigated the effect of exercise on tibial translation (25) what may play an important role in stabilising the knee (31) and there is some evidence of the use of neuromuscular electrical stimulation (NMES) in order to restore and improve quadriceps function (23). However, there are contradictory results about the effects of training methods on the knee joint stabilization (25). More research is needed to determine the efficacy of various proprioceptive feedback mechanisms and the ultimate capacity of neuromuscular responses to stiffen the joint and protect the ACL under sudden loading conditions (41). In this sense, and considering that neuromuscular factors that contribute to

knee stability include active muscle stiffness (38), muscle coactivity (21) and reflexive muscular activation (10), whole body vibration (WBV), which is a new kind of somatosensory stimulus for proprioception has been shown to affect all these variables (6).

WBV increase muscle strength (27) and improve neuromuscular performance based on an increase in the synchronisation activity of the motor units (6), what might have an important role on neuromuscular control of the knee joint (31). However, there is a lack of scientific support about the effects of WBV on knee proprioceptors. Only Moezy et al. (32) compared the effects of WBV training and conventional therapy on knee proprioception and postural stability in ACL reconstructed subjects. Authors reported improved proprioception and balance after WBV but greater improvement of postural stability in the WBV group in comparison with conventional training.

It was suggested that vibration stimulate the skin receptors, muscle spindles, joint mechanoreceptors and changes in vestibular system (6). It seems that during a WBV loading skeletal muscles undergo small changes in muscle length, including activation of muscle spindles, mediation of the neural signals by afferent channels, and activation of muscle fibers via large alpha-motor neurons and may contribute to joint stability by modulating muscle stiffness via reflex action on gamma-motoneurons (44). This might cause an increase in recruitment of the motor units through activation of muscle spindles and therefore a more efficient use of the positive proprioceptive feedback what was suggested to result in increased muscle strength due to neural adaptation (45).

One may argue that WBV affects the reflex activity of the muscles which act as synergists to the ACL and thus the neuromuscular control of the knee joint. However, to the best of our knowledge, no study has investigated the effects of WBV training on knee proprioception before. Just one study aimed to investigate the effect of a single WBV exposure on the reflex activity of the H and on functional knee stability (31). Authors suggested that a single session of WBV results in a decrease in anterior tibial translation that may play an important role in stabilizing the knee. No studies have investigated the differences between men and women when controlling the knee during a single-legged drop landing after the exposure to WBV. Therefore the purpose of this study was to determine whether gender differences existed in muscle activity and knee kinematics in healthy people when performing a landing maneuver after the exposure to WBV. We hypothesized that the exposure to WBV would result in: (1) differences in lower limb kinematics. Females would exhibit decreased vertical ground reaction forces (GRFs) compared to males, (2) decreased knee flexion angle during a single-leg -landing task in both genders, (3) differences in muscle activation timing. Concurrently, we presumed that vibration would result in increased activation of the H, mainly in females (with a tendency to lower activation of H) and that knee joint control would be increased, (4) an increase of muscle reflex activity which may in turn affect neuromuscular knee stabilization in both gender. We also hypothesized that some characteristic differences exist between the lower limb kinetics (knee and ankle acceleration) of male and female participants.

METHODS

Experimental Approach to the Problem

There are gender differences in neuromuscular and biomechanical function what may explain the different rates of injury in men and women. The different activation strategies or kinematics patterns contributes to an increased knee injury rate in females which may also be due to the lower muscle stiffness produced by females. It is widely accepted that neuromuscular control, joint stiffness or the efficacy proprioceptive feedback mechanisms, can improve joint stability and decrease the incidence of ACL injuries. WBV has been reported to improve all these mechanism although no study has investigated the effects of WBV training on knee proprioception before and neither the differences between men and women when controlling the knee while landing after the exposure to WBV. To observe the differences in the muscle activity and knee kinematics between males and females before and after the exposure to WBV, 45 healthy individuals performed three pretest single-leg drop landings from 30 cm and after 3 min recovery they completed 1 min of WBV (30 Hz – 4 mm) before a new landing. In all attempts, knee angles, vertical ground reaction forces and the time to stabilize the knee were assessed. Surface EMG in rectus femoris (RF) and H and knee and ankle accelerometry signals were also acquired. All outcomes were compared before and after WBV using a repeated-measures two-way ANOVA (group × measurement time). The results of this study would potentially provide additional insight into the mechanisms of ACL injury and would provide information for the development of injury-prevention programs that differentiate specific responses to WBV for both genders.

Subjects

Eighty-one subjects from the student population at University of Seville were invited by mail and by word of mouth to participate in the study. Fifty subjects volunteered to participate. Medical histories were reviewed by a physician to assess suitability for the study and exclusion criteria included the presence of lower extremity injury within six months prior to data collection. Five subjects did not fulfill the inclusion criteria (one male had severe chondromalacia, one male and one female meniscal tears and one male and one female a grade 2 or greater ligament injury) and were excluded from the study. Subjects with a history of minor strains, sprains, or chronic conditions such as tendinitis or bursitis in the dominant extremity that had completely healed or were causing no pain at the time could be included in the study. Forty-five healthy individuals, 30 males (22 ± 3 yr; 76.8 ± 8.8 kg; 179.0 ± 6.8 cm) and 15 females (22 ± 3 yr; 61.0 ± 7.7 kg; 161.9 ± 7.2 cm) participated in this study. To verify that sport experience and training history were similar between the sexes, data on sport activity and training history were collected on each subject, including running, practice, and weight-lifting activities of the previous month. Participants had to be physically active, participating in a minimum of 20 min of physical activity three times per week. All subjects played in intramural sports leagues at the university but had not participated in regular resistance or jump-training programs during the last 12 months. All subjects had a very similar training volume (minimum 3 per week and maximum 4 per week), broken up into 1-hour sessions. Participants were asked to not perform heavy exercise during the 48 h prior to the test. Each subject was informed of all procedures, potential risks, and benefits associated with the study

and were free to withdraw from the study at any time. All experimental procedures were performed in accordance with the Helsinki Declaration and subjects provided both verbal and written consent before participating. Procedures were approved by the institutional Human Research Ethics Committee.

Procedures

All subjects were familiarized with the test procedures during the pretest orientation session. They were instructed on, and provided with a demonstration of, the correct performance of the jump exercise to be assessed during the test session. All tests were preceded by a 5-min. warm-up consisting in cycling on a cycloergometer (Ergoline 900®, Ergometrics, Bitz, Germany) at 60 W (60 rpm) and warm-up was followed by five 30-cm single-legged drop landings until they demonstrated the correct technique.

Participants performed the first single-leg drop landing onto a squared zone (50 x 40 cm) delimited into the force plate. After 1 min recovery this action was repeated twice (again with 1 min recovery between trials). After 3 min recovery participants were placed on the vibrating platform and completed one bout of 1 min (30 Hz – 4 mm). Immediately after the vibration participants performed again the single-leg drop landing. All research was done during a period (between February and March) in which the participants were competing in their respective intramural leagues. In addition, all testing procedures were performed during the same period (between 10:00 and 12:00 am) in a room at an ambient temperature 22–24°C. All subjects had a typical Spanish breakfast and water intake was ad libitum.

Electromyography

EMG signals of the dominant leg were collected. In accordance with the guidelines of SENIAM Project (19), self-adhesive bipolar surface electrodes (diameter: 1.5 cm, interelectrode distance: 3 cm; Blue Sensor®, Medicotest A/S, Olstykke, Denmark) were placed at 50% on the line from the anterior superior iliac spine to the superior part of the patella, to record the RF signal and for recording H parallel to the muscle approximately half the distance from the gluteal fold to the back of the knee (semitendinosus /semimembranosus muscles). The reference electrode was placed over the patella. Signals were acquired using a wireless system (bioPLUX, Lisbon, Portugal).

EMG signals were first processed removing the y axis offset, by subtracting its mean value. It was applied a band-stop filter with a stop band of 2 Hz centered on 50 Hz and the signals were then rectified and normalized to the respective maximum value. After applying a smoothing filter with a moving average window of 400 points the EMG activation areas were determined as those were the resultant signal had an amplitude bigger than 0.1. For both RF and H EMG signals the neuromuscular pre-activity (pre150 and pre50) which refers to the EMG 150 and 50 ms prior to toe-down and the pos-activation periods (pos150 and pos50), first 150 ms and 50 ms after to toe-down were defined. In each landing the EMG signals Root Mean Square (EMG_{RMS}) on each period were computed and after obtaining the frequency spectra signals by applying to the Fast Fourier Transform algorithm the respective mean frequency values were also calculated. A quadriceps-to-hamstring (RF/H) pre-activity ratio was calculated by dividing RF activity by H activity.

Accelerometry

A tri-axial accelerometer (xyzPLUX®; PLUX - Wireless Biosignals, Lisbon, Portugal) was used to measure accelerations onto participant's ankle and knee. The sensors were set to measure accelerations within ± 3 g range. Accelerometers were stuck onto skin at tibial condyle level and at the peroneal malleolus level. Accelerations signals provided information related to participant's knee and ankle oscillations. Signals were pre-processed in order to exclude influence of gravity. In order to consider only vibration-induced muscle displacements, the signals provided by the accelerometer were low-pass filtered by an application of a smoothing filter with a moving average window of 10 points. Accelerations in medial-lateral (ML) and antero-posterior (AP) axis 60 ms after to the toe-down were considered for both knee and ankle. For each time point the signals were rectified and then the mean values were computed.

Drop landings

Participants performed 3 single-legged drop landings from a 30-cm platform onto a force plate (MuscleLab; Ergotest, Langesund, Norway) set at a sampling rate of 600 Hz and were used to measure GRFs, to indicate time phases of initial ground contact (PF1) and maximum vertical GRF (PF2) acting as key reference points for kinematic analyses but also to determine the time to stabilize the knee, defined as the eccentric contact time (s). Peak GRF during landing was defined as the highest value attained from the force-time record for the landing phase (11). GRF data were normalized by each participant's body mass. Participants wore no shoes to avoid it possible influence on the landing phase and were required to cross their arms over their chest and begin each trial in single-limb stance on the dominant leg. They then dropped off the platform and landed on the force plate using the same leg. Data were sampled and processed using a dedicated PC system (MuscleLab; Ergotest, Langesund, Norway).

Whole body vibration

All participants were familiarized with the vibrating platform (Power Plate®, North America Inc., Northbrook, IL) and the proper positioning. During the test subjects should to hold half squat position on the platform (with a 100◦ knee flexion controlled by electronic goniometer). WBV stimulus was induced to the plantar surfaces of the feet at a frequency of 30 Hz with a peak-to-peak displacement of 4 mm, considered the optimal combination to get the greater muscle performance (9).

Joint Kinetics

Three reflective markers were placed over the lateral malleolus, lateral condyle and greater trochanter. Two-dimensional sagittal-plane-projection angle of knee was measured during all tasks. A digital video camera was placed at the height of the subject's knee, 2 m beside to the subject's landing target and aligned perpendicularly to the sagittal plane. The digital images were imported into a digitizing software program (Quintic 4®, Quintic Consultancy Ltd., United Kingdom). The knee flexion angle in touchdown and the knee flexion angle when the maximal GRF was reached were determined.

Statistical analyses

The data represent means and the standard deviations (SD). Possible statistical differences were analyzed using a repeated-measures two-way ANOVA (group × measurement time). One-way analysis of variance tests were used to analyze the difference between male and female subjects in all kinematics variables. Mean EMG data for the participants were analyzed for differences between the two groups by using a multivariate analysis of variance and then by using a one-way analysis of variance for results for each individual muscle. The level of significance was set at $p < 0.05$. All statistical analyses were performed using the SPSS, 15.0 (SPSS, Inc., Chicago, IL, USA) statistical software package.

RESULTS

Table 1 shows the results of the kinetic variables during the landing phase before and after WBV. Gender differences in both the knee flexion angle in touchdown ($p = 0.02$) and the knee flexion angle when the maximal GRF was reached ($p = 0.03$) during the post-contact phase of the jump were found in the pretest. In addition, during this phase females demonstrated greater PF2 ($p = 0.02$) compared with males. After WBV no significant differences were found for the GRF or the knee flexion angles. However, there was a trend toward a different PF2 ($p = 0.06$). Thus a decrement of 6% was found in females while males even experienced an increment (4%). The time to stabilize the knee was significantly lower in both males and females ($p < 0.05$) after WBV, although no gender differences were found.

Table 1. Vertical ground reaction forces and kinematic data during 30-cm single-legged drop landings before and after WBV.

	Pretest			**Postest**		
	Males	Females	*p*	Males	Females	*p*
PF1 (BW)	2.70 (1.12)	2.69 (0.96)	.960	2.72 (0.91)	2.96 (1.05)	.454
PF2 (BW)	6.44 (1.50)	8.49 (2.58)	.002*	6.73 (1.87)	7.99 (2.22)	.065
T_Stab (s)	1.92 (0.53)	2.04 (0.64)	.548	1.76 (0.53)	1.57 (0.34)	.214
Angle1 (°)	142.41 (9.93)	151.00 (12.22)	.021*	147.96 (8.38)	147.00 (5.99)	.711
Angle2 (°)	124.07 (8.97)	130.15 (6.52)	.034*	124.79 (8.61)	128.23 (6.36)	.205

Data are reported as mean (SD); PF1= First peak vertical force value; PF2= Second peak vertical force value; BW= Times body weigh; T_stab= Time to stabilize the knee; Angle1 = Knee flexion angle in touchdown; Angle2 = Knee flexion angle when the maximal vertical ground reaction force was reached. * $p < 0.05$ (P values are for Inter-group differences).

The magnitude of the EMG activation and the activation ratios in RF and H are reported in table 2. During the pretest no gender differences in the magnitude of muscle activation during the pre-contact phase of the jump were found for RF. Significant differences in EMG_{RMS} activity was showed in H 50 ms before activation in females compared with males. During the post-contact phase of the jump, males demonstrated greater RF activation ($p = 0.26$) compared with females. When the EMG activity was assessed after WBV no significant differences were found. In the pre-contact phase of the jump, males showed a trend toward a greater EMG frequency of the RF ($p = 0.076$) than females and although none significant, the EMG_{RMS} of the

H decreased in females after WBV (27%; p = 0.475). On the other hand, during the post-contact phase, the activation of RF increased in females (4%; p = 0.687) while a decrement in H activation was experienced (4%; p = 0.999).

Table 2. EMG activity during 30-cm single-legged drop landings before and after WBV.

	Pretest			**Postest**		
	Males	Females	*P*	Males	Females	*p*
RMS_pre50_RF	0.06 (0.35)	0.07 (0.35)	.266	0.05 (0.03)	0.05 (0.02)	.658
Freq_pre50_RF	131.98 (20.23)	128.02 (19.29)	.558	138.06 (16.60)	127.71 (17.87)	.076
RMS_pos50_RF	0.09 (0.02)	0.09 (0.02)	.477	0.10 (0.03)	0.09 (0.02)	.854
Freq_pos50_RF	128.23 (16.39)	121.04 (23.50)	.263	123.95 (15.97)	126.15 (22.28)	.719
RMS_pre50_H	0.08 (0.04)	0.12 (0.06)	.048*	0.10 (0.05)	0.08 (0.05)	.239
Freq_pre50_H	161.13 (14.93)	157.67 (6.09)	.428	153.81 (11.64)	155.44 (14.64)	.701
RMS_pos50_H	0.11 (0.04)	0.11 (0.04)	.746	0.11 (0.05)	0.09 (0.03)	.329
Freq_pos50_H	146.72 (25.29)	136.41 (44.02)	.826	143.98 (17.01)	130.81 (44.69)	.171
Ratio RF/H_preRMS	0.77 (0.51)	0.82(0.92)	.794	0.73 (0.69)	.071 (0.25)	.954
Ratio RF/H_preFreq	0.82 (0.14)	0.81 (0.13)	.801	0.90 (0.13)	0.83 (0.15)	.111
Ratio RF/H_posRMS	0.98 (0.52)	0.98 (0.58)	.998	1.01 (0.49)	1.08 (0.36)	.651
Ratio RF/H_posFreq	0.90 (0.20)	0.82 (0.21)	.280	0.88 (0.18)	0.89 (0.18)	.866

Data are reported as Mean (SD); RMS_pre50: pre-activation (50 ms before ground contact); Freq_pre50: preactivation frequency values; RMS_pos50: pos-activation (50 ms after the end of activation); Freq_pos50: posactivation frequency values; Ratio RF/H: RF to H activation ratios during the pre- and post-contact phases; RF: Rectus femoris; H: Hamstrings. * $p < 0.05$ (P values are for Inter-group differences).

Timing of Activation statistical analysis in RF and H (Figure 1.) revealed that in the pre-contact phase of the jump, 150 ms before the activation both males and females showed a similar response. However 50 ms before the activation females showed a greater EMG_{RMS} in both RF and H (Figure 1a-b). After WBV no significant differences were found for the muscles assessed during the pre- and post-contact phase of the jump (Figure 1c-d). Although a greater activation of the H was found in females 150 ms before the ground contact.

RF to H activation ratios (RMS and frequency) during the pre- and post-contact phases of the drop landing before and after WBV between males and females are also showed in Table 2. No significant differences were found for the activation ratios when the activation of the RF and H are averaged and expressed in a ratio. In the pretest, during the post-contact phase of the jump, males demonstrated a higher RF/H activation ratio than women (p = 0.280). When the analysis was performed after WBV males increased the activation 50 ms before the ground contact while females showed a greater activation in the post-contact phase. In none of the cases significant differences were found.

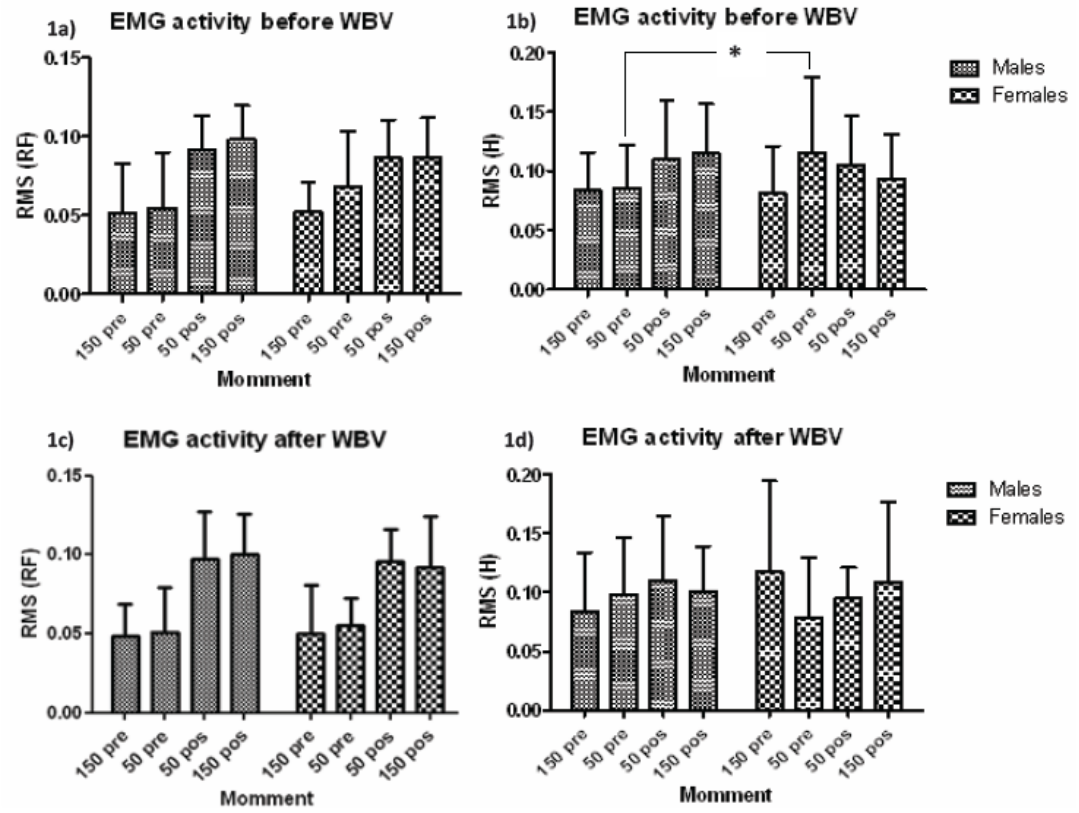

Figure 1. Comparison of EMG_{RMS} in RF (1a) and H (1b) during the first 150 ms and 50 ms before ground contact and during the subsequent 50 ms and 150 ms between males and females before and after WBV (1c, 1d). Mean values (SD) are displayed. * Denotes significant differences between genders.

Finally the acceleration of knee and ankle during the drop landings before and after WBV are showed in Table 3. No significant differences were found during the pre- or post-contact phase neither before nor after WBV. However, in the pretest, males displayed a greater AP knee acceleration (12%; $p = 0.160$) and a lower ML knee acceleration (14%; $p = 0.122$) than females. Regarding the ankle females showed again a greater ML acceleration (14%; $p = 0.147$). After WBV females experienced a decrement in knee (10%; p = 0.963) and ankle (9%; $p = 0.997$) ML acceleration.

Table 3. Acceleration data during 30-cm single-legged drop landings before and after WBV.

	Pretest			**Postest**		
	Males	Females	*p*	Males	Females	*p*
AP_Knee	1.66 (0.43)	1.46 (0.40)	.160	1.76 (0.36)	1.54 (0.45)	.095
ML_Knee	1.42 (0.40)	1.65 (0.50)	.122	1.41 (0.44)	1.49 (0.49)	.604
AP_Ankle	2.32 (0.39)	2.29 (0.32)	.765	2.29 (0.41)	2.36 (0.45)	.623
ML_Ankle	0.86 (0.32)	1.00 (0.19)	.147	0.89 (0.27)	0.91 (0.27)	.839

Data are reported as Mean (SD); AP: Antero-posterior axis; ML: Medial-lateral axis. Acceleration 60 ms after the ground contact with or without WBV in both knee and ankle. P values are for Inter-group differences.

DISCUSSION

The purpose of this study was to observe the differences in the muscle activity and knee kinematics during 30-cm single-legged drop landings between males and females before and after the exposure to WBV. The specific aim of this research was to evaluate the gender differences in knee stability in response to WBV, which had not been previously addressed. The main finding of the present study is that while females displayed a significantly greater GRF and H activity before the ground contact, an acute bout of WBV might reduce GRF and H activity in females increasing co-contraction. On the other hand, no gender differences in neuromuscular activity of the quadriceps were observed after WBV. Finally, WBV decreases females ML acceleration in both knee and ankle.

Biomechanical and neuromuscular imbalances were reported in order to explain the different rates of knee injury in males and females. In this sense, the results of the examination of gender differences during single-legged drop landings presented in the present study confirmed previous research findings that females land with increased GRF (22). Considering that PF2 was previously matched with the moment when ACL resists the largest strain during the landing (37), the results of this study indicate that females may be at a greater risk of injury. However, PF2 decreased in this population group after WBV which was reported to reduce the risk of injury during the landing movement (1). In addition, females landed with a greater knee extension which has also been cited as a predisposing factor to knee injury (36). Markolf et al. (28) reported that quadriceps forces can produce anterior tibial translation and increases in ACL mainly when the knee is flexed 40 degrees or less. In the current study both males (38°) and females (29°) displayed lower degrees. It seems that the neuromuscular system may attempt to prevent falls during unilateral landings by limiting excessive knee flexion (3) and this may also be the reason why after WBV there was a light decrement in the knee flexion angle in touchdown. This is consistent with the results reported by Gehring et al. (14) indicating that a simultaneous activation of all the aspects of the quadriceps muscle may likely lead to a better control of the frontal plane motion in the knee joint.

Another important finding in the current study was related to the neuromuscular control of the lower extremity which may be related to the incidence of ACL injuries (4). There is evidence in the literature reporting gender-specific muscle activation strategies and differences in timing or even the muscle stiffness (33,49).

Differences between males and females in muscular activation during jumping activities have been reported in the literature. While most studies support a tendency to higher activation of quadriceps and lower activation of H or even higher EMG activity means (50) in females compared to males, others did not report pre-activity patterns for the RF or H muscles (7,43,46). Our results neither showed differences in the pre-activation phase, which is consistent with Cowan and Crossley (8) who demonstrated that there were no differences in the onset of EMG or peak activity of the thigh and leg muscles between genders.

In the present study, females showed greater activation of the H than males during the pre–contact phase of the jump, which contrasts with Bencke and Zebis (2) who found lower H activation during 50 ms prior to initial ground contact, indicating lower H force in the first part of ground contact for the female subjects. Most research examining this issue has failed to find

significant gender differences in H activation upon landing during functional movements (7,30,35). Although Sell et al. (40) also found a greater H activation in females which suggest females may be H dominant. This situation was reported to reduced the ACL load due to H are synergistic to the ACL. However, as females relied more on their H, the initial increased use of these muscles in comparison to RF muscles could place greater stress on the ACL in these females' athletes (2). A greater H pre-activity was found 150 ms before the activation in females but this response was just seen in males 50 ms before the activation. These findings were partially explained by Melnyk et al. (31) suggesting that a short bout of WBV causes an increase in the short latency responses activity of the H and does not influence the medium latency responses activity of the H. In addition Krosshaug et al. (24) showed that the timing of non-contact ACL injury ranges from 17 to 50 ms after initial ground contact and this leave no time for mechano-sensory feedback mechanisms to prevent injury which suggest that a different mechanism may have occurred after WBV in this study.

Some gender differences in the timing of H and RF muscle activation have also been demonstrated in the literature (11,30). However, both seem to employ a similar sequence of muscle activation (5). The ratio of the H to the RF activation is reportedly important as a risk factor of ACL injury (48). In a study by Hanson et al. (17) a lower H to quadriceps activation ratios were found in female than male soccer players during a standardized side-cutting maneuver. This finding is consistent with others who report higher H to quadriceps activation ratios for males, compared with females, during functional movements (34,35). However, in the current study no significant differences were found in activation ratios between males and females before or after the WBV.

Finally it was suggested that both muscle stiffness and muscle coactivity may also contribute to knee stability (21). Some authors reported that H stiffness is significantly greater in males than in females and this may potentially contribute to longer electromechanical delay and a lesser rate of muscle force production in response to joint perturbation (4). Voluntary responses are too slow to protect the joint. However, reflexive muscular activation may be sufficient to elicit a protective stiffening response (42). In fact, the greater muscle activation the greater joint stiffness (10). The results of the current study indicate that after WBV there were no significant differences, although a decrement in post-activation frequency H values was found in females together with an increase RF activity. This may indicate that the females were attempting to use their quadriceps muscles to maintain the position of the knee.

Both preparatory and reactive muscle activity assist in regulating muscular stiffness, and increased muscular stiffness provides greater joint stability and protection against joint injury (38). In this sense WBV was suggested to control knee position during dynamic movement by the nervous and muscular systems, increasing the coactivation of the muscles surrounding the joint (32). However, in the current study these different muscle activation strategies between genders are not apparent which may indicate that the vibratory stimulus was not enough to induce muscle coactivation. These results contrast with Moezy et al. (32) who found that WBV resulted in a greater amount of antagonist coactivation. One possible explanation for this finding may be the double reciprocal inhibition in which antagonist muscle pairs are simultaneously active (39). Adequate co-contraction of the H during explosive movements is extremely important for dynamic knee joint stabilization (2) and these authors reported that

WBV had a greater effect for knee stability than conventional training due to WBV resulted in a greater amount of antagonist coactivation. In addition, WBV may induce the reflex action on gamma motoneurons modulating muscle stiffness and this might also explain possible gender differences in this phenomenon considering that subjects had difficulty controlling force production during vibration and greater levels of coactivation are needed to control movements and therefore this situation may require a greater response of the proprioceptive system (44). Another possible explanation of our results after WBV might be due to improved synchronization of the motor units and improved co-contraction of synergist muscles which could improve joint stability (21). This explanation may be more consistent attending to the kinetics improvements achieved in the current study.

Some authors have reported that knee injury is related to decreased knee flexion at initial contact, increased RF EMG activity but also increased knee valgus during unilateral landings (20,36). One of the most intriguing results of this study is the significant effect of gender on the lower limb acceleration. To our knowledge, this is the first investigation which has evaluated the acceleration suffered by the knee and ankle during landing. As such, direct comparison of our reported values to previous literature is not possible. However, Chappell et al. (7) showed that females exhibit greater anterior shear force on tibia during landing compared to males. Gender differences in muscle reflex in response to tibial internal/external rotation and anterior translation of the knee have also been examined (41). The results showed in the current study are consistent with previous literature but just in the AP axis. However, gender differences have shown that the participating females showed a greater (non-significant) ML acceleration than their counterpart males in both knee and ankle, and this absence of muscle control of ML knee motion has been suggested to result in high valgus knee torques and high GRF (47). These gender differences in joint kinematics suggest that increased dynamic knee valgus contributes to ACL non-contact injury risk in women (48).

When acceleration was assessed after WBV an increment in the AP axis for the knee was found in males (6%) and females (5%). Kvist et al. (26) indicated that exercise affects tibial translation in a different manner depending on gender, although authors reported that training resulted in a post-exercise increase in tibial translation just in the male athletes. In the current study, no gender differences could be found. One possible explanation of the kinetic characteristics found might be related to the fatigue resulting from WBV due to Chappell et al. (7) reported that subjects land with significantly increased peak proximal tibial anterior shear forces, increased valgus moments and decreased knee flexion angles during landings in fatigue conditions and it was found that fatigue resulted in increased knee internal rotation, adduction, and abduction moments, with the latter being more pronounced in females (29). However, Fagenbaum and Darling (12) interpreted the increased knee flexion acceleration during landing as a potential injury prevention mechanism; therefore the observed effect of WBV may play an important role in stabilizing the knee, mainly in the females ML activity. In general, ML muscle control of the knee joint is necessary since medial joint compression may be an ACL protective mechanism as it can avoid excessive abduction displacement (20,33).

In conclusion, female display significantly greater H EMG activity in the pre-activation period during single-legged drop landings before WBV than their male counterparts. In addition gender differences in the knee flexion angles, GRF and ML acceleration were reported. After

WBV there were no significant differences between males and females. However, females experienced a decrement in knee and ankle ML acceleration with no changes in the EMG what may suggest an increase in the synchronization activity of the motor units or even muscle co-contraction.

PRACTICAL APPLICATIONS

Numerous studies have demonstrated gender differences in the performance of single-legged landings, a common athletic maneuver that is important in cutting or jumping. These differences in neuromechanical function and musculotendinous stiffness may contribute to the greater incidence of ACL injury in females (Blackburn et al., 2009). Our comparison of kinematics and neuromuscular responses in male and female subjects to a WBV perturbation provides new insight into the control of knee joint loading. In particular, our results may suggest that interventions based on WBV may offer the potential for increased rate and magnitude of knee muscles recruitment and an increase in the synchronization activity which has been suggested to reduce the rate of injuries in this particular joint.

The present study indicates a possible benefit to using WBV as a preventive activity in actions involving explosive motions (e.g. jumping). However, the gender differences reported in knee stability in response to WBV underline the necessity to perform specific neuromuscular training programs based on WBV together with instruction of the proper technique which can assist the clinician in understanding the mechanisms necessary to protect the joint and prevent injury under sudden loading conditions. However, more research is needed in order to fully understand how WBV affect muscle activation and stiffness and possible gender differences. Specifically, the results of the present study indicate that WBV affects knee stability in a different manner depending on gender. Therefore, due to these differences, professionals might consider using this activity with some caution and always the use of WBV should be determined on an individualized basis.

REFERENCES

1. Abián, J, Alegre, LM, Lara, AJ, Rubio, JA, and Aguado, X. Landing differences between men and women in a maximal vertical jump aptitude test. *J Sports Med Phys Fitness* 48(3): 305-10, 2008.
2. Bencke, J, and Zebis, MK. The influence of gender on neuromuscular pre-activity during side-cutting. *J Electromyogr Kinesiol* 21(2): 371-5, 2011.
3. Benjaminse, A, Habu, A, Sell, TC, Abt, JP, Fu, FH, Myers, JB, and Lephart, SM. Fatigue alters lower extremity kinematics during a single-leg stop-jump task. *Knee Surg Sports Traumatol Arthrosc* 16(4): 400-7, 2008.
4. Blackburn, JT, Bell, DR, Norcross, MF, Hudson, JD, and Engstrom, LA. Comparison of hamstring neuromechanical properties between healthy males and females and the influence of musculotendinous stiffness. *J Electromyogr Kinesiol* 19(5): e362-9, 2009.

5. Cammarata, ML, and Dhaher, YY. Evidence of gender-specific motor templates to resist valgus loading at the knee. *Muscle Nerve* 41(5): 614-23, 2010.
6. Cardinale, M, and Bosco, C. The use of vibration as an exercise intervention. *Exerc Sport Sci Rev* 31(1): 3–7, 2003.
7. Chappell, JD, Creighton, RA, Giuliani, C, Yu, B, and Garrett, WE. Kinematics and electromyography of landing preparation in vertical stop-jump: risks for noncontact anterior cruciate ligament injury. *Am J Sports Med* 35(2): 235–41, 2007.
8. Cowan, SM, and Crossley, KM. Does gender influence neuromotor control of the knee and hip? *J Electromyogr Kinesiol* 19(2): 276-82, 2009.
9. Da Silva-Grigoletto ME, de Hoyo M, Sañudo B, Carrasco L, García-Manso JM. Determining the optimal whole-body vibration dose–response relationship for muscle performance. J Strength Cond Res, 2011 [in press].
10. Dhaher, YY, Tsoumanis, AD, Houle, TT, and Rymer, WZ. Neuromuscular reflexes contribute to knee stiffness during valgus loading. *J Neurophysiol* 93: 2698–2709, 2005.
11. Ebben, WP, Fauth, ML, Petushek, EJ, Garceau, LR, Hsu, BE, Lutsch, BN, and Feldmann, CR. Gender-based analysis of hamstring and quadriceps muscle activation during jump landings and cutting. *J Strength Cond Res* 24(2): 408–415, 2010.
12. Fagenbaum, R and Darling, WG. Jump landing strategies in male and female college athletes and the implications of such strategies for anterior cruciate ligament injury. *Am J Sports Med* 31: 233–240, 2003.
13. Ford, KR, Myer, GD, and Hewett, TE. Valgus Knee Motion during Landing in High School Female and Male Basketball Players. *Med Sci Sports Exerc* 35(10): 1745–1750, 2003.
14. Gehring, D, Melnyk, M, and Gollhofer, A. Gender and fatigue have influence on knee joint control strategies during landing. *Clin Biomech (Bristol, Avon)* 24(1): 82-7, 2009.
15. Griffin, LY, Agel, J, Albohm, MJ, Arendt, EA, Dick, RW, Garrett, WE, Garrick, JG, Hewett, TE, Huston, L, Ireland, ML, Johnson, RJ, Kibler, WB, Lephart, S, Lewis, JL, Lindenfeld, TN, Mandelbaum, BR, Marchak, P, Teitz, CC, and Wojtys, EM. Noncontact anterior cruciate ligament injuries: risk factors and prevention strategies. *J Am Acad Orthop Surg* 8(3): 141-50, 2000.
16. Griffin, LY, Albohm, MJ, Arendt, EA, Bahr, R, Beynnon, BD, Demaio, M, Dick, RW, Engebretsen, L, Garrett, WE Jr, Hannafin, JA, Hewett, TE, Huston, LJ, Ireland, ML, Johnson, RJ, Lephart, S, Mandelbaum, BR, Mann, BJ, Marks, PH, Marshall, SW, Myklebust, G, Noyes, FR, Powers, C, Shields, C Jr, Shultz, SJ, Silvers, H, Slauterbeck, J, Taylor, DC, Teitz, CC, Wojtys, EM, and Yu, B. Understanding and preventing noncontact anterior cruciate ligament injuries: a review of the Hunt Valley II meeting, January 2005. *Am J Sports Med* 34: 1512–1532, 2006.
17. Hanson, AM, Padua, DA, Troy, BJ, Prentice, WE, and Hirth, CJ. Muscle activation during sidestep cutting maneuvers in male and female soccer athletes. *J Athl Train* 43(2): 133–43, 2008.
18. Harmon, KG, and Ireland, ML. Gender differences in noncontact anterior cruciate ligament injuries. *Clin Sports Med* 19: 287–302, 2000.
19. Hermens, HJ, Freriks, B, Merletti, R, Stegeman, D, Blok, J, and Rau, G. European recommendations for surface electromyography, results of SENIAM project. 8th ed. Enschede: Roessingh Research and Development; 1999.

20. Hewett, TE, Myer, GD, and Ford, KR. Anterior cruciate ligament injuries in female athletes: Part 1, mechanisms and risk factors. *Am J Sports Med* 34: 299–311, 2006.
21. Jordan, MJ, Norris, SR, Smith, DJ and Herzog, W. Vibration Training: An overview of the Area, Training Consequences, and Future Consideration. *J Strength Cond Res* 19: 459-466, 2005.
22. Kernozek, TW, Torry, MR, Van, H, Cowley, H, and Tanner, S. Gender differences in frontal and sagittal plane biomechanics during drop landings. *Med Sci Sports Exerc* 37: 1003–1012, 2005.
23. Kim, KM, Croy, T, Hertel, J, and Saliba, S. Effects of neuromuscular electrical stimulation after anterior cruciate ligament reconstruction on quadriceps strength, function, and patient-oriented outcomes: a systematic review. *J Orthop Sports Phys Ther* 40(7): 383-91, 2010.
24. Krosshaug, T, Nakamae, A, Boden, BP, Engebretsen, L, Smith, G, Slauterbeck, JR, Hewett, TE, and Bahr, R. Mechanisms of anterior cruciate ligament injury in basketball: video analysis of 39 cases. *Am J Sports Med* 35(3): 359–67, 2007.
25. Kvist, J, Cunningham, D, and Tigerstrand-Wejlemark, H. Gender differences in post-exercise sagittal knee translation: a comparison between elite volleyball players and swimmers. *Knee* 13(2): 132-6, 2006.
26. Kvist, J. Sagittal tibial translation during exercises in the anterior cruciate ligament deficient knee. *Scand J Med Sci Sports* 15(3): 148– 58, 2005.
27. Marín, PJ and Rhea, MR. Effects of vibration training on muscle strength: A meta-analysis. *J Strength Cond Res* 24(2): 548–556, 2010.
28. Markolf, K, O'Neil, G, and Jackson, S. Effects of applied quadriceps and hamstrings muscle loads on forces in the anterior and posterior cruciate ligaments. *Am J Sports Med* 32: 1144–1149, 2004.
29. McLean, SG, Felin, RE, Suedekum, N, Calabrese, G, Passerallo, A,and Joy, S. Impact of fatigue on gender-based high-risk landing strategies. *Med Sci Sports Exerc* 39: 502–514, 2007.
30. Medina, JM, Valovich, McLeod, TC, Howell, SK, and Kingma, JJ. Timing of neuromuscular activation of the quadriceps and hamstrings prior to landing in high school male athletes, female athletes, and female non-athletes. *J Electromyogr Kinesiol* 18(4): 591-7, 2008.
31. Melnyk, M, Kofler, B, Faist, M, Hodapp, M, and Gollhofer, A. Effect of a whole-body vibration session on knee stability. *Int J Sports Med* 29(10): 839-44, 2008.
32. Moezy, A, Olyaei, G, Hadian, M, Razi, M, and Faghihzadeh, S. A comparative study of whole body vibration training and conventional training on knee proprioception and postural stability after anterior cruciate ligament reconstruction. *Br J Sports Med* 42(5):373-8, 2008.
33. Myer, GD, Ford, KR, and Hewett, TE. The effects of gender on quadriceps muscle activation strategies during a maneuver that mimics a high ACL injury risk position. *J Electromyogr Kinesiol* 15(2): 181–9, 2005.
34. Nagano, Y, Ida, H, Akai, M, and Fukubayashi, T. Gender differences in knee kinematics and muscle activity during single limb drop landing. *Knee* 14(3): 218–23, 2007.
35. Padua, DA, Carcia, CR, Arnold, BL, and Granata, KP. Gender differences in leg stiffness and stiffness recruitment strategy during two-legged hopping. *J Motor Behav* 37: 111–125, 2005.

36. Pappas, E, Hagins, M, Sheikhzadeh, A, Nordin, M, and Rose, D. Biomechanical differences between unilateral and bilateral landings from a jump: gender differences. *Clin J Sport Med* 17(4): 263-8, 2007.
37. Pflum, MA, Shelburne, KB, Torry, MR, Decker, MJ, and Pandy, MG. Model prediction of anterior cruciate ligament force during drop-landings. *Med Sci Sports Exerc* 36: 1949–1958, 2004.
38. Riemann, BL, and Lephart, SM. The sensorimotor system, part I: the physiologic basis of functional joint stability. *J Athl Train* 37(1): 71–9, 2002.
39. Rothmuller, C, and Cafarelli, E. Effect of vibration on antagonist muscle coactivation during progressive fatigue in humans. *J Physiol* 485(3): 857-64, 1995.
40. Sell, TC, Ferris, CM, and Abt, JP. The effect of direction and reaction on the neuromuscular and biomechanical characteristics of the knee during tasks that simulate the noncontact anterior cruciate ligament injury mechanism. *Am J Sports Med* 34: 43–54, 2006.
41. Shultz, SJ, Perrin, DH, Adams, MJ, Arnold, BL, Gansneder, BM, and Granata, KP. Neuromuscular Response Characteristics in Men and Women After Knee Perturbation in a Single-Leg, Weight-Bearing Stance. *J Athl Train* 36(1): 37-43, 2001.
42. Shultz, SJ, and Perrin, DH. Using surface electromyography to assess sex differences in neuromuscular response characteristics. *J Athl Train* 34(2): 165-76, 1999.
43. Sigward, SM, and Powers, CM. The influence of gender on knee kinematics, kinetics and muscle activation patterns during side-step cutting. *Clin Biomech (Bristol, Avon)* 21(1): 41–8, 2006.
44. Sjolander, P, Johansson, H, and Djupsjobacka, M. Spinal and supraspinal effects of activity in ligament afferents. *J Electromyogr Kinesiol* 12: 167–176, 2002.
45. Trans, T, Aaboe, J, Henriksen, M, Christensen, R, Bliddal, H, and Lund, H. Effect of whole body vibration exercise on muscle strength and proprioception in females with knee osteoarthritis. *Knee* 16(4): 256-61, 2009.
46. Urabe, Y, Kobayashi, R, Sumida, S, Tanaka, K, Yoshida, N, Nishiwaki, GA, Tsutsumi, E, and Ochi, M. Electromyographic analysis of the knee during jump landing in male and female athletes. *Knee* 12(2): 129–34, 2005.
47. Wikstrom, EA, Tillman, MD, Chmielewski, TL, and Borsa, PA. Measurement and evaluation of dynamic joint stability of the knee and ankle after injury. *Sports Med* 36(5): 393–410, 2006.
48. Yamazaki, J, Muneta, T, Ju, YJ, and Sekiya, I. Differences in kinematics of single leg squatting between anterior cruciate ligament-injured patients and healthy controls. *Knee Surg Sports Traumatol Arthrosc* 18(1): 56-63, 2010.
49. Zazulak, BT, Ponce, PL, Straub, SJ, Medvecky, MJ, Avedisian, L, and Hewett, TE. Gender comparison of hip muscle activity during single-leg landing. *J Orthop Sports Phys Ther* 35: 292–299, 2005.
50. Zeller, BL, McCrory, JL, Kibler, WB, and Uhl, TL. Differences in kinematics and electromyographic activity between men and women during the single-legged squat. *Am J Sports Med* 31(3): 449–456, 2003.

A.3 *BIOSIGNALS 2012*

Brake Response Time Before and After Total Knee Arthroplasty - Tracking Possible Effects of the Surgery Technique on Motor Performance: Report of Two Cases.

BRAKE RESPONSE TIME BEFORE AND AFTER TOTAL KNEE ARTHROPLASTY

Tracking Possible Effects of the Surgery Technique on Motor Performance: Report of Two Cases

Carlos J. Marques [1, 2], Rui Santos [4], Hugo Gamboa [4], Frank Lampe [3], João Barreiros [1], Jan Cabri [5]
[1] *Faculty of Human Kinetics at the Technical Universitty of Lisbon, Lisbon , Portugal;* [2] *Physikal Therapy and Rehabilitation Department and* [3]*Joint Replacement Center at the Schön Klinik Hamburg Eilbek, Hamburg, Germany;* [4]*Physics Department of the Sciences and Technology Faculty at the New University of Lisbon, Lisbon, Portugal;* [5] *Department of Physical Performance at the Norwegian School of Sport Sciences, Oslo, Norway*
carlos.marques@web.de, rui_pss@hotmail.com, hgamboa@fct.unl.pt, flampe@schoen-kliniken.de*, jbarreiros@fmh.utl.pt, jan.cabri@nih.no*

Keywords: Total Knee Replacement; Minimally Invasive Surgery; Brake Response Time; Reaction Time; Automobile Driving

Abstract: After total knee arthroplasty (TKA) patients often ask when they can resume car driving. This question was the aim of some studies in the past, however no study was found on the possible effects of different surgery techniques on brake response time (BRT). A randomized controlled trial on the effects of two surgery techniques (minimally invasive vs. standard approach) on BRT was designed. In this paper the motor performance of two female patients was compared. Surgery had different effects on the mean BRT of both Patients. The mean BRT of the MIS Patient wasn't increased 7 days after surgery, while the BRT of the Patient undergoing standard surgery was increased by 46.8% at the same time.

1 INTRODUCTION

Patients undergoing total knee arthroplasty (TKA) frequently ask when they can resume car driving. Six studies on this topic were published in the past years (Dalury et al., 2010, Liebensteiner et al., 2010, Marques et al., 2008a, Marques et al., 2008b, Pierson et al., 2003, Spalding et al., 1994). All studies investigated the effects of TKA on brake response time (BRT), an important human factor used in accident prevention research.

The results document a BRT increase after right TKA. The time frame needed for the BRT to return to preoperative values varied and ranged from 8 (Pierson et al., 2003) to 4 weeks (Dalury et al., 2010). In the study by Dalury and colleagues (2010), where the patients were submitted to "contemporary TKA with less tissue disruption", the BRT of all patients returned to preoperative values 4 weeks after surgery. A small group of patients reached the preoperative values already 2 weeks after surgery.

The BRT can be fractionated in reaction time (RT) and movement time (MT). The RT, also called neurological time, is the time required for stimulus perception, response selection and response initiation. The MT can be subdivided in foot transfer time (FTT) and brake pedal travelling time (BPTT).

In the studies where the components of the BRT (RT and MT) were investigated (Spalding et al., 1994, Marques et al., 2008b, Marques et al., 2008a, Dalury et al., 2010) it was observed that ten days after TKA the central components of the task were not affected once RT was not changed.

Total knee arthroplasty seems to affect peripheral aspects related with the execution of the movement and the soft tissue lesion may be the cause of such performance impairments.

Minimal invasive surgery (MIS) techniques for TKA have been used for several years as an alternative to standard approaches. Supporters of MIS techniques go from the assumption that a smaller soft tissue injury with a reduction of the muscle quadriceps lesion leads to a faster rehabilitation with better early functional outcomes, less pain and shorter stay duration. To the best of our knowledge we don't know of any available data on

the effects of different surgery techniques on motor performance while executing an emergency brake in a car simulator. The purpose of this study is to compare the effects of MIS and Standard approach for TKA on BRT components. Once the study is ongoing the data of two cases will be reported.

2 METHODS AND MATERIALS

2.1 Design

A randomized controlled trial with one between-subject factor (surgery technique: MIS or Standard) and one within-subject factor (time: one day before and 7 days, 30 and 40 days after surgery) was designed (Marques et al., 2011). After consent to participate the patients were randomly assigned to MIS or standard approach surgery. The patients were blinded to the surgery technique they underwent and they all received the same standard physiotherapy treatments.

One experienced orthopaedic surgeon performed all surgeries. In the operation room a concealed envelope was opened and the surgeon got to know which technique he would have to perform.

The MIS technique used was the mini-midvastus approach (Haas et al., 2006). The peri-patellar approach with inversion of the patella was standard. Independently from the surgery technique all operations were performed with the use of the OrthoPilot navigation system and all patients got a Columbus total knee endoprosthesis (BBraun Aesculap, Germany).

The study protocol was approved by the Ethics-Committee of the Federal State of Hamburg, Germany (Project Nr.: PV3349). The trial registration number at the German Clinical Trial Database (DRKS) is: DRKS00000552.

2.2 Participants

The patient selection is taking place at the Schön Klinik Hamburg Eilbek in Hamburg, Germany. The patients addressed the clinic for elective primary right TKA and were asked if they were car drivers. If the patient drove regularly (at least once a week) he/she was informed about the study and asked for consent.

The patient selection started on January 10th 2011 and is still ongoing. Eleven patients have signed the informed consent until now, of which the complete data of 8 Patients is available: MIS n=5 (4 male; 1 female); Standard approach n=3 (1 male; 2 female). Because the number of cases is still small and the distribution of male and female patients in the groups is unlike, we will present only the primary outcome results of two female patients (Pat. A and Pat. B).

2.3 Instruments / Equipment

The patients performed the emergency brakes in a car simulator (Fig.1) which was built based on a European middle class car an already used in two former studies (Marques et al., 2008a, Marques et al., 2008b).

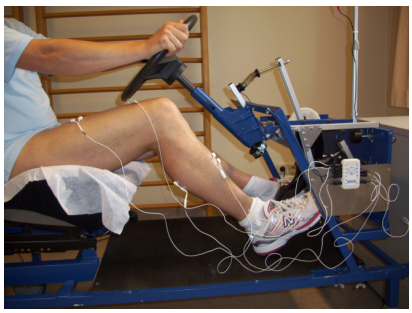

Figure 1: Car simulator with bioPLUX Research system.

The data acquisition system consists of a BioPlux Research system with wireless connectivity via Bluetooth (PLUX – Wireless Biosignals, S. A.), one trigger to command the stimulus light (red LED) turn on/off and two load cells connected with the break and accelerator pedals.

2.4 Study Outcomes

The primary outcomes of the study are the brake response time (BRT), which is time frame between the onset of the red LED and the achieving of a brake force on the brake pedal of 150N (ms). The BRT was fractionated in reaction time (RT), foot transfer time (FTT) and brake pedal travelling time (BPTT).

2.5 Procedures

The assessments took place in a closed room to avoid secondary distraction sources. A trained physiotherapist performed all tests.

After sitting down in the car simulator the patients were required to adjust the seat in order to find a comfortable position. A simple and a more complex

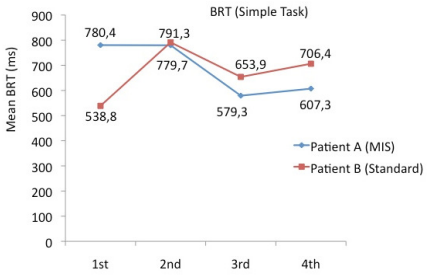

Figure 2: Mean BRT values across the four measurements

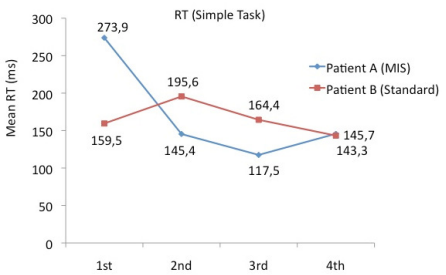

Figure 3: Mean RT values across the four measurements

task were used to assess the components of BRT. At each measurement day patients performed 5 practice and 10 test trials for each task.

2.7 Data analysis

Two types of signals were collected: the digital signal from the light trigger and the force signals from the accelerator and brake pedal load cells. The digital signal was used to slice the signals in the 10 break trials for each task. The force signals were calibrated considering that in the initial instant the foot is not pressing any of the pedals and the acquired value in the initial 100ms was considered the zero of the load cells.

After the pre-processing steps, the onset points of the force signals were detected by applying a signal-independent algorithm, which marks significant events in a signal, based on a morphological analysis approach (Santos et al., 2012) and the values of the variables were detected.

3 RESULTS

Patient B is 15 years older then patient A. Despite that difference patient B had faster baseline performances in both tasks when compared with patient A.

	Patient A	Patient B
Age (y)	61	76
Body weight (Kg)	71	74
Stature (cm)	167	175
Technique	MIS	Standard

Table 1: Demographic data of both patients.

The effects of TKA on BRT are different when comparing the data of both cases in the simple task (Fig. 2). Seven days after surgery the mean BRT of Patient B (Standard) had increased by 46.8% while the mean BRT of Patient A remained practically unchanged (decreased 0.08% from the first to the second measurement). From the second to the third measurement the mean BRT had decreased by 25.7% and 17.3% for patients A and B respectively. Thirty-two days after surgery patient A performed on average 201.1ms quicker then at baseline, while the mean BRT of patient B was still 115.1ms increased when compared with baseline.

The BRT increased due to an MT increase. The RT (Fig. 3) decreased for both patients across the time, with exception of patient B, who's RT had increased by 22.6% from the first to the second measurement.

The analysis of the MT components (FTT and BPTT) revealed that the BRT increased mainly due to an increase of the FTT. The FTT (Fig. 4) had increased by 57.8% (189.7ms) and 53.7% (144.6ms) from the first to second measurement respectively for patient A and B. At 40 days the mean FTT values of both patients were still over baseline (see Figure 5).

The BPTT decreased across the time for Patient A, however, it increased by 65% for patient B between the 1st and second measurement (Fig. 6), showing that surgery techniques might have had different effects on this variable.

4 DISCUSSION

Total knee Arthroplasty reduces pain and increases function and health related quality of life in patients with knee impairments resulting from osteoarthritis. Many patients undergoing TKA want to know when they can return to car driving after surgery. The available evidence, on which doctors can rely to advice these patients, is few.

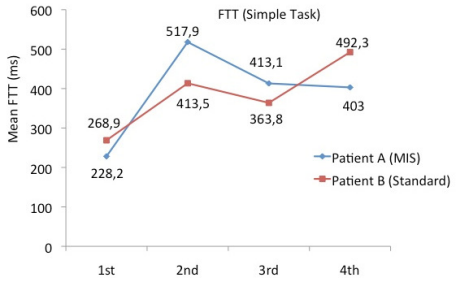

Figure 4: Mean FTT values across the four measurements

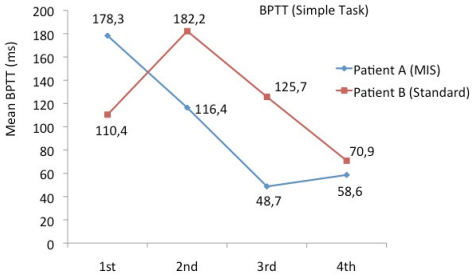

Figure 5: Mean BPTT values across the four measurements

There is no evidence whether different surgery techniques for TKA can influence the BRT recovery of the patients.

Based on the results of two cases we can report that surgery had different effects on the mean BRT of both Patients. The mean BRT of the MIS Patient wasn't increased 7 days after surgery, while the BRT of the Patient undergoing standard surgery was increased by 46.8% at the same time.

The components of MT (FTT and BPTT) characterize two distinguished parts of the leg movement. While during the FTT the leg is being moved in an open system, with the foot having no contact with the pedals, during the BPTT the leg is being moved in a closed system, with the foot pressing the brake pedal and the knee making an extension. The performance pattern of the patients in the open system (FTT) is very similar (Fig. 4), with both patients showing a performance increase after surgery followed by a decrease. On the other hand, in the closed system (BPTT), the patient's performance provides an interesting difference, with the MIS patient having no performance decrease after surgery (Fig. 5).

In order to find out, whether the observed trends are related with the surgery technique the patients underwent and not due to inter-subject variations, a bigger sample is necessary.

ACKNOWLEDGEMENTS

We thank the Technical Department at the Schön Klinik Hamburg-Eilbek for the technical changes and adaptations made in the car simulator.

REFERENCES

DALURY, D. F., TUCKER, K. K. & KELLEY, T. C. (2010) When Can I Drive?: Brake Response Times After Contemporary Total Knee Arthroplasty. Clin Orthop Relat Res.

HAAS, S. B., MANITTA, M. A. & BURDICK, P. (2006) Minimally invasive total knee arthroplasty: the mini midvastus approach. Clin Orthop Relat Res, 452, 112-6.

LIEBENSTEINER, M. C., KERN, M., HAID, C., KOBEL, C., NIEDERSEER, D. & KRISMER, M. (2010) Brake response time before and after total knee arthroplasty: a prospective cohort study. BMC Musculoskeletal Disorders.

MARQUES, C. J., BARREIROS, J., CABRI, J., CARITA, A. I., FRIESECKE, C. & LOEHR, J. F. (2008a) Does the brake response time of the right leg change after left total knee arthroplasty? A prospective study. Knee, 15, 295-8.

MARQUES, C. J., CABRI, J., BARREIROS, J., CARITA, A. I., FRIESECKE, C. & LOEHR, J. F. (2008b) The effects of task complexity on brake response time before and after primary right total knee arthroplasty. Arch Phys Med Rehabil, 89, 851-5.

MARQUES, C. J., GAMBOA, H., LAMPE, F., BARREIROS, J. & CABRI, J. (2011) Muscle activations thresholds before and after total knee arthroplasty - protocol of a randomized comparison of minimally invasive vs. standard approach. Proceedings of the International Conference on Bio-inspired Systems and Signal Processing. Rome, Italy.

PIERSON, J. L., EARLES, D. R. & WOOD, K. (2003) Brake response time after total knee arthroplasty: when is it safe for patients to drive? J Arthroplasty, 18, 840-3.

SANTOS, R., SOUSA, J., B., S., MARQUES, C. J. & GAMBOA, H. (2012) Biosignals Event Detection: A morfological Signal-Independent Approach. Proceedings of the International Conference on Bio-inspired Systems and Signal Processing. Vilamoura, Portugal.

SPALDING, T. J., KISS, J., KYBERD, P., TURNER-SMITH, A. & SIMPSON, A. H. (1994) Driver reaction times after total knee replacement. J Bone Joint Surg Br, 76, 754-6.